2012

GLYCEROLIPIDS AND THE PLANT CUTICLE CONTRIBUTE TO PLANT IMMUNITY

Qing-Ming Gao
University of Kentucky, qgao2@g.uky.edu

STUDENT AGREEMENT:

I represent that my thesis or dissertation and abstract are my original work. Proper attribution has been given to all outside sources. I understand that I am solely responsible for obtaining any needed copyright permissions. I have obtained and attached hereto needed written permission statements(s) from the owner(s) of each third-party copyrighted matter to be included in my work, allowing electronic distribution (if such use is not permitted by the fair use doctrine).

I hereby grant to The University of Kentucky and its agents the non-exclusive license to archive and make accessible my work in whole or in part in all forms of media, now or hereafter known. I agree that the document mentioned above may be made available immediately for worldwide access unless a preapproved embargo applies.

I retain all other ownership rights to the copyright of my work. I also retain the right to use in future works (such as articles or books) all or part of my work. I understand that I am free to register the copyright to my work.

REVIEW, APPROVAL AND ACCEPTANCE

The document mentioned above has been reviewed and accepted by the student's advisor, on behalf of the advisory committee, and by the Director of Graduate Studies (DGS), on behalf of the program; we verify that this is the final, approved version of the student's dissertation including all changes required by the advisory committee. The undersigned agree to abide by the statements above.

Qing-Ming Gao, Student

Dr. Aardra Kachroo, Major Professor

Dr. Lisa J. Vaillancourt, Director of Graduate Studies

GLYCEROLIPIDS AND THE PLANT CUTICLE CONTRIBUTE TO PLANT IMMUNITY

DISSERTATION

A dissertation submitted in partial fulfillment of the requirements
for the degree of Doctor of Philosophy in the
College of Agriculture at the
University of Kentucky

By
Qing-Ming Gao

Lexington, Kentucky

Director: Dr. Aardra Kachroo, Associate Professor, Plant Pathology Department,
Lexington, Kentucky

2012

ABSTRACT OF DISSERTATION

GLYCEROLIPIDS AND THE PLANT CUTICLE CONTRIBUTE TO PLANT IMMUNITY

The conserved metabolites, oleic acid (18:1), a major monounsaturated fatty acid (FA), and glycerol-3-phosphate (G3P) are obligatory precursors of glycerolipid biosynthesis in plants. In *Arabidopsis*, the *SSI2*-encoded SACPD is the major isoform that contributes to 18:1 biosynthesis. Signaling induced upon reduction in oleic acid (18:1) levels not only upregulates salicylic acid (SA)-mediated responses but also inhibits jasmonic acid (JA)-inducible defenses. I examined the transcription profile of *ssi2* plants and identified two transcription factors, *WRKY50* and *WRKY51*. Although the *ssi2 wrky50* and *ssi2 wrky51* plants were constitutively upregulated in SA-derived signaling, they were restored in JA-dependent defense signaling. Not only did these plants show JA-inducible *PDF1.2* expression, but they were also restored for basal resistance to the necrotrophic pathogen, *Botrytis cinerea*. Overall, my results show that the WRKY50 and WRKY51 proteins mediate both SA- and low 18:1-dependent repression of JA signaling in *Arabidopsis* plants.

My studies also show that cellular G3P levels are important for plant defense to necrotrophic pathogens. I showed that G3P levels are induced in *Arabidopsis* in response to the necrotrophic fungal pathogen *B. cinerea*. G3P-dependant induction of basal defense is not via the activities of other defense-related hormones such as SA, JA or the phytoalexin camalexin. Arabidopsis mutants unable to accumulate G3P (*gly1*, *gli1*) showed enhanced susceptibility to *B. cinerea*.

Previous studies in our lab identified acyl-carrier protein 4 (ACP4), a component of FA and lipid biosynthesis, as an important regulator of plant systemic immunity. *ACP4* mutant plants were defective in systemic acquired resistance (SAR) because they contained a defective cuticle. I further investigated the role of the plant cuticle in SAR by studying the involvement of long-chain acyl-CoA synthetases (*LACS*), a gene family involved in long-chain FA and cuticle biosynthesis, in SAR. In all, eight *lacs* mutants (*lacs1, lacs2, lacs3, lacs4, lacs6, lacs7, lacs8, lacs9*) were isolated and characterized. Six mutants were compromised in SAR. Together, my studies show that the various LACS

isoforms contribute differentially to both cuticle formation and systemic immunity in *Arabidopsis*.

Keywords: Fatty acid, Glycerol-3-phosphate, Transcription factors, Systemic Acquired Resistance, Cuticle

Qing-Ming Gao

April 13, 2012

GLYCEROLIPIDS AND THE PLANT CUTICLE CONTRIBUTE TO PLANT IMMUNITY

By

Qing-Ming Gao

Dr. Aardra Kachroo
Director of Dissertation

Dr. Lisa J. Vaillancourt
Director of Graduate Studies

April 13, 2012
Date

DEDICATED TO MY BELOVED PARENTS

ACKNOWLEDGEMENTS

First of all, I would like to express my sincere gratitude to my advisor Dr. Aardra Kachroo. I am lucky to have Dr. Aardra Kachroo as my advisor and happy to work with her. In last five years, her constant motivation and support greatly help me to complete my dissertation. I thank Dr. Pradeep Kachroo for his help in executing the experiments and suggestions during my lab meetings. I am very grateful to Dr. Ludmila Lapchyk for her generous support during my Ph.D. study. I would like to thank Amy Crume for her excellent work in maintaining our plant growth facility. I would like to say thanks to all the past and present members of Dr. Kachroo lab for their kind help.

I sincerely thank all my committee members, Dr. David Smith, Dr. Arthur Hunt, Dr. Christopher Schardl, and the outside examiner Dr. Christoph Benning, for their valuable suggestions during my committee meetings and useful comments on my dissertation. My special thanks to Dr. David Smith and Dr. Arthur Hunt for writing recommendation letters for me and other generous help.

Many thanks to Mr. John Johnson for help me with fatty acid analysis, Dr. Duroy Navarre for salicylic acid estimation, Dr. Keshun Yu for cutin monomer analysis, Dr. John Browse for *gly1-1* seeds, Dr. Jian-Min Zhou for *gli1* seeds, Dr. Jane Glazebrook for providing camalexin standard and *pad3* seeds, Dr. Fred Ausubel for *sid2* seeds, Dr. John Turner for *coi1* seeds, Dr. Paul Staswick for *jar1* seeds, Dr. Barbara Kunkel for *avrRpt2* strain, and Kansas Lipidomic Research Center for lipid analysis.

Finally, I would like to thank all my friends and family members for their support and encouragement in last five years.

TABLE OF CONTENTS

LIST OF TABLES

LIST OF FIGURES

CHAPTER ONE

INTRODUCTION

The increasingly changing global climate and fast-growing human population have augmented worldwide concerns related to the security of our food supply. These concerns are further intensified by pathogen-related crop losses; each year, about 15% of food production is lost due to infections by plant pathogens (McDonald, 2010). Controlling plant infectious diseases is therefore an immediate concern, especially for plant pathologists.

The better we understand how pathogens cause diseases and how plants defend themselves, the better we should be able to control plant diseases. The use of "model" species in plant biology research is undeniably advantageous and has been successfully applied to improve the production of a variety of crops (Rafalski, 2010; Wulff et l., 2011). *Arabidopsis thaliana* is widely used for studies in plant biology with a large number of available tools and resources (Nishimura and Dangl, 2010; Serino and Gusmaroli, 2011). Consequently, studies in this plant have rapidly increased our knowledge of many aspects of plant growth and development. My research is particularly pertinent to plant defense to microbial pathogens and is directly applicable to commodity crops. I use the "model" plant *Arabidopsis* for a major portion of my research. In crop plant, my research involves the examination of defense-related aspects in soybean.

Plants are static and challenged by various biotic and abiotic stresses during their different growing stages in nature. With extensive studies in past decades, we learned that plants have evolved different defense systems, such as non-host resistance, basal defense and *R*-mediated resistance (Eulgem 2005). For the pathogens which have narrow host range, for example, host from one or two genus, the other plants are all non-host. In non-host resistance, physical barriers, such as cuticle, cell wall, and antibiotic metabolites can repulse non-host pathogens. Meanwhile, general elicitors from host pathogens, also called pathogen-associated molecular patterns (PAPMs), like flagellin from gram

negative bacteria, can induce basal defense (Thordal-Christensen 2003). By contrast, host pathogens can suppress basal defense by *AVR* elicitors. Meanwhile, plants evolved various Resistance (*R*) genes and trigger *R* gene-mediated resistance through an incompatible interaction (Jones and Dangl 2006; Jones and Dangl 2006). The R gene-mediated resistance is very specific, and normally each avirulence (*avr*) gene of pathogens is recognized by one Resistance (*R*) gene directly or indirectly in plant host. The sign of this gene-for-gene interaction is hypersensitive response (HR), which restricts pathogens spread in infected tissues.

Many studies indicated that plant hormones act as signal molecules in plant defense, such as jasmonic acid (JA), salicylic acid (SA), ethylene, abscisic acid (ABA), gibberlic acid, brassinosteroids (BRs), and cytokinin (Shah 2003; Lorenzo and Solano 2005; Mauch-Mani and Mauch 2005). JA is an important phytohormone involved in response to abiotic stress, such as wounding and water deficiency, and also involving in many plant physiological progresses, such as root growth, senescence and pollen maturation (Wasternack 2007; Balbi and Devoto 2008). For biotic stress, JA mediated-pathway is primarily effective against necrotrophic pathogens and insects although there are exceptions to this (Beckers and Spoel 2006; Beckers and Spoel 2006; Halim, Vess et al. 2006; Halim, Vess et al. 2006). SA is a well-known phytohormone and many studies already showed its important role in plant defense. For example, SA level is increased after biotrophic pathogen infection and can activate pathogen-related (*PR*) gene expression and induce resistance to bacterial and oomycete pathogens (Malamy, Carr et al. 1990; Shah, Kachroo et al. 2001). In transgenic plant *NahG* (bacterial salicylate hydroxylase gene), SA is conjugated to catechol and plants show susceptibility to pathogens (Gaffney, Friedrich et al. 1993). However, application of the functional analog of SA, benzo (1, 2, 3) thiadiazole-7-carbothioic acid S-methyl ester (BTH), can activate *PR*-gene expression and plants show more resistance to pathogens (Ward, Uknes et al. 1991; Friedrich, Lawton et al. 1996). Also, SA is required in systemic acquired resistance (SAR) (Gaffney, Friedrich et al. 1993; Ryals, Neuenschwander et al. 1996; Durrant and Dong 2004). The important molecular component in SA pathway is *NPR1* (non-expressor of *PR* genes), also known as *NIM1* (non-inducible immunity)/*SAI1* (salicylic acid-

insensitive), functions downstream of SA (Cao, Bowling et al. 1994; Delaney, Friedrich et al. 1995; Shah, Tsui et al. 1997).

Emerging evidence strongly indicates that all of these different pathways overlap at some point, such as plant defense is actually a coherence of many pathways functioning together. More and more evidence indicated that there is cross-talk between different defense signaling pathway, such as SA/JA, JA/ABA, and JA/ethylene (Lorenzo and Solano 2005; Beckers and Spoel 2006; Halim, Vess et al. 2006). The crosstalk between SA and JA pathways has particularly been the majority of many investigations.

The SA and JA pathways can function synergistically or antagonistically to mediate plant defense. Normally, SA induces some marker genes, such as *PR-1*, *PR-2* and *PR-5*, and confers resistance to biotrophic pathogens which grow and reproduce in live cells. SA-mediated resistance is abolished in *npr1* mutant and transgenic *NahG* plants. Meanwhile, JA can induce some marker genes, such as *PR-3*, *PR-4* and *PDF1.2*, and confer resistance to necrotrophic pathogens which kill the live cells and obtain nutrients from dead tissue (Thomma, Eggermont et al. 1998). Exogenous SA treatment can suppress JA-mediated defense to necrotrophic pathogen (*Alternaria brassicicola*) (Spoel, Johnson et al. 2007). Compared with water treatment, the plants showed susceptibility to *A. brassicicola* and very low level expression of *PDF1.2* in SA treated plants. Furthermore, same results were observed in plants inoculated with virulent *P. syringae*. Interestingly, this suppression was abolished in the *sid2* and *npr1* mutants, suggesting that the suppression requires SA accumulation and occurs in a *NPR1*-dependent manner. Surprisingly, in systemic tissues of virulent *P. syringae* strain-inoculated plants, this suppression was not observed. This result indicated that plants have a fine spatial control of the SA-JA antagonistic relationship. Also, avirulent strains carrying *Avr* effectors (*avrRpm1* and *avrRpt2*), which could trigger *R-gene* mediated defense and induce cell death in plant tissues, failed to suppress the JA pathway in local and systemic tissues. Thus, plants can minimize the opportunity of necrotrophic pathogen attack when they activate the SA pathway to defend themselves against biotrophic pathogens. Conversely, the virulent *P. syringae* can synthesize coronatine, a structural mimic of JA. Transferred into host cells,

coronatine can suppress the SA-pathway and induce susceptibility to virulent *P. syringae* in un-inoculated leaves. Howeve, coronatine couldn't induce susceptibility to insect pathogen (cabbage looper, *Trichoplusia ni*) in systemic tissues a(Cui, Bahrami et al. 2005).

A synergistic example of the JA-SA relationship was found in ISR (induced systemic resistance) and SAR (systemic acquired resistance). ISR is induced by nonpathogenic *Pseudomonas rhizobacteria* in soil and is dependent on JA/ethylene pathway, and SAR is induced by *avirulent* pathogens and is dependent on SA pathway. ISR and SAR induce resistance to many pathogens, such as virus, fungus and bacteria (Durrant and Dong 2004; Beckers and Spoel 2006). JA-dependent ISR pathway and SA-dependent SAR pathway were compatible and showed an additive effect in defense to *P. syringae*. Both pathways required *NPR1*, but the direct crosstalk between ISR and SAR was not found (Pieterse, Van Pelt et al. 2000).

In addition to these phytohormones, fatty acids (FAs) are also involved in plant defense signaling (Vijayan, Shockey et al. 1998; Li, Liu et al. 2003). In Dr. Aardra Kachroo's my PI's lab, we are working on a mutant involved in FA biosynthesis, which shows very interesting defense-related phenotypes. Originally, the mutant was identified in the screening of suppressor of SA-insensitivity 2 (*ssi2*). *SSI2* encodes stearoyl-acyl carrier protein desaturase (S-ACP-DES), which desaturates stearic acid (18:0)-ACP to oleic acid (18:1)-ACP. The EMS-mutagenesis-generated *ssi2*, as a result, the level of 18:1 in *ssi2* mutant is pretty low, compared with wide type (Co-0). The *ssi2* mutant shows constitutive *PR*-gene expression, high endogenous SA level, spontaneous lesions, more resistance to bacterial and oomycete pathogens. Meanwhile, JA-mediated signaling pathway is impaired in *ssi2* mutant. Three suppressors of *ssi2* mutant, *act1* (plastid glycerol-3-phosphate acyl-transferase), *gly1* (glycerol-3-phosphate dehydrogenase) and *acp4* (acyl-carrier protein 4), can rescue the *ssi2* defense-related phenotypes including JA-mediated signaling pathway. Our results indicated that oleic acid (18:1) level could regulate SA and JA defense pathways in plants (Kachroo, Lapchyk et al. 2003; Kachroo, Venugopal et al. 2004). Another WRKY family member, WRKY70, has been shown to

be involved in SA-JA pathway crosstalk. WRKY70 is an activator of the SA pathway, and a repressor of the JA pathway (Li, Brader et al. 2004). However, the mechanisms underlying this regulation are still unlcear.

Another part of my PhD thesis is to understand the roles of the primary metabolite glycerol-3-phosphate (G3P) and the plant cuticle in mediating basal and induced plant defenses. Classical studies in plant pathology implied defense-signaling pathways as separate from primary metabolism in plants. However, recent evidence implicates a number of primary metabolic pathways and their components as interfacing with plant defense. Studies in Dr. Aardra Kachroo's laboratory have demonstrated novel roles for primary metabolites such as fatty acids, components of glycerolipid metabolism, and the plant cuticle in mediating plant defense against a variety of pathogens. The ability to induce defense signaling in moderate levels and specifically only in response to or in anticipation of pathogen infection is highly desirable. Characterizing the roles of various primary metabolic components is particularly attractive as it will enable the development of novel and sustainable strategies for crop improvement.

G3P is a conserved metabolite in many organisms. In plants, G3P is generated through glycerol via glycerol kinase (*GK*), or the reduction of dihydroxyacetone phosphate (DHAP) via G3P dehydrogenase (*G3Pdh*). The plastidal G3P acyltransferase (*ACT1*) is another enzyme tightly associated with G3P metabolism because it acylates G3P with the fatty acid oleic acid (18:1) to form lyso-phosphatidic acid. This is the first committed step for lipid biosynthesis via the prokaryotic pathway in plants. G3P metabolism is important also for maintaining the homeostasis of other primary metabolites, such as FAs, lipids and sugars. Previously, we reported that cellular G3P levels were induced in *Arabidopsis* in response to the hemibiotrophic pathogen, *Colletotrichum higginsianum,* and increased accumulation of G3P-enhanced resistance to this pathogen. Correspondingly, mutant plants (*gly1*) defective in *G3Pdh* showed more susceptibility to *C. higginsianum*, whereas overexpression of *GK* increased resistance. This G3P-mediated induction of basal defense is independent of signaling induced by the defense-related phytohormones salicylic acid, jasmonic acid, and ethylene pathway (Chanda et al., 2008). *C.*

higginsianum in the initial stages of infection *C.higginsianum* behaves as a true biotroph later switching to the necrotrophic phase of growth, which kills host tissue. Although different pathogens evolve specific features contributing to pathogenicity, many also share conserved mechanisms (Choquer *et al.* 2007). Therefore, it is reasonable to speculate that this G3P-mediated basal defense might also protect against true necrotrophs.

Botrytis cinerea (teleomorph: *Botryotinia fuckeliana*), the causal agent of grey mold disease, is the most important necrotrophic plant pathogen. This ascomycete pathogen can infect more than 200 dicot plants in field and greenhouse during growing season or post-harvest, including vegetables (i.e. lettuce, beans, tomato), fruits (i.e. grape, apple, strawberry), oil crops (i.e. sunflower) and forage (i.e. alfalfa). This necrotrophic pathogen poses special challenges to pathologists, breeders, and growers in particular due to its long-lived survival structures, wide host range, and high variability in strains and populations. Current, available strategies for controlling such pathogens include developing new fungicides and generating resistant hosts. Several fungicides targeting fungal respiration, microtubule assembly, or sterol synthesis were developed in the past three decades. However, the related increase in cost of crop production and the rapid development of fungicide-insensitive pathogen populations has impaired the efficacy of this approach. Furthermore, use of fungicide is not a sustainable solution and could be detrimental to the environment and human health in the long run, due to long term retention of harmful chemicals in the soil. Developing truly sustainable strategies for counteracting plant pathogens such as *B. cinerea* requires a better understanding of the physiology of the plant during the disease process. In this study, I have shown the role of G3P and its metabolizing enzymes in mediating defense against the necrotrophic pathogen, *B. cinerea.*

In our previous studies on *acp4* (acyl-carrier protein 4) mutant, a suppressor of *ssi2*, I have shown the role for acyl-carrier protein 4 (*ACP4*), a component of FA and lipid biosynthesis, in mediating systemic immunity in plants. This work showed that mutations in the *ACP4* gene not only affect plant cuticle formation, but also basal resistance to

necrotrophic pathogens (*B. cinerea*) and the ability to induce systemic resistance. Further characterization showed that the plant cuticle is essential for the perception of a mobile signal that is generated in the primary infected tissues and later translocated to systemic parts of the plant to induce immunity against secondary infections.

The plant cuticle is a hydrophobic layer that covers the aerial surface of plants and forms the first line of contact with the environment. It is known to fulfill important roles in controlling water loss, gas exchange, UV irritation, organ development and pathogen entering. The cuticle layer consists of two types of lipids: cuticular waxes and cutin polymers. The plant cuticle was primarily thought to serve a passive role in plant defense by acting as a physical barrier to pathogen ingress. However, recent studies have demonstrated that the cuticle may also play a more active, signaling role and participate in innate immune response. For example, exogenous application of cutin monomers confers enhanced resistance to several fungal pathogens. Furthermore, plants containing defective cuticles show enhanced resistance to fungal pathogens, such as several cuticle defective mutants (*lacs2/bre1/sma4*, *att1*, *bodyguard*, *lacerata*) show increased tolerance to *B. cinerea*. However, the mechanisms are not well studied. In the third part of my study, I further investigated the role of the plant cuticle in basal defense and SAR by studying the long chain acyl-CoA synthetases (*LACS*) gene family which are involved in long chain FA and cuticle biosynthesis in plants.

CHAPTER TWO

MATERIALS AND METHODS

Plant growth conditions

Arabidopsis seeds were sown on bedding plant containers (Hummert International, USA) filled with commercial soil mixture (PROMIX, Premier Horticulture Inc, Canada), and subject to cold treatment at 4 ^{o}C overnight for synchronized germination. The next day, seeds were transferred to a MTPS 144 (Conviron, Canada) walk-in chamber. Two weeks after germination, the *Arabidopsis* seedlings were transplanted into individual pots (4 seedlings per pot), and the plants were grown at 22 ^{o}C, 65% relative humidity under fluorescent light illumination and a 14h light, 10h dark cycle. The photon flux density (PFD) of the light period was ~106 µmoles m^{-2} s^{-1} (measured by a digital light meter, Phytotronic Inc, USA). All experiments utilized four week-old *Arabidopsis* plants grown in the same conditions unless otherwise noted.

Mutant screening and genetic analysis

The seeds for single mutants (T-DNA insertion mutants) were obtained from ABRC. The genotypes used in this study are listed in Table 2.1. For genetic crosses, flowers from the recipient genotype were emasculated and pollinated with donor pollen. The wild-type (WT) and mutant alleles were identified by PCR, cleaved amplified polymorphic sequences (CAPS) (Konieczny and Ausubel, 1993), or derived (d)-CAPS (Neff et al., 1998) analysis. Homozygous T-DNA insertion lines were verified by sequencing PCR products obtained with primers specific for the T-DNA left border in combination with gene-specific primers. The primers used for genotyping are listed in Table 2.2. F2 plants showing WT genotype at mutant loci were used as controls in all experiments.

Generation of transgenic plants

Full-length *GLY1* cDNA was amplified as *NcoI*/*XbaI*-linked PCR products using specific primers (Forward: ATTACCATGGCGGCTTCGGTGCAACC, Reverse:

CGGGATCCTCATACTTCTTCAATCTGA) and cloned downstream of double 35S promoters in a pRTL2.GUS vector. For *Arabidopsis* transformation, the fragment containing the 35S promoter, *GLY1* cDNA, and the terminator was removed from pRTL2 vector and cloned into the *HindIII* site of the binary vector pBAR1. After confirmation by sequencing, the pBAR1-*GLY1* construct was transformed into *Agrobacterium tumefaciens* strain MP90 and transformed into Col-0 plants as described below.

Agrobacterium tumefaciens strain MP90 was cultured overnight (12-16 hours, 29 ^{o}C, 250 rpm) in 500 mL LB and the culture were centrifuged for 20 min at 6,000 rpm (GS-6R centrifuge, Beckman) to pellet cells. The pellet was dissolved into one liter transformation solution (one liter containing 2.15 g Murashige and Skoog basal salt mixture, 30 g sucrose, 0.5 mL of Silwett-77, adjusted to pH 5.7 with 1 M KOH). Plant transformation was carried out using the floral-dip method (Cloughand Bent, 1998). Briefly, the transformation solution was added to square containers (~500 mL) and the whole above-ground parts of plants (~ 4 week-old) were immersed (pot upside-down) into the solution. After 15-30 seconds, the pots were removed and the treated plants were placed under a transparent plastic dome for 12-24 h. Subsequently, the treated plants were transferred into growth chamber and were ready for seed collection in following 2-3 weeks. Transgenic seeds (F1) were selected for kanamycin resistance (seedlings grown on 50 ug/ml Kanamycin) or resistance to the herbicide BASTA sprayed on whole plants after germination.

Bacterial transformation

Both heat-shock and electroporation methods were used for bacterial transformation in this study. For preparing heat-shock competent cells, a single isolated colony of *Escherichia coli* strain DH5α (Invitrogen) was cultured overnight in 5 mL LB broth at 37 ^{o}C with shaking at 200 rpm. One mL inoculum from overnight-grown culture was added into 100 mL fresh LB broth, grown to an OD of 0.5 (A_{600}) and chilled on ice for 15 min. The cells were collected by centrifugation at 3000 rpm for 10 min at 4 ^{o}C, and the pellet was suspended in 50 mL ice-cold Tfb I buffer (30 mM KAc pH 5.8, 100 mM $RbCl_2$, 10 mM $CaCl_2$ and 15% glycerol). After 30 min on ice, the cells were centrifuged at 3000

rpm for 10 min and the pellet was re-suspended in 5 mL of ice-cold Tfb II buffer (10 mM MOPS pH 6.5, 75 mM $CaCl_2$ 10 mM $RbCl_2$, 15% glycerol). After 15 min on ice, the cells were dispensed as 100 µL aliquots in 1.5 mL microfuge tubes and stored at -80 ^oC until further use. For heat-shock transformation, ~50 ng of DNA was mixed with 100 µL of competent cells, incubated on ice for 30 min, followed by heat shock at 42 ^oC for 90 sec. The transformed cells were chilled on ice for 5 min, mixed with 1 mL of LB broth and incubated at 37 ^oC for 1 h. The transformed cells were spun down at 2000 rpm for 30 sec and then plated on LB agar plates containing appropriate antibiotic(s). The plates were incubated at 37 ^oC overnight and positive transformants were identified by colony PCR and confirmed by sequencing.

For preparing electroporation competent cells, a single isolated colony of *A. tumefaciens* strain MP90 or LBA4404 was cultured overnight in 5 mL LB broth at 29 ^oC. One milliliter inoculum from overnight-grown culture was added into 100 mL fresh LB broth, grown to an OD of 0.5 (A_{600}) and chilled on ice for 15 min. The cells were collected at 3000 rpm for 10 min at 4 ^oC, and the pellet was suspended in cold autoclaved 8.0% glycerol. The cells were dispensed as 20 µL aliquots in 1.5 mL microfuge tubes and stored at -80 ^oC till further use. For electroporation transformation, ~50 ng of DNA was mixed with 20 µL of competent cells, placed in a pre-cooled cuvette and given a pulse at 2500 volts (12.5 kV/cm). The suspension was transferred to a 1.5 mL microfuge tube containing 1 mL LB broth and incubated for 1 h at 29 ^oC. The treated cells were plated on LB agar plates containing appropriate antibiotic(s) and incubated overnight at 29 ^oC. The positive colonies were identified by colony PCR and confirmed by sequencing

Pathogen infection

Hyaloperonospora arabidopsidis

The asexual conidiospores of *H. arabidopsidis* were maintained on the susceptible host *Arabidopsis thaliana* ecotype Nossen (Nö) or Nö *NahG* (bacterial salicylate hydroxylase) (Shah et al., 2001). The spores were collected from infected leaves by agitation in sterile water and counted with a hemocytometer under a microscope (Olympus, USA). The final concentration of spore suspension was adjusted to 10^5 per mL. Two-week-old seedlings

were sprayed with spore suspension, covered with a transparent plastic dome and transferred to a MTR30 reach-in chamber (Conviron, Canada) maintained at 17 ^{o}C, 98% relative humidity and 8 h (light) 16 h (dark) cycle. Disease symptoms of inoculated plants were scored at ~14 dpi and the conidiophores were counted under the dissecting microscope. Each experiment was repeated at least three times.

Pseudomonas syringe pv. *tomato*

The *P. syringe* virulent strain DC3000 containing empty pVSP61 vector, and the avirulent derivatives *avrRpt2* (containing pVSP61-*avrRpt2*), *avrRps4* (containing pVSP61-*avrRps4*) or *avrRpm1* (containing pVSP61-*avrRpm1*) were cultured overnight in King's B broth containing 25 µg/mL rifampicin and 50 µg/mL kanamycin (Gold Biotechnology, USA). The bacterial cells were collected at 3000 rpm for 10 min, washed and re-suspended in 10 mM $MgCl_2$, quantified using a spectrophotometer (A_{600}) and diluted to a final density of 10^5 or 10^7/mL (as indicated for each experiment). The bacterial suspension was injected into the abaxial surface of the leaf using a 1 mL needle-less syringe. Mock control plants were injected with 10 mM $MgCl_2$. Four replicates (three leaf discs per replicate) from each inoculated genotype were collected at 0, 3 or 6 dpi. The leaf discs were homogenized in 10 mM $MgCl_2$ by blue pestle (Fisher Scientific, USA), diluted 10^3 or 10^4 fold and plated on King's B agar plates containing appropriate antibiotics. The plates were incubated at 29 ^{o}C for two days and colonies were counted using a Colony counter (Fisher Scientific). Each experiment was repeated at least three times.

Colletotrichum higginsianum

C. higginsianum Sacc. (IMI 349063) obtained from CABI Biosciences (Egham, Surrey, U.K.) was maintained on oat meal agar (Difco). The spores were harvested from two-week-old plates by agitating mycelia in sterile water followed by filtration through two layers of miracloth (Calbiochem, Gremany). The spores were washed once, collected by centrifugation at 3000 rpm for 10 min and re-suspended in sterile water. The spore concentration was determined using a hemocytometer under a microscope and diluted to 10^5 or 10^6 spores/mL for inoculation. The plants were inoculated by spray (50 mL per

tray) or spot method (10 μL spot/leaf). The inoculated plants were covered with a transparent plastic dome and transferred to a Conviron PGV36 walk-in chamber. Disease symptoms of inoculated plants were scored at 3-9 dpi. The disease severity of spray-inoculated leaves was assessed based on the amount of necrotic lesions present on the leaves. The lesion size on the spot-inoculated leaves was measured using a digital Vernier caliper (Fisher, USA). Each experiment was repeated at least three times.

Botrytis cinerea

The *B. cinerea* strain was kindly provided by Dr. Bart Thomma (Wageningen University, The Netherlands). The fungal strain was maintained as a silica stock and grown on V8 agar plates (one liter contained 200 mL V8 juice, 3 g $CaCO_3$, 15 g agar, pH 7.2) to generate inoculum. Sub-culturing was carried out every 2 weeks. A 5 × 5 mm agar cube was cut from the edge of a fungal colony, and put in the center of new V8 plates. Sub-culture only can be done 2-3 times through plates to plates, and then the new culture should start from stock. The conidia were harvested from two-week-old culture by agitating mycelia in sterile water followed by filtration through two layers of miracloth. The conidia were washed once at 3000 rpm for 10 min and re-suspended in sterile water. The conidia concentration was determined using a hemocytometer under a microscope and diluted to 2×10^5 or 10^6 per mL for inoculation. The plants were inoculated by spray (2×10^5 conidia per mL, 50 mL per tray) or spot method (10^6 conidia per mL, 10 μL spot/leaf). The inoculated plants were covered with a transparent plastic dome and transferred to a Conviron PGV36 walk-in chamber. Disease symptoms of inoculated plants were scored at 3-7 dpi. The disease severity of spray-inoculated leaves was assessed based on the amount of necrotic lesions present on the leaves. The lesion size on the spot-inoculated leaves was measured using a digital Vernier caliper. Each experiment was repeated at least three times.

Collection of phloem exudate

Leaf exudate was collected as described (Maldonado *et al.*, 2002). The plants were induced for SAR by inoculation with *P. syringe* virulent strain carrying pVSP61-*avrRpt2*

(10^6 CFU/mL). 12-24 h later, leaf petioles were excised, surface-sterilized in 50 % ethanol, and 0.0006 % bleach, rinsed in 1 mM EDTA and submerged in 2 mL 1 mM EDTA containing 100 µg/mL ampicillin. The phloem exudates were collected up to 48 h in growth chamber and then infiltrated into healthy wild-type plants and different mutant plants. Infiltrated leaves and systemic leaves were collected at 2 dpi for RNA extraction. For SAR analysis, *P. syringe* virulent strain DC3000 (10^5 CFU/mL) was inoculated in the systemic tissues 2 dpi after exudate infiltration.

Trypan blue staining

The samples (4-6 leaves per sample) were vacuum-infiltrated with trypan blue stain solution (10 mL acidic phenol, 10 mL glycerol, and 20 mL sterile water with 10 mg of trypan blue). Once the infiltration was completed, the samples were placed in a heated water bath (~90 ^oC) for 2 min and incubated at room temperature for 4-10 h. The samples were destained using chloral hydrate (25 g/10 mL sterile water; Sigma, USA) for 2-4 h on shaker, mounted on a glass slide with glycerol and observed for cell death under a compound microscope. The samples were photographed using an AxioCam camera (Zeiss, Germany) and images were analyzed using Openlab 3.5.2 software (Improvision).

Toluidine blue staining

Toluidine blue staining was carried out as described earlier (M. Bessire *et al.*, 2007). Leaves from 3-4 week-old plants were immersed in 0.05 % (w/v) toluidine blue (Sigma, USA) for 5-10 min and washed gently with water to remove excess stain.

Scanning electron microscopy (SEM)

For SEM analysis, both abaxial and adaxial surfaces of leave and stem samples were mounted on a sample holder with 12 mm conductive carbon tabs (Ted Pella Inc.), and sputter-coated with gold-palladium. The samples were observed on a Hitachi S-3200 SEM with and without backscatter detector at 5 and 20 kV.

Transmission electron microscopy (TEM)

For TEM analysis, leaves were cut into 3 mm × 3 mm sections and fixed with paraformaldehyde and embedded in epon-araldite. The samples were sectioned on a Reichert-Jung Ultracut E Microtome with a Diatome diamond knife and observed under a Philips Tecnai Biotwin 12 TEM.

Chlorophyll leaching and water loss assay

For chlorophyll leaching assay, 100 mg fresh leaves were gently agitated in 5 mL 80 % ethanol in dark at room temperature. The absorbance of each sample was measured at 664 and 647 wavelength on a spectrophotometer. The concentration of total chlorophyll per gram of fresh weight was determined by the formula: total chlorophyll = 7.93 (A_{664}) + 19.3 (A_{647}).

Glycerol, G3P, SA, BTH and JA treatments

Glycerol (50 mM; VWR), G3P (10 or 25 mM; Sigma), SA (500 μM, pH 7.0; Sigma) and BTH (100 μM; CIBA-GEIGY Ltd) were prepared in sterile water. JA (50 μM; Sigma) was first dissolved in 200 μL100% ethanol and then diluted in sterile water. MeJA (10%; Aldrich) was first dissolved in methanol and then diluted in sterile water. Glycerol, SA, BTH and JA were sprayed and only JA-treated plants were covered with a transparent plastic dome to maintain the humidity. G3P was injected into leaves with 1 mL needless syringe.

Hydrogen peroxide levels and paraquat treatment

For determination of hydrogen peroxide levels, 50 mg of leaf tissue was homogenized in 1 mL of Tris-HCl (40 mM pH 7.0). The samples were incubated for 1 h in dark after addition of 20 μM of 2', 7'-dichlorofluorescein and of 20 μg/ml horse radish peroxidase, followed by measurement of absorption at 488 nm (excitation) and 523 nm (emission). The levels of hydrogen peroxide were calculated as μmol/mg protein by extrapolating from a reference curve generated using known amounts of hydrogen peroxide. For paraquat treatments, paraquat was prepared in sterile water and leaves were spot-inoculated with 10 μL of 5, 10, 15, 25 or 50 μM solutions. Lesion sizes were measured at

48 h post paraquat application using Vernier calipers.

Fatty acid profiling

For FA profiling, leaves were placed in 2 mL of 3% H_2SO_4 in methanol containing 0.001% butylated hydroxytoluene (BHT). After 30 min incubation at 80 ^oC in a water bath, the samples were cooled for 5 min at room temperature in a chemical hood, and then 1 mL of hexane with 0.001% BHT was added. After vortexing briefly, the hexane phase was transferred to glass vials (National Scientific) for gas chromatography (GC) analysis (G1800B GCD system, HP). 1 µL samples were analyzed by GC on a Varian FAME 0.25 mm × 50 m column and quantified with flame ionization detection. The identities of the peaks were determined by comparing the retention time with known FA standards. Mole values were calculated by dividing peak area by molecular weight of the respective FA.

Lipid profiling

For total lipid extraction, 6 to 8 fresh leaves were kept at 75 ^oC in a water bath in isopropanol containing 0.01% BHT for 15 min. Next, 1.5 mL chloroform and 0.6 mL water were added and lipids were extracted by agitating the samples on a shaker for 1 h at room temperature. The lipids were re-extracted in chloroform: methanol (2:1) mixture for 2-5 times until the leaves were completely bleached. The aqueous content in the extraction was removed by partitioning with 1M KCl and water. The lipid extract (~ 20 mL) was completely dried under a gentle stream of nitrogen gas and re-dissolved in 0.5 mL chloroform in a glass vial. Lipid analysis and acyl group identification were carried out using the automated electrospray ionization-tandem mass spectrometry facility at the Kansas Lipidomics Research Center.

Extraction and quantification of salicylic acid and SAG

Salicylic acid (SA) and SAG were extracted from 300 mg of fresh leaves using anisic acid as internal standard. Samples were analyzed on an Agilent 1100 (Agilent Technologies, Palo Alto, CA, USA) with diode-array detector and fluorescence-array detector detection, using a Novapak C18 column (Waters, Milford, MA, USA). Sample

extraction and analysis was carried out in collaboration with Dr. Duroy Navarre (USDA-ARS, Prosser, Washington).

Extraction and quantification of jasmonic acid

For jasmonic acid (JA) extraction, fresh leaves (0.5 g to 1 g) were ground in liquid nitrogen and extracted in 100% methanol using dihydro-JA (DJA; Sigma) as internal standard. The extract was acidified to pH $\leq$ 4 with 1M HCl and passed through tC-18 Sep-Pak columns (Waters: 500mg: 3mL) which were pre-equilibrated with 75% methanol containing 0.2% acetic acid. The column-purified extract was saturated with sodium chloride and re-extracted in diethyl ether. The ether extract was completely dried under a gentle stream of nitrogen gas and methylated using diazomethane. The oxylipins were solublized in 0.5 mL hexane and dried to 10 µL under a gentle stream of nitrogen gas. Sample (1 µL) was injected into GC attached to Electron Ionization Detector (Hewlett Packard, GCD Systems). The JA peaks were identified by mass spectrometric (MS) analysis. The peak area and the ratio between JA/DJA were used to calculate the amount of JA in the samples and expressed as nmol/g FW.

Extraction and quantification of camalexin

For camalexin estimations, 100 mg of fresh leaf tissue was incubated in 400 mL of 80% methanol at 80 ^{o}C in a water bath for 20 min. The extract was concentrated to 75 mL under a gentle stream of nitrogen gas followed by addition of 75 mL of chloroform. The samples were vortexed, centrifuged at 3000 rpm for 10 min and dried under a gentle stream of nitrogen gas. The dried samples were re-dissolved in 50 µL chloroform and spotted on silica gel-TLC plate (Whatman; 60A^{o}, 20 x 20 cm, 250 mM thickness). The chromatogram was developed using 100 mL ethyl acetate: hexane (100:15) solvent system and the camalexin was visualized as blue spots under ultra-violet light. The camalexin spots were removed from the TLC plate, extracted in methanol and the fluorescence was measured using a fluorimeter (315 nm excitation and 385 nm emission wavelengths) (SPECTRA max2, Molecular Devices, USA). The concentrations of camalexin were determined as ng/g FW by extrapolating from a reference curve generated using known amounts of commercially available camalexin.

Extraction and quantification of glycerol-3-phosphate

For extraction of glycerol-3-phosphate (G3P), 300 mg of fresh leaf tissue was ground in 80% ethanol using 2-deoxyglucose (Sigma, USA) as internal standard. The extract was boiled for 5 min in a water bath, cooled on ice and centrifuged at 6000 rpm for 10 min to remove the plant debris. The supernatant was completely freeze-dried and rehydrated in 1 mL sterile water. Then the extract was purified by passing through 0.45µ Nylon columns (Corning Inc., USA). The extracts were run on PA1 columns and ion chromatography (ICS-3000, Dionex Inc., USA) was conducted. The quantification of G3P was based on the peak areas of standard G3P sample (Sigma, USA) and internal standard 2-deoxyglucose.

Wax component analysis

About 500 mg fresh rosette leaves of 4-week-old plants were taken and immediately immersed in 10 mL chloroform for 10 sec at room temperature. The chloroform was transferred to another glass tube and the leaves were again extracted with 10 mL chloroform for 10 sec. The combined chloroform extract (total 20 ml) was amended with 20 µg of tetracosane (c24) as an internal standard. The solvent in the extract was evaporated to about 1 mL under a stream of nitrogen and transferred into a 2 mL glass vial. When the extract was dried completely with the nitrogen gas, about 10 drops of diazomethane was added and then vortexed to methylate the free FAs. Once the diazomethane was evaporated, 100 µL of pyridine and 100 µL of acetic anhydride were added into the vial and the extract was kept at 60 °C for 1 h. The extract was completely dried again under a stream of nitrogen gas and re-dissolved in 0.5 ml of heptane: toluene (1:1. v/v). The extract was washed with 400 µ1 of 1% $NaHCO_3$ and 1 µL of the extract was injected for GC analysis.

Cutin monomer analysis

For cutin monomer analysis, fresh leaf or stem tissue was quenched in 100 mL of 80 °C isopronanol for 10 min. The tissues were finely ground with a Polytron and incubated overnight in isopropanol in a 250 mL glass flask at room temperature and agitated at 180 rpm on a rotary shaker. The extract was filtered and the insoluble reside was re-extracted

by shaking overnight with 100 mL of chloroform: methanol (2:1 v/v). The extract was filtered again and re-extracted with 100 mL of chloroform: methanol (1:2 v/v). The residue was air-dried for two days and then dried under vacuum for two more days. The dried residue (~ 0.2 g) was heated at 60 °C with stirring in 8 mL of methanol containing 7.5% (v/v) methyl acetate and 4.5% sodium methoxide (w/v), and methyl-heptadecanoate and pentadecalactone were added as internal standards (1 mg/g dried residue). After 24 h, to acidify the extract, 2 mL glacial acetic acid followed by 8 mL of water were added. The monomer products were extracted into methylene dichloride (10 mL) and the organic phase was washed three times with 0.9% KCl. The organic phase was dried over anhydrous sodium sulfate under nitrogen gas, and was re-dissolved in 0.1 mL of pyridine and 0.1 mL of acetic anhydride and heated at 60 °C for 60 min. The extract was dried again under nitrogen gas and re-dissolved in 0.5 mL of heptane: toluene (1:1. v/v). Finally, the extract was washed with an equal volume of 1% $NaHCO_3$ and 1 µL of the extract was injected for GC analysis.

DNA extraction

Small-scale DNA extraction was carried out from a single *Arabidopsis* leaf. Leaf samples were frozen in liquid nitrogen and ground with disposable pestle (Fisher Scientific, USA). The extract was suspended in 150 µL of DNA extraction buffer containing 200 mM Tris, 25 mM EDTA, 1% SDS and 250 mM NaCl. The homogenate was mixed with 75 µL of phenol: chloroform: isoamyl alcohol (25:24:1) and centrifuged for 10 min at 12,000 rpm. The supernatant was transferred and precipitated with 100 µL of isopropanol and centrifuged for 10 min at 12,000 rpm. The DNA pellet was air-dried and re-suspended in 30-60 µL of sterile water or Tris:EDTA (10:1 pH 8.0) buffer.

RNA extraction

RNA extraction was carried out using Trizol reagent (Invitrogen, USA). About 100 mg samples of *Arabidopsis* leaves were collected in 1.5 mL eppendorf tubes and frozen in liquid nitrogen, ground with disposable pestles and each was suspended in 1 mL of Trizol. The homogenates were each mixed ewith 200 µL of chloroform and the samples were centrifuged at 12,000 rpm for 12 min. Each supernatant was transferred into a new

eppendorf tube and precipitated with 0.5 mL of isopropanol for 1 h at room temperature and then centrifuged at 12,000 rpm for 12 min. Each RNA precipitate was washed once with 75% alcohol, air-dried and re-suspended in 30-40 µL of DEPC-treated water.

Reverse transcriptase-polymerase chain reaction (RT-PCR)

For cDNA synthesis, 5 µg total RNA was denatured at 65 ^{o}C in a water bath and annealed to 1 µL oligo dT_{17} (0.5 µg/µL). The reaction mixture was supplemented with 1 µL reverse transcriptase (200 U/µL, Invitrogen, USA), 1 µL RNAase inhibitor (40U/µL, Invitrogen, USA), 1 µL 10 mM dNTPs and 2 µL 100 mM DTT and incubated at 42 ^{o}C in a water bath for 1 h. The reaction was stopped by incubating the tube at 65 ^{o}C for 15 min and subsequently used for RT-PCR.

Northern blot analysis

The RNA was quantified by a spectrophotomer (A_{260}) and 7 µg of total RNA was electrophoresed on 1.5% agarose gel containing 3% formaldehyde and 1 × MOPS. The MOPS buffer was prepared by mixing 4.18 g MOPS, 680 mg NaOAc, 37 mg EDTA in 1 L sterile water and adjusted to pH 7.0. Before loading, RNA was mixed with 16 µL denature mixture (1 mg/mL ethidium bromide, 0.39 × MOPS, 13.7% formaldehyde and 39% formamide), denatured at 65 ^{o}C for 15 min, chilled on ice for 5 min and mixed with 2 µL of RNA loading dye (50% glycerol, 1mM EDTA, 0.4% bromophenol blue and 0.4% xylene cyanol).

For northern blot analysis, RNA was transferred onto Hybond-NX (GE Healthcare) nylon membrane. After overnight capillary transfer, RNA was cross-linked fixed under UV for 0.9 min in a CL-1000 ultraviolet Cross-linker (UVP). The membrane was washed in 2 × SSC for 30 min, dried at 65 ^{o}C for 10 min and used for hybridization. The membrane was hybridized in sodium phosphate buffer (pH 7.0) containing sheared salmon sperm DNA (100 µg/mL), 7% SDS and 1.25 mM EDTA.

For probe synthesis, the DNA fragment was amplified from wild-type plant cDNA with specific primers and confirmed by sequencing. The gel-purified DNA fragment was

denatured at 90 ^{o}C in a water bath for 5 min , immediately chilled on ice for 5 min and mixed well with 1 μL Klenow enzyme (NEB, 2000 U/mL), 2 μL 10 × BSA and 10 μL labeling mixture (containing hexanucleotide primers, dATP, dGTP, dTTP) and 25 μCi α-^{32}P-dCTP (Perkin Elmer, USA). The reaction was incubated at 37 ^{o}C for 1 h and purified by MicroSpin G-50 Sephadex column (GE Healthcare). The labeled DNA fragment was denatured by 14 μL 2N NaOH for 15 min, neutralized with 1M Tris pH 7.5 for 15 min and added to the hybridization buffer. Hybridization was routinely carried out overnight at 60 ^{o}C in hybridization oven (Labnet International Inc.). The hybridized membrane was washed twice at 60 ^{o}C with 2 × SSC, 0.5% SDS and once at 60 ^{o}C with 1 × SSC, 0.1% SDS solutions. The membrane was exposed to a Storage Phosphor Screen (Amersham Biosciences) overnight and scanned on a Typhoon 9400 Variable Mode Imager (GE Healthcare). The signal intensity was quantified by ImageQuant TL V2005 software.

Transcriptional profiling

Total RNA was isolated from four-week-old plants using TRIzol as described above. The experiment was carried out in triplicate and a separate group of plants was used for each set. RNA was processed and hybridized to the Affymetrix Arabidopsis ATH1 genome array GeneChip following the manufacturer's instructions. All probe sets on the Genechips were assigned hybridization signal above background using Affymetrix Expression Console Software v1.0. A one-way ANOVA test, followed by post hoc two sample *t*-tests was used to analyze the data. The *P* values were calculated individually and in pair-wise combination for each probe set. The identities of the *WRKY* genes were obtained from the Arabidopsis information resource (www.arabidopsis.org).

Sequencing

The sequencing reaction was carried out in 10 μL total volume containing 100-200 ng of PCR products or gel-purified DNA (Qiagen, CA, USA), 3 μL of 5 μM sequencing primer, 0.5 μL of Big Dye and 2 μL 5 × sequencing buffer (Applied Biosystems, UK). The reaction product was precipitated with 2 μL 3 M NaOAc, 2 μL 125 mM EDTA and 50 μL 100% ethanol, washed with 300 μL 70% alcohol and air-dried before submitting to

sequencing facility at the Advanced Genetic Technologies Center (AGTC), University of Kentucky.

Protein extraction

For total protein, 50-200 mg fresh plant tissues were thoroughly ground with liquid nitrogen and 1-2 mL protein extraction buffer (50 mM Tris-Cl, pH 7.5, 150 mM NaCl, 1 mM EDTA, 10% glycerol, 5 mM DTT, 0.5% Triton-X-100, and 1 × protease inhibitor cocktail). The extract was centrifuged at 12,000 rpm for 15 min at 4 ^{o}C, and the supernatant was transferred to a new 1.5 mL eppendorf tube. The protein concentration was determined by using the Bio-Rad protein assay kit.

For membrane fractionation extraction, tissues were ground in liquid nitrogen and suspended in extraction buffer (50 mM Tris-MES, pH 8.0, 0.5 M sucrose, 1 mM $MgCl_2$, 10 mM EDTA, 10 mM EGTA, 10 mM asocorbic acid, 5 mM DTT, 1 × protease inhibitor cocktail) (Sigma-Aldrich, USA). All fractionation steps were carried out at 4 ^{o}C. The total extract (T) was centrifuged at 10, 000 × g for 10 min. The supernatant (S) was centrifuged again at 125, 000 × g (45,000 rpm) for 1 h to remove any insoluble material. The pellet (membrane fraction) was re-suspended in a detergent-free buffer (5 mM potassium phosphate, pH 7.8, 2 mM DTT, 1 × protease inhibitor cocktail).

Western blot analysis

For running SDS-PAGE gel, 10 μg protein samples were mixed with 3 × loading buffer (3.0 mL H_2O, 1.2 mL 1 M Tris-HCl pH 6.8, 2.4 mL glycerol, 0.48 SDS, 60 μL 10% bromophenol blue. and 1.5 mL β–mercaptoethanol) and the samples were boiled at 100ºC for 5 min. The samples were run on a SDS-PAGE minigel (6 × 9 cm) at 100 V in 1 × running buffer (14.4 g glycine, 3 g Tris-base, 1 L H_2O) until the bromophenol blue reached the bottom of the gel.

For protein transferring, PVDF membrane (Immun-Blot, Bio-Rad) was pre-wet in methanol and other materials were pre-wet in 1 × transferring buffer (3.2 g Tris-base, 15 g glycine, 1 L H_2O), and the materials were stacked in the transferring case (following the order: sponge, Whatman paper, membrane, protein gel, Whatman paper, sponge). The

protein gel was transferred at 400 A for 1 h on ice with the Bio-Rad mini-gel box electro-transfer. After transferring, PVDF membranes were stained in Ponceau-S solution (40% methanol, 15% acetic acid, 0.25% Ponceau-S). The membranes were distained by rinsing in deionized water for 2-4 times.

For western blotting analysis, the membrane was first blocked in 10 mL 5% non-fat dry milk dissolved in 1 × TBST buffer (5 mM Tris-base, 20 mM NaCl, pH 7.4, 0.1% Tween 20) for 1 h on a shaker. After blocking, the primary antibody was added into fresh 10 mL 5% non-fat dry milk dissolved in 1 × TBST buffer and incubated on a shaker for 2-4 h. The membrane was washed three times for 15 min with 1 × TBST buffer, and then the secondary antibody (HRP-conjugated, Sigma) was added and incubated on a shaker for 2-4 h. The membrane was washed for three times, developed with ECL kit (1 mL/membrane) (Super-Signal, Thermo Scientific) and exposed to autoradiography film (Santa Cruz Biotechnology, USA).

Agrobacterium-mediated transient expression

For transient gene expression analysis, *A. tumefaciens* strain LBA4404 carrying pGWB or pSITE vector integrated with target gene was grown overnight at 29 ^{o}C on LB broth containing appropriate antibiotics. The *A. tumefaciens* cells were collected at 3,000 rpm for 10 min and re-suspended in induction buffer (10 mM MES, pH 5.6, 10 mM MgCl2, and 150 μM acetosyringone) and incubated at room temperature for 3 h prior to infiltration into *Nicotiana benthamiana* leaves. The *N. benthamiana* plants were transferred into a growth chamber and the samples were collected 12-48 h post infiltration.

Protein localization and Bi-molecular fluorescence (Bi-FC) assays

For determining protein localization, to tag the target protein with green fluorescent protein (GFP) or red fluorescent protein (RFP), the proteins were fused into pSITE-3CA-GFP or pSITE-3CA-RFP vectors and the constructs were transformed into *A. tumefaciences* strain LBA4404. *Agrobacterium* strains carrying various tagged proteins were infiltrated into wild-type *N. benthamiana* plants or GFP-tagged endoplasmic

reticulum (ER) or RFP-tagged ER transgenic plants. After 24 h or 48 h, water-mounted sections of leaf tissues (~ 5 mm × 5 mm) were scanned with an Olympus FV 1000 microscope (Olympus America) equipped with a water immersion PLAPO60XWLSM 2 (NA 1.0) objective and lasers spanning the spectral range of 405-633 nm. The software Olympus FLUOVIEW 1.5 was used to operate the confocal microscope, acquire images and export TIFF files.

For Bimolecular fluorescence (Bi-FC) assays, the various target proteins were fused to the N/C-terminal halves of E-yellow fluorescent protein (YFP) (nEYFP/cEYFP) in the pSITE-3CA-EYFP vectors. The various constructs were transformed into *A. tumefaciences* LBA4404 strain. To check the protein-protein interaction, *Agrobacterium* strains carrying various proteins were infiltrated in pair into wild-type *N. benthamiana* plants or CFP-H2B-tagged *N. benthamina* transgenic plants expressing nuclear-localized CFP. The water-mounted sections of leaf tissues were examined by confocal microscopy 48 h later. The CFP and YFP overlay images or GFP and RFP overlay images (40 ×) were acquired at a scan rate of 10 ms/pixel.

Table 2.1. Seed materials used in the study.

Sl No.	Mutants and transgenic seeds	References
1	Columbia-0 (Col-0)	Kachroo et al. (2003)
2	Nossen (Nö)	Kachroo et al. (2001)
3	Landsberg *erecta* (L*er*)	Aarts et al. (1998)
4	Wassilewskija (Ws-0)	Aarts et al. (1998)
5	Dijon (Di-17)	Kachroo et al. (2000)
6	*gly1-1*	Miquel (1998), Kachroo et al. (2004)
7	*act1*	Kunst et al. (1988), Kachroo et al. (2003)
8	*gli1* (*nho1*)	Kang et al. (2003), Kachroo et al. (2005)
9	35S-*GLI1*	Kang et al. (2003)
10	35S-*GLY1*	Chanda et al. (2008)
11	*ssi2*	Kachroo et al. (2001)
12	*eds1-1*	Parker et al. (1996)
13	*eds1-2*	Aarts et al. (1998)
14	*eds5-1*	Nawrath et al. (2002)
15	*pad4-1*	Jirage et al. (1999)
16	*sid2-1*	Wildermuth et al. (2001)
17	Nö-*nahG*	Yamamotoj et al. (1965)
18	*npr1-1*	Cao et al. (1997)
19	*npr1-5*	Shah et al. (1997)
20	*fab2*	Lightner et al. (1994), Kachroo et al. (2001)
21	*pad3*	Glazebrook and Ausubel (1994)
22	*etr1-1*	Chang et al. (1993)
23	*jar1*	Staswick et al. (1992)
24	*coi1*	Xie et al. (1998)
25	*wrky25*	Present work
26	*wrky46*	Present work
27	*wrky50*	Present work
28	*wrky51*	Present work
29	*wrky53*	Present work
30	*wrky60*	Present work
31	*wrky70*	Present work
32	*lacs1*	Present work
33	*lacs2-1*	Present work
34	*lacs2-3*	Present work
35	*lacs3*	Present work
36	*lacs*4	Present work
37	*lacs*6	Present work
38	*lacs*7	Present work
39	*lacs*8	Present work
40	*lacs*9	Present work
41	*acp4*	Present work

Table 2.1 continued

43	*ssi2 act1*	Kachroo et al. (2003b)
44	*ssi2 sid2*	Kachroo et al. (2005)
45	*ssi2 nahG*	Shah et al. (2001)
46	*ssi2 eds1-2*	Kachroo et al. (2005)
47	*ssi2 eds5-1*	Kachroo et al. (2005)
48	*ssi2 pad4*	Kachroo et al. (2005)
49	*eds1-1 sid2*	Present work
50	*pad3 act1*	Present work
51	*sid2 act1*	Present work
52	*gly1 gli1*	Present work
53	*gli1* 35S-*GLY1*	Present work
54	*gly1 act1*	Present work
55	*gli1 act1*	Present work
56	*wrky50 wrky51*	Present work
57	*ssi2 wrky50*	Present work
58	*ssi2 wrky51*	Present work
59	*ssi2 wrky46*	Present work
60	*ssi2 wrky53*	Present work
61	*ssi2 wrky60*	Present work
62	*ssi2 wrky70*	Present work
63	*lacs*1 *lacs*7	Present work
64	*lacs*7 *lacs*8	Present work
65	*ssi2 eds1-1 sid2*	Present work
66	*ssi2 eds1-2 sid2*	Present work
67	*ssi2 eds5 sid2*	Present work
68	*ssi2 wrky50 wrky51*	Present work
69	*ssi2 wrky50 wrky51*	Present work

Table 2.2. List of primers used in this study. The name, sequence and the purpose for which the primers were used are listed. The enzymes used for dCAPS or CAPS markers are mentioned in parenthesis.

Name	Primer	Purpose (enzyme)
ssi2	TTG GTG GGG GAC ATG ATC ACA GAA GA AAG TAG GAC TAG CAC CTG TTT CAT CC	dCAPS (Nsi I)
fab2	CCA ATC AAG TAC TGA ATG GTC TTG GCA ACC CCA GGA TTT CTT	CAPS (Sau96A I)
gly1-1	AAC CGA TGT TCT TGA GCG TAC TCG CCAG CAA CAA CCT AAA AAC CCC CAG ATT C	dCAPS (BstN I)
gly1-3	GGT CTG GAG CTT AAT ACT CTT AAG AGT ATT AAG CTC CAG ACC	CAPS (Bcc I)
eds1-1	CGA GGT GCT CGG TTT ATT G AAA TGT CGA TGG TAG TTT GC	dCAPS (Mse I)
pad4-1	ACC GAG GAA CAT CAG AGG TAC AAA TTC GCA ATG TCG AGT GGC	CAPS (BsmF I)
eds5-1	CAA ATC AAC ATT TGT TTC CTG TGT TTT TG CAT GAA GAA AGG TAT AAG CAG TCT ATG GAT	dCAPS (Sau3A I)
sid2-1	CTG TTG CAG TCC GAA AGA CGA CTA GAG CTG ATC TGA TCC CGA	CAPS (Mfe I)
Actin	CAC TGT GCC AAT CTA CGA GGG TT ACA ATTT TCC CGC TCT GCT GTT GTG	q-RT-PCR
β-tubulin	CGT GGA TCA CAG CAA TAC AGA GCC CCT CCT GCA CTT CCA CTT CGT CTT C	RT-PCR
gli1	CAG AGA GAG ACT ACT GTT GTT TGG A CTG CAG ATG GAG CTG GTA CGA GCA TC	dCAPS (BStN I)
act1	GCC ATC AAG TGT TCA TCT ACT GGA AGT CAT ACA AGG TTG CTA	CAPS (BsmF I)
coi1	GGT TCT CTT TAG TCT TTA C CAG ACA ACT ATT TCG TTA CC	CAPS (Xcm I)
pad3	GCT TCC CAT CAT CGG AAA CTT TAG AGA TTT ATC CCG TAC CCG	CAPS (Hind III)
npr1-5	GAG GAC ACA TTG GTT TATA CTC CAA GAT CGA GCA GCG TCA TCT TC	CAPS (Nla IV)
eds1-2	ACA CAA GGG TGA TGC GAG ACA GTG GAA ACC AAA TTT GAC ATT AG	Genotyping
nahG	GGC TTG CGC ATC CGT ATC GTC GGC GCC ATG GGC CCG ATA GGC TTC TCG	Genotyping
NPT (Kan)	CAA GAT GGA TTG CAC GCA GGT GCT CTT CAG CAA TAT CAC GGG	Genotyping (detect the presence of binary vector containing kanamycin)

Table 2.2 continued

HPT (Hyg)	ACC TAT TGC ATC TCC CGC CGT CCG GAT GCC TCC GCT CGA AGT	Genotyping (detect the presence of binary vector containing hygromycin)
GLY1	ATT ACC ATG GCG GCT TCG GTG CAA CC CGG GAT CCT CAT ACT TCT TCA ATC TGA	Genotyping
PDF1.2	AAT GAG CTC TCA TGG CTA AGT TTG CT AAT CCA TGG AAT ACA CAC GAT TTA GC	PCR
GK	ATG GCA AAA GAA AAT GGA TTT TTA GAT AGA GAG GTC AGC GAG	PCR
SSI4	CTC AAG AGA GTA TGC TTC TCT TTC- CAT AAC CC CTG GTT TGG TCT TCA TGA GAC TCC ATGAG	RT-PCR
RPS2	ATG GAT TTC ATC TCA TCT CTT TAT AAT CTC CGC GAG CCG GCG	RT-PCR
RPS4	ATG GAG ACA TCA TCT ATT TCC ACT G AAT TCC GGG CAT CCC AAC AAC TCC A	RT-PCR
RPM1	GCA TAC ATG GGA CCT AGG TTG CGT TTT GCACAA GG GCC TTG GCC GCC TAA GAT GAG AGG CTC AC	RT-PCR
SNC1	ATG GAG ATA GCT TCT TCT TCT ATC AGG TGG AGA GTC TTT CCC	RT-PCR
EDS1	CCG CTC GAG ATG GCG TTT GAA GCT CTT ACC GTA GTC TAG ATC AGG TAT CTG TTA TTT CAT CC	RT-PCR
EDS5	CAA AAC AAG ACG GAT CCC GGT CAG AGA TTT GAT GTT GCG CTT C	RT-PCR
G3PdH	ATT ACC ATG GCG GCT TCG GTG CAA CC CGG GAT CCT CAT ACT TCT TCA ATC TGA	RT-PCR
GK	ATG GCA AAA GAA AAT GGA TTT TTA GAT AGA GAG GTC AGC GAG	RT-PCR

CHAPTER THREE

REPRESSION OF JASMONIC ACID-INDUCIBLE DEFENSE RESPONSES REQUIRES THE WRKY50 AND WRKY51 PROTEINS [Ψ]

[Ψ] The results shown in this chapter were published in the following journal:

1. Qing-Ming Gao, Srivathsa Venugopal, Duroy Navarre, and Aardra Kachroo. (2010). Repression of jasmonic acid-inducible defense responses requires the *WRKY*50 and *WRKY*51 proteins. Plant Physiol 155:464-476. www.plantphysiol.org, "Copyright American Society of Plant Biologists"

INTRODUCTION

Plants, like animals, have evolved to develop immunity against a wide variety of microbial pathogens, including basal immunity against virulent pathogens, resistance (R) protein-mediated immunity against species-specific pathogens, and systemic immunity against secondary pathogens. R-mediated signaling is well known to induce a very rapid and efficient immune response and is often associated with the development of a hypersensitive reaction (HR), a form of programmed cell death, at the site of pathogen entry (Dangl *et al*., 1996). The resulting necrotic lesions are one of the first visible manifestations of pathogen-induced defense responses and are thought to aid the confinement of the pathogen to the dead cells.

Downstream signaling induced in response to *R* gene activation is commonly mediated by one or more phytohormones. Of these, defense signaling mediated by salicylic acid (SA) and jasmonic acid (JA) have been widely studied. The two phytohormones frequently act antagonistically to mediate defense against specific types of pathogens (Kunkel and Brooks, 2002; Glazebrook et al., 2005; Koornneef and Pieterse, 2008; Spoel and Dong, 2008). For example, accumulation of SA antagonizes JA-mediated responses (Doherty et al., 1988; Peña-Cortés et al., 1993; Gupta et al., 2000; Spoel et al., 2003). Infection with virulent *Pseudomonas syringae* induces SA-derived signaling and enhances susceptibility to *Alternaria brassicicola* by inhibiting JA-mediated defense responses in *Arabidopsis* (Spoel et al., 2007). Conversely, JA-derived signaling antagonizes SA-mediated responses, such as the suppression of host SA-derived responses by the bacterial phytotoxin coronatine, a structural analogue of JA (Zhao et al., 2003; Brooks et al., 2005; Cui et al., 2005). Characterization of mutants affected simultaneously in both pathways has led to the identification of several molecular components that mediate cross-talk between SA- and JA-derived signaling pathways (Petersen et al., 2000; Spoel et al., 2003, Li et al., 2004, Kachroo et al., 2007a).

The Arabidopsis mutant, *ssi2* (suppressor of SA insensitive 2) is one such mutant that is affected in both SA- and JA-derived signaling (Kachroo et al., 2001). *SSI2* encodes a

plastid-localized stearoyl-acyl carrier protein desaturase (SACPD) that desaturates stearic acid to oleic acid (18:1) in the plant chloroplast. The *ssi2* mutant plants are stunted in size, exhibit HR-like cell death lesions on their leaves, accumulate high levels of SA, and overexpress pathogenesis-related (*PR*) genes. Consequently, these plants exhibit enhanced resistance to bacterial and oomycete pathogens (Kachroo et al., 2001, 2003, 2004 & 2005). In contrast to the upregulation of the SA pathway, *ssi2* mutant plants are defective in JA-mediated defense responses. Although, *ssi2* plants are not altered in the perception or biosynthesis of JA, these plants are unable to induce defensin (*PDF1.2*) expression in response to JA. Consequently, these plants are hypersusceptible to necrotrophic pathogens such as *Botrytis cinerea* (Kachroo et al., 2001). Lowering the levels of SA via expression of a bacterial SA hydroxylase does not restore JA-derived responses in *ssi2* plants, indicating that high SA alone is not responsible for the non-induction of JA-responsive defenses in these plants (Kachroo et al., 2001). Characterization of *ssi2* suppressors has shown that the altered defense-related phenotypes of *ssi2* are the result of reduction in 18:1 levels (Kachroo et al., 2003, 2004, 2005, 2007b, Chandra-Shekara et al., 2007; Xia et al., 2009). Furthermore, this ability to induce altered defense responses upon reduction in 18:1 levels is conserved amongst diverse plants, including soybean and rice (Kachroo et al., 2008; Jiang et al., 2009). A large majority of the *ssi2* suppressors restore 18:1 levels in *ssi2* plants resulting in the normalization of both SA- and JA-mediated signaling (Kachroo et al., 2003, 2004, 2007b, Xia et al., 2009).

The *ssi2*-related defense phenotypes can also be induced in wild-type plants by exogenous application of glycerol. Exogenous glycerol is metabolized to glycerol-3-phosphate (G3P), which serves as a substrate for the *ACT1*-encoded G3P acyltransferase. Increased G3P levels promote the ACT1-catalyzed acylation of 18:1 onto the G3P backbone, thereby lowering 18:1 levels. This, in turn, induces defense responses resulting in cell death, *PR-1* expression, SA accumulation, and enhanced resistance to bacterial and oomycee pathogens (Kachroo et al., 2003, 2004, 2005, 2007b; Chandra-Shekara et al., 2007). The glycerol-derived effect is specific because a mutation in *ACT1* renders plants non-responsive to glycerol; *act1* mutant plants are unable to acylate G3P and therefore

unable to deplete 18:1 in response to glycerol.

Signaling induced in response to SA and JA is often mediated by defense-related transcription factors including those belonging to the WRKY family of proteins (Eulgem and Somssich, 2007). For example, the WRKY25 protein negatively regulates SA-responsive *PR-1* expression and resistance to *P. syringae* (Zheng et al., 2007), whereas WRKY33 positively regulates JA-inducible *PDF1.2* expression (Zheng et al., 2006). Overexpression of WRKY33 enhances resistance to necrotrophic fungi but increases susceptibility to *P. syringae*. Several WRKY proteins are also involved in SA-JA cross-talk, such as WRKY62, which likely participates in the SA-derived suppression of JA responses (Mao et al., 2007). The WRKY70 protein suppresses the expression of JA-responsive genes. Furthermore, expression of the *WRKY70* transcript is upregulated by SA and downregulated by JA, indicating that WRKY70 may be involved in integrating SA- and JA-derived signaling pathways (Li et al., 2004). Likewise, WRKY41 may also be involved in cross-talk between the SA- and JA-derived pathways, since overexpression of *WRKY41* simultaneously induces *PR-5* expression and suppresses JA-responsive *PDF1.2* expression (Higashi et al., 2008).

The Arabidopsis genome contains 74 *WRKY* genes and several of these are induced in response to pathogen infection and/or exogenous application of SA (Dong et al., 2003). Here, I examined the involvement of WRKY proteins in mediating the altered SA- and JA-derived responses in *ssi2* plants was examined. Genome-wide transcriptional profiling showed that several *WRKY* genes were induced in the low 18:1-containing *ssi2* plants. Second-site mutations in two of these (*WRKY50* and *WRKY51*) restored JA-inducible *PDF1.2* expression and basal resistance to *B. cinerea* in the *ssi2* plants, suggesting that WRKY50 and WRKY51 might serve as positive regulators of SA-mediated signaling, but negative regulators of JA-mediated signaling.

RESULTS

A second-site mutation in *WRKY70* does not alter *ssi2*-related phenotypes

The well-characterized role of WRKY70 in mediating SA-JA cross-talk, together with the fact that *ssi2* plants are impaired in JA-derived defense signaling, prompted this investigation the role of WRKY70 in *ssi2*-mediated signaling. Since the *WRKY70* transcript is SA-inducible (Li et al., 2004), the levels of *WRKY70* expression between wild-type and *ssi2* mutant plants were first compared. Northern blot analysis showed that *WRKY70* transcription was, indeed, induced in *ssi2* (high SA) compared to wild-type plants (Figure 3.1A). Interestingly, compared to wild-type plants, *WRKY70* was also induced in *ssi2 sid2* plants, which contain basal levels of SA due to a mutation in the *SID2*-encoded isochorishmate synthase (Wildermuth et al., 2001). This indicated that induction of the *WRKY70* transcript in *ssi2* plants was regulated in an SA-independent manner. To test the role of *WRKY70* in *ssi2*-derived defense signaling, I isolated a knockout (KO) mutation in this gene. Lines carrying T-DNA insertion in *WRKY70* were screened for homozygous insertion mutants (Table 3.1). RT-PCR analysis of cDNA from the *wrky70* line did not detect any *WRKY70* transcript, confirming the presence of a KO mutation in this gene (Figure 3.2). The *wrky70* mutant plants, which were morphologically similar to wild-type plants (data not shown), were then crossed with *ssi2* plants. The *ssi2 wrky70* double-mutant plants segregated in a Mendelian double recessive manner. Consistent with their segregation, the *ssi2 wrky70* plants showed *ssi2*-like phenotypes (Figure 3.1B); the *ssi2 wrky70* plants were stunted in morphology, showed HR-like cell death on their leaves, and constitutively expressed high levels of the *PR-1* gene (Figure 3.1C). Consistent with their phenotypes, *ssi2 wrky70* double-mutant plants showed *ssi2*-like 18:1 levels (Table 3.2).

To determine if the *wrky70* mutation restored JA-responsive *PDF1.2* expression in *ssi2* plants, I applied exogenous JA to wild-type, *ssi2*, *wrky70* and *ssi2 wrky70* plants. As expected, *PDF1.2* induction was detected in wild-type and *wrky70* plants, but not in the *ssi2* or *ssi2 wrky70* plants (Figure 3.1D). Together, these results indicate that absence of *WRKY70* does not restore the altered SA-/JA-derived defense signaling in *ssi2* plants.

Reduction in 18:1 levels induces the expression of several *WRKY* genes

Next, I used two parallel approaches to identify other *WRKY* genes that might regulate the altered SA- and/or JA-derived signaling in *ssi2* plants. These included genome-wide transcriptional profiling of *WRKY* genes between wild-type and *ssi2* plants and expression analysis of known *WRKY* transcription factors that participate in cross-talk between SA and JA pathways. Genome-wide transcriptional profiling was carried out using Affymetrix ATH1 GeneChip arrays. Using this analysis, seventeen *WRKY* genes (including *WRKY70*) were found to be induced in *ssi2* plants, but only three of these were also induced in *ssi2 sid2* plants (Table 3.3). Strikingly, several *WRKY* genes, including *WRKY50* and *WRKY51*, were not detected in the GeneChip arrays or in many of the publicly available arrays. Using these approaches I identified nineteen *WRKY* genes that were induced in *ssi2* plants (data not shown). Northern analysis of the *WRKY* genes identified in the genome-wide and targeted expression profiling showed that only *WRKY46*, *WRKY50*, *WRKY51*, *WRKY53* and *WRKY60* were induced in an SA-independent manner in *ssi2 sid2* plants (Figure 3.2A). To confirm this further, I analyzed the expression of these *WRKY* genes in glycerol-treated wild-type and *sid2* plants, since exogenous glycerol application mimics *ssi2*-like phenotypes in wild-type plants by lowering 18:1 levels. As expected, glycerol application lowered 18:1 levels to induce defense phenotypes in both wild-type and *sid2* plants (Figure 3.3A). The glycerol-treated *sid2* plants did not accumulate any SA (Figure 3.3B) but showed induction of *WRKY46*, *WRKY50*, *WRKY51*, *WRKY53* and *WRKY60* genes (Figure 3.4A, right panel). These *WRKY* genes were thus considered candidate genes that might participate in the *ssi2*-mediated induction of defense responses.

Mutations in *WRKY50* and *WRKY51* restore JA responsiveness in *ssi2* plants

To study the roles of *WRKY46*, *WRKY50*, *WRKY51*, *WRKY53* and *WRKY60* genes in *ssi2*-mediated signaling I first isolated knockout (KO) mutations in these genes. Lines carrying T-DNA insertions in the target genes were screened for homozygous insertional mutants (Table 3.1). RT-PCR analysis of cDNA from the *wrky46*, *wrky50*, *wrky51*, *wrky53* or *wrky60* lines did not detect any transcript for the respective gene, confirming the presence of KO mutations in each gene (Figure 3.4B). All *wrky* mutants were

morphologically similar to wild-type plants (Figure 3.5A) and were crossed with *ssi2* plants. The *ssi2 wrky* double-mutant plants segregated in a Mendelian double-recessive manner and all double-mutants showed *ssi2*-morphology and constitutive cell death (Figure 3.6B & Figure 3.4C). Interestingly, the *ssi2 wrky46, ssi2 wrky50, ssi2 wrky51* and *ssi2 wrky53* double-mutant plants accumulated significantly lower levels of SA and SAG, compared to the *ssi2* single mutant (Figure 3.4D). SA and SAG levels in *ssi2 wrky60* plants were also lower than those in *ssi2* plants but they were over four–fold higher than those in any of the other *ssi2 wrky* double mutants. Regardless of their SA levels, all *ssi2 wrky* plants expressed high levels of the *PR-1* gene, likely because the SA/SAG levels in these were still higher (up to five–fold) than those in wild-type plants (Figure 3.4E). Consistent with their morphological and defense phenotypes, 18:1 levels of *ssi2 wrky46*, *ssi2 wrky50*, *ssi2 wrky51*, *ssi2 wrky53* and *ssi2 wrky60* double-mutant plants were similar to that of *ssi2* (Table 3.3).

To determine if the *wrky 46, 50, 51, 53* or *60* mutations restored JA-responsive *PDF1.2* expression in *ssi2* plants, I applied exogenous JA to wild-type, *ssi2*, *ssi2 wrky46*, *ssi2 wrky50*, *ssi2 wrky51*, *ssi2 wrky53*, and *ssi2 wrky60* plants. As expected, *PDF1.2* induction was detected in wild-type but not *ssi2* plants. Interestingly, *ssi2 wrky50* and *ssi2 wrky51* plants showed induction of *PDF1.2*, although these levels were lower than in wild-type plants (Figure 3.7A). The *ssi2 wrky46*, *ssi2 wrky53* and *ssi2 wrky60* plants did not induce *PDF1.2* expression in response to JA, similar to *ssi2* plants. The *wrky* single mutants did not exhibit basal *PDF1.2* expression and did induce *PDF1.2* expression in response to exogenous JA, similar to wild-type plants (Figure 3.6B). Together these results showed that the *ssi2 wrky50* and *ssi2 wrky51* mutants are able to induce *PDF1.2* expression in response to JA in spite of their low 18:1 levels.

This analysis of *ssi2* suppressors has shown that restoration of wild-type-like phenotypes in *ssi2* plants relies upon the restoration of 18:1 levels in these plants. The only exception is the *ssi2 eds1 sid2* triple-mutant plants, which show wild-type-like morphology in spite of containing *ssi2*-like levels of 18:1 (Figure 3.5C). The *ssi2 eds1 sid2* plants are also restored in all the SA-related phenotypes associated with the *ssi2* mutation (Venugopal et

al., 2009). To determine if JA responsiveness was associated with 18:1 levels, the SA pathway and/or morphological phenotype, I next tested JA-responsive *PDF1.2* expression in the *ssi2 sid2 eds1* plants. Northern blot analysis showed that, unlike *ssi2 wrky50* or *ssi2 wrky51,* the *ssi2 eds1 sid2* plants were unable to induce *PDF1.2* in response to JA (Figure 3.6C). This indicates that basal levels of 18:1 are essential for JA-inducible expression of *PDF1.2* and that this phenotype is independent of morphological size. Furthermore, these data suggest that *WRKY50* and *WRKY51* act as negative regulators of JA-responsive *PDF1.2* expression downstream of 18:1 levels.

Since the WRKY50 and WRKY51 negatively regulate JA-derived *PDF1.2* expression in *ssi2* plants, I tested if these proteins did the same in the wild-type background. SA is known to repress the JA-inducible expression of *PDF1.2* in Arabidopsis (Spoel et al., 2003). Therefore, I tested *PDF1.2* expression in wild-type, *wrky50* and *wrky51* single-mutant plants, and the *wrky50 51* double-mutant plants that were treated with JA in the presence of water (water+JA) or SA (SA+JA). As expected, the SA+JA-treated wild-type plants induced very low levels of *PDF1.2* in comparison to water+JA-treated plants (Figure 3.6D). In contrast, both the *wrky50* single mutant, and the *wrky50 51* double mutants induced *PDF1.2* expression at levels comparable to the corresponding water+JA-treated plants, and much higher than the SA+JA-treated wild-type plants. The SA+JA-treated *wrky51* single mutant also induced *PDF1.2* at levels higher than the correspondingly treated wild-type plants. However, these levels were much lower than those in the SA+JA-treated *wrky50* single mutant, or the *wrky50 51* double-mutant plants (Figure 3.6D). Together, these results indicate that WRKY50 and WRKY51 negatively regulate the repression of JA-inducible *PDF1.2* expression under low 18:1 conditions in *ssi2* plants, as well as in the presence of SA in wild-type plants.

Second-site mutations in *wrky50* or *51* restore basal resistance to *Botrytis cinerea* in *ssi2* plants

The *ssi2* plants exhibit enhanced susceptibility to *B. cinerea* as compared to wild-type plants, possibly due to their inability to induce JA-responsive defense signaling (Kachroo

et al., 2001). Since the *wrky50* or *51* mutations both restored JA-responsive *PDF1.2* expression in *ssi2* plants, I determined whether these mutations also restored basal resistance to *B. cinerea* in *ssi2* plants. Wild-type and mutant plants were inoculated with *B. cinerea* and the plants monitored for *PDF1.2* expression and disease progression. As expected, *B. cinerea* infection induced *PDF1.2* expression in wild-type, but not *ssi2* plants. Consistent with their JA-inducible *PDF1.2* expression, *ssi2 wrky50* and *ssi2 wrky51* plants also induced *PDF1.2* in response to *B. cinerea* (Figure 3.8A). In contrast, and consistent with their inability to respond to JA, *ssi2 wrky46*, *ssi2 wrky53* and *ssi2 wrky60* plants did not induce *PDF1.2* expression in response to *B. cinerea* (data not shown).

Analysis of disease progression up to 9 days post inoculation (dpi) showed that the *ssi2* plants developed profuse necrosis and succumbed to *Botrytis* infection within 9 dpi (Figure 3.8B & C). In contrast, wild-type plants were more resistant, with nearly 35% of the plants surviving infection at 9 dpi (Figure 3.8B & C). Interestingly, and congruent to their JA/pathogen-inducible expression of *PDF1.2*, *ssi2 wrky50* and *ssi2 wrky51* plants were resistant to infection by *B. cinerea*; ~ 30-35 % of these plants survived infection at 9 dpi. In contrast, *ssi2 wrky46*, *ssi2 wrky53* or *ssi2 wrky60* plants were as susceptible to *B. cinerea* as *ssi2* plants (Figure 3.8B & C). The enhanced resistance conferred by the *wrky50* and *51* mutations was specific to the *ssi2* background, since the single mutant plants (*wrky46, 50, 51, 53,* and *60*) exhibited wild-type-like response to *B. cinerea* (Figure 3.8A-3.8C). Together, these results show that second-site mutations in *WRKY50* or WRKY*51* restore *PDF1.2* expression as well as resistance to *B. cinerea* in *ssi2* plants.

Since WRKY proteins are known to function redundantly (Eulgem and Somssich, 2007), I next tested if *WRKY50* and *WRKY*51 contributed additively to increased *PR-1* expression or the repression of JA responses in *ssi2* plants. The triple-mutant *ssi2 wrky50 wrky51* plants were generated and analyzed for *PR-1* expression and resistance to *B. cinerea*. Northern blot analysis showed that the *ssi2 wrky50 wrky51* triple-mutant plants continued to express the *PR-1* gene constitutively, similar to the *ssi2 wrky50* or *ssi2 wrky51* double-mutant plants (Figure 3.9). The *ssi2 wrky50 wrky51* plants also induced

similar levels of *PDF1.2* in response to *B. cinerea* infection and exogenous JA as the double-mutant plants (Figures 3.8A and data not shown). Furthermore, basal resistance to *B. cinerea* was not further improved in the *ssi2 wrky50 wrky51* plants (Figure 3.8B & C). Together, these results show that *WRKY50* and *WRKY51* do not function additively in repressing defense to *B. cinerea* under low 18:1 conditions.

Mutations in *WRKY50* or *WRKY51* do not alter sensitivity to, or the production of, reactive oxygen species

The *ssi2* mutant accumulates high levels of reactive oxygen species (ROS), and increased ROS levels are known to be associated with enhanced susceptibility to necrotrophs, including *B. cinerea* (Govrin and Levine, 2000). Conversely, tolerance to ROS has been associated with increased resistance to necrotrophic pathogens (Glazebrook, 2005). Therefore, I tested whether the restored basal resistance to *B. cinerea* in the *ssi2 wrky50* or *ssi2 wrky51* plants was due to alterations in responses to, or the production of, ROS in these plants. I first tested the possible involvement of the various *WRKY* genes in sensitivity to ROS production. Changes in gene expression in response to exogenous H_2O_2 application were analyzed. As reported previously (Miao et al., 2004), the *WRKY53* transcript was induced in plants treated with H_2O_2. Northern blot analysis did not detect increased expression of any of the other *WRKY* genes analyzed (Figure 3.10A). Next, I analyzed the *wrky* single-mutant plants for sensitivity to paraquat (1,1′-dimethyl-4,4′-bypiridilium), an agent that promotes ROS formation by inhibiting electron transport during photosynthesis (Farrington et al., 1973; Hiyama et al. 1993). Various concentrations of paraquat (5 - 50 μM) were spot-inoculated on wild-type and *wrky* mutant leaves and the lesion sizes were measured 48 h later. None of the *wrky* single-mutants showed significant differences in paraquat-derived lesion formation as compared to wild-type plants (Figure 3.10B, data shown for 15 μM paraquat).

Finally, I evaluated the levels of ROS in wild-type, *ssi2,* and *ssi2 wrky* double-mutant plants, before and after inoculation with *B. cinerea*. The basal levels of ROS in *ssi2, ssi2 wrky50* and *ssi2 wrky51* plants were ~ 2–fold higher than in wild-type plants (Figure

3.10C). Inoculation of *B. cinerea* increased ROS levels in wild-type plants by > 2−fold. In contrast, the *B. cinerea*-responsive increase in ROS levels was only > 1.2−fold in the *ssi2, ssi2 wrky50* or *ssi2 wrky51* plants. Furthermore, no appreciable differences were observed between the basal or pathogen-induced ROS levels of *ssi2, ssi2 wrky50*, or *ssi2 wrky51* plants. Together, these results showed that restoration of resistance to *B. cinerea* in the *ssi2 wrky50* or *ssi2 wrky51* plants was not due to their altered sensitivity to, or endogenous levels of, ROS.

WRKY51 mediates defense against _P. syringae_ in the _ssi2_ and wild-type backgrounds

Since the *ssi2* mutation confers enhanced resistance to bacterial pathogens, I next tested the response of the *ssi2 wrky50* and *ssi2 wrky51* double-mutant plants to virulent and avirulent *P. syringae*. The *ssi2* plants accumulated ~ 25−fold lower virulent bacteria than wild-type plants (Col-0). In comparison, *ssi2 wrky50* and *ssi2 wrky51* double-mutant plants accumulated similar levels of virulent bacteria as wild-type plants (Figure 3.7A). As in the case of virulent bacteria, *ssi2* plants accumulated ~ 31−fold reduced levels of avirulent bacteria (*avrRpt2*) than wild-type plants (Figure 3.7B). However, in contrast to their response to virulent bacteria, the *ssi2 wrky50* and *ssi2 wrky51* double-mutant plants showed partial loss of *ssi2*-mediated enhanced resistance to *avrRpt2* bacteria (Figure 3.7B). Together, these results suggest that mutations in *WRKY50* and *51* are required for *ssi2*-mediated enhanced resistance to virulent and avirulent bacteria.

The above results and the fact that WRKY proteins are known to mediate defense responses, prompted me to examine the pathogen response of the *wrky* single-mutant plants. The *wrky46*, *wrky50* and *wrky60* plants accumulated similar levels of virulent *P. syringae* as wild-type plants (Figure 3.11A). In contrast, *wrky51* or *wrky53* plants consistently accumulated 6−fold more virulent bacteria than wild-type plants ($P<0.05$). Inoculation with avirulent bacteria showed that bacterial proliferation in the *wrky46*, *wrky50, wrky51* or *wrky60* mutants was not significantly altered as compared to wild-type plants (Figure 3.11B). In contrast, *wrky53* plants were significantly more susceptible ($P<0.05$), accumulating 3−fold increased avirulent bacteria compared to wild-type plants

(Figure 3.11B). These results show that WRKY51 is required for basal resistance, while WRKY53 participates in both basal and R-mediated defense to *P. syringae*.

To determine if enhanced susceptibility was due to impaired SA pathway, I evaluated SA responsiveness of *wrky51* and *wrky53* plants; exogenous SA induced wild-type like levels of the SA-responsive marker, *PR-1* (Figure 3.11C). SA application also restored wild-type like resistance to virulent bacteria (Figure 3.11D). These results show that *wrky51* and *wrky53* plants are not impaired in SA responsiveness and likely function upstream of SA. This is further corroborated by the fact that WRKY51 and WRKY53 contribute to SA accumulation in *ssi2* plants (Figure 3.4D).

DISCUSSION

The Arabidopsis *ssi2* mutant plants are constitutively upregulated in SA-derived signaling, and concomitantly defective in their ability to induce JA-responsive defenses. As a result, these plants exhibit enhanced resistance to biotrophic pathogens but show heightened susceptibility to necrotrophs. This is in agreement with the fact that SA-mediated signaling often contributes to defense against biotrophs, whereas defense to many necrotrophic pathogens requires JA-derived signaling (Glazebrook, 2005). SA is also well known to antagonize JA signaling, and this antagonism is mediated via the signaling component NPR1 (non-expression of *PR1*) and the WRKY62 protein (Spoel et al., 2003; Mao et al., 2007). However, lowering SA levels neither restores the morphological phenotypes nor relieves the inhibition of JA-derived responses in *ssi2* plants. Furthermore, both *ssi2 npr1* and *ssi2 NPR1* plants remain defective in JA-mediated induction of *PDF1.2* as well as in resistance to *B. cinerea* (Kachroo et al., 2001). This indicates that the inhibition of JA-mediated defenses in *ssi2* plants is not due to antagonism from their increased SA levels or heightened SA-derived signaling. Thus, the *ssi2* mutant provides a unique avenue to identify molecular components that mediate cross-talk between the SA and JA pathways, but are not involved in the SA-mediated antagonism of the JA pathway.

Suppressor analysis has shown that repression of the JA pathway in the *ssi2* plants can only be relieved when their 18:1 levels are increased to wild-type-like or higher. Second site mutations in *ACT1*, *GLY1* or *ACP4* all restore 18:1 levels as well as both SA- and JA-derived signaling in *ssi2* plants (Kachroo et al., 2003 & 2004; Xia et al., 2009). On the other hand, although simultaneous mutations in *EDS1* and *SID2* restore the morphological and constitutive *R* gene expression phenotypes (Venugopal et al., 2009), the *ssi2 eds1 sid2* plants are neither restored for 18:1 levels nor JA-inducible *PDF1.2* expression. Thus, EDS1 and SA function redundantly and downstream of 18:1 levels to modulate resistance to biotrophic pathogens, but do not participate in the low 18:1-regulated repression of JA signaling (Figure 3.12). Like EDS1 and SA, WRKY50 and 51 also function downstream of 18:1 levels; the *ssi2 wrky50* and *ssi2 wrky51* plants contain *ssi2*-like (low) levels of 18:1. However, unlike *eds1 sid2*, the *wrky50* or *wrky51* mutations restore the ability of *ssi2* plants to induce JA-responsive *PDF1.2* expression as well as basal resistance to the necrotrophic pathogen *B. cinerea*. Interestingly, although *wrky50* or *wrky51* mutations do not abolish constitutive cell death, *PR-1* expression or enhanced resistance to *P. syringae*, they do lower SA levels in the *ssi2* plants. However, the SA levels in *ssi2 wrky50* or *ssi2 wrky51* plants are still higher than those in wild-type plants, and these levels might be sufficient to induce *PR-1* expression and enhance resistance to *P. syringae*. The high SA in *ssi2* plants is unlikely to antagonize JA-inducible *PDF1.2* expression because *ssi2 sid2* plants, which are unable to accumulate SA, continue to be repressed in JA-inducible *PDF1.2* expression. Moreover, second-site mutations in *WRKY 46* or *53* also lower SA level, but do not restore JA-induced signaling in *ssi2* plants. These results further suggest that the SA-mediated antagonism of the JA pathway is indirect and likely involves various intermediates (like WRKY50 and 51), which are constitutively upregulated in the *ssi2* background.

The *ssi2* plants exhibit constitutive cell death, and increased cell death has been associated with enhanced pathogenicity of necrotrophic pathogens such as *B. cinerea* (Govrin and Levine, 2000). Furthermore, *ssi2* plants contain high levels of ROS, which are known to induce cell death and facilitate the spread of necrotrophic pathogens. In fact, many necrotrophs including *Botrytis* are known to induce ROS production in the

host, to enhance pathogenicity (von Tiedemann, 1997, Govrin and Levine, 2000, Dickman et al., 2001; Govrin et al., 2006). Likewise, increased sensitivity to oxidative stress is also associated with susceptibility to *B. cinerea* (Tierens et al., 2002; Mengiste et al., 2003; Veronese et al., 2004). The *ssi2* plants exhibit spontaneous cell death as well as accumulate increased levels of ROS (Kachroo et al., 2001). However, cell death and ROS likely do not account for the increased susceptibility of *ssi2* plants to *B. cinerea*, since the *ssi2 wrky50* and *ssi2 wrky51* double mutants also show constitutive cell death and accumulate *ssi2*-like levels of ROS. This is also consistent with the fact that *WRKY50* or *WRKY51* transcripts are not inducible by hydrogen peroxide and the *wrky50* or *wrky51* single mutants show wild-type-like sensitivity to paraquat. Thus, the restoration of basal resistance to *B. cinerea* in the *ssi2 wrky50* or *ssi2 wrky51* plants may not be associated with sensitivity to/accumulation of ROS, or the cell death phenotype.

The Arabidopsis genome encodes 74 *WRKY* genes and many of the encoded proteins function directly/indirectly in defense signaling against microbial pathogens (Pandey and Somssich, 2009). This is consistent with my findings here that KO mutations in either *WRKY51* or *53* lower basal resistance to *P. syringae*. Furthermore, *WRKY53* also participates in *R*-mediated resistance to *AvrRPT2*-expressing *P. syringae*. In addition to pathogen or pathogen-derived elicitors, many *WRKY* genes are induced in response to high SA (Dong et al., 2003). Of the SA-inducible *WRKY* genes, *WRKY46*, *50*, *51*, *53, 60* and *70* are also induced in response to a reduction in 18:1 levels. Furthermore, this low 18:1-inducible expression of *WRKY46*, *50*, *51*, *53, 60* and *70* is independent of high SA, since these genes continue to be induced in *ssi2 sid2* as well as glycerol-treated *sid2* plants, which are unable to accumulate high SA. This raises the possibility that some or all of the WRKY46, 50, 51, 53, 60 and 70 proteins, might regulate defense gene expression and, thereby, the altered signaling in *ssi2* plants. Indeed, many defense-related genes, including *PR-1*, contain W-boxes (WRKY-binding sites) in their promoter regions (Maleck et al., 2000, Yu et al., 2001). In fact, overexpression of WRKY70 was associated with increased expression of *PR-1* as well as enhanced resistance to *P. syringae* (Li et al., 2004). Clearly though, constitutive *PR-1* expression in *ssi2* plants is not the result of

increased expression of *WRKY70* (or *WRKY46*, *50*, *51*, *53* and *60*), since all of the *ssi2 wrky* double mutants continue to overexpress *PR-1*.

WRKY proteins are characterized by the presence of one or two highly conserved domains carrying the WRKYGQK sequence and a zinc-binding motif at the N-terminal end (Eulgem et al., 2000). WRKY proteins bind specific DNA sequences termed W-box elements in the promoters of target genes and the promoters of several defense-related genes, including *PR* genes, contain W-boxes (Eulgem, 2006). Mounting evidence shows that, in addition to inducing gene expression, WRKY proteins can also serve as transcriptional repressors (Rushton et al., 2010). This raises the possibility that WRKY50 and/or WRKY51 directly repress *PDF1.2* expression, although WRKY proteins have not been reported to regulate the expression of JA signaling components. Absence of these proteins, then, relieves this repression to restore JA-derived signaling and, thereby, resistance to *B. cinerea* in the *ssi2 wrky50* and *ssi2 wrky51* plants. Analysis of the 5' upstream sequences of *PDF1.2* did not detect sequences corresponding to the minimal W-box domain (C/TTGACC/T, Rushton et al., 1996; Eulgem et al., 2000). However, the absence of W-boxes does not rule out the possibility for WRKY50/51 as regulators of *PDF1.2* expression, since some WRKY proteins do bind non-W box sequences as well (Rushton et al., 2010). Interestingly, a preliminary analysis did detect W-box sequences in several other JA-inducible/metabolizing genes (Table 3.4) such as *VSP2* (vegetative storage protein 2), *OPR3* (oxophytodienoic acid reductase 3) and *AOS* (allene oxide synthase). Functional analyses of these W box-like sequences could reveal an as yet unidentified role for WRKY proteins in modulating the JA signaling pathway.

Table 3.1. T-DNA insertional lines used for analysis of WRKY function.

Gene	ID	Salk Line	Insertion	Mutant Designation
WRKY46	At2g46400	Salk_134310	Exon III	*wrky46-1*
WRKY50	At5g26170	Salk_045803	5' UTR	*wrky50-1*
WRKY51	At5g64810	Salk_022198	Intron II	*wrky51-1*
WRKY53	At4g23810	Salk_034157	Exon II	*wrky53-1*
WRKY60	At2g25000	Salk_120706	Exon I	*wrky60-1*
WRKY70	At3g56400	Salk_025198	Exon I	*wrky70-1*

Table 3.2. FA composition of leaf tissues from *SSI2*, *ssi2* and the *ssi2 wrky46*, *50*, *51*, *53* or *60* double mutants.

Genotype	FA content (mol%)							
	16:0	**16:1**	**16:2**	**16:3**	**18:0**	**18:1**	**18:2**	**18:3**
SSI2	15.7	4.0	0.9	15.1	1.3	2.7	14.6	45.7
	±0.4[a]	±0.2	±0.1	±0.5	±0.4	±0.1	±0.2	±0.5
ssi2	14.2	2.3	0.4	10.1	13.6	0.6	13.5	45.2
	±0.4	±0.0	±0.0	±0.3	±0.5	±0.0	±0.3	±0.4
ssi2	15.3	2.4	0.4	8.8	10.4	0.9	14.6	47.1
wrky46	±0.1	±0.1	±0.0	±0.1	±0.4	±0.1	±0.2	±0.7
ssi2	15.3	2.7	0.4	8.3	10.3	1.2	14.4	47.4
wrky50	±0.4	±0.1	±0.0	±0.2	±0.5	±0.2	±0.5	±1.3
ssi2	15.7	2.5	0.3	7.7	9.4	1.0	14.2	49.1
wrky51	±0.1	±0.2	±0.0	±0.4	±0.4	±0.2	±0.5	±1.3
ssi2	16.4	2.2	0.3	8.8	9.8	0.8	14.4	47.2
wrky53	±0.3	±0.2	±0.0	±0.2	±0.4	±0.1	±0.9	±1.2
ssi2	15.8	2.4	0.4	8.5	11.5	1.1	14.1	46.3
wrky60	±0.5	±0.1	±0.0	±0.4	±0.6	±0.1	±0.1	±0.5
ssi2	12.8	3.6	0.2	11.7	15.8	1.2	16.2	38.4
wrky70	±0.2	±0.1	±0.2	±0.3	±0.4	±0.01	±0.7	±0.4

[a] ± indicates standard deviation (n=5).

Table 3.3. Fold change in transcript levels of *WRKY* genes in *ssi2* or *ssi2sid2* mutant plants compared to Col-0 plants ($P < 0.05$)

Genes	**Gene ID**	***ssi2*/Col-0**	***ssi2sid2*/Col-0**
AtWRKY17	At2g24570	2.21315789	–
AtWRKY47	At4g01720	3.359375	–
AtWRKY48	At5g49520	3.4402277	–
AtWRKY70	At3g56400	3.44956602	–
AtWRKY55	At2g40740	4.96059113	–
AtWRKY45	At3g01970	5.06530214	–
AtWRKY30	At5g24110	5.56363636	–
AtWRKY31	At4g22070	5.83480826	–
AtWRKY40	At1g80840	6.46308432	–
AtWRKY33	At2g38470	6.81128163	–
AtWRKY71	At1g29860	7.09090909	–
AtWRKY72	At5g15130	7.40952381	–
AtWRKY60	At2g25000	7.65981432	2.812665782
AtWRKY53	At4g23810	11.6026365	5.077526679
AtWRKY46	At2g46400	18.5101918	12.65527578
AtWRKY75	At5g13080	27.4978942	–
AtWRKY58	At3g01080	76.1315789	–

Table 3.4 JA-responsive/metabolizing genes containing putative W-box elements in their 5' upstream regions

Gene	Gene ID	W-box sequence	Position
VSP2	At5g24770	TTGACC	-1274 and -1258
CHI-B	At3g12500	TTGACT	-1628
OPR3	At2g06050	TTGACC	-59
AOS	At5g42650	TTGACC	-1906
LOX2	At3g45140	TTGACT	-1677

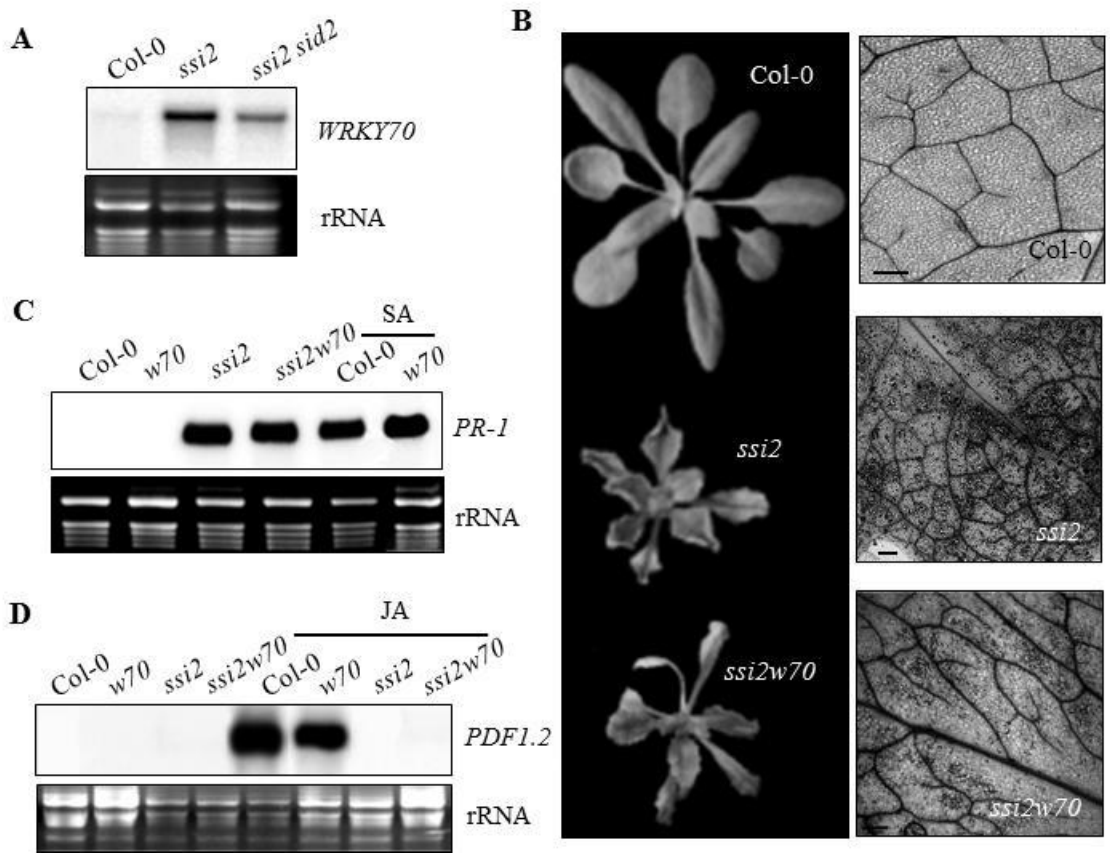

Figure 3.1. Effect of second-site mutation in *WRKY70* in *ssi2* plants. (**A**) Northern blot analysis showing expression of *WRKY70* gene in the indicated genotypes. Ethidium bromide staining of rRNA was used as a loading control. (**B**) Morphology and cell death phenotypes of wild-type (Col-0), *ssi2* and *ssi2 wrky70* (*ssi2w70*) plants. Microscopy of trypan blue-stained leaves is shown in the right panels. Scale bars represent 270 microns. (**C & D**) Northern blot analysis showing basal and salicylic acid (SA)-responsive expression of the *PR-1* gene (**C**) or basal and jasmonic acid (JA)-responsive expression of *PDF1.2* (**D**) in indicated genotypes. *w70* denotes the *wrky70* single-mutant. Ethidium bromide staining of rRNA was used as a loading control.

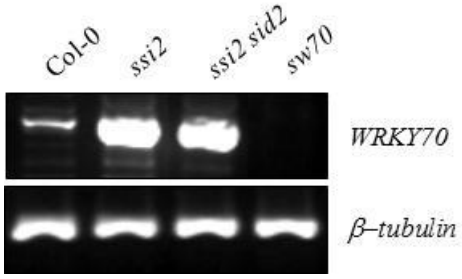

Figure 3.2. Expression of the *WRKY70* transcript in wild-type (Col-0), *ssi2*, *ssi2 sid2* and *ssi2 wrky70* (*sw70*) plants. *β*–tubulin levels were used as internal control for cDNA amounts.

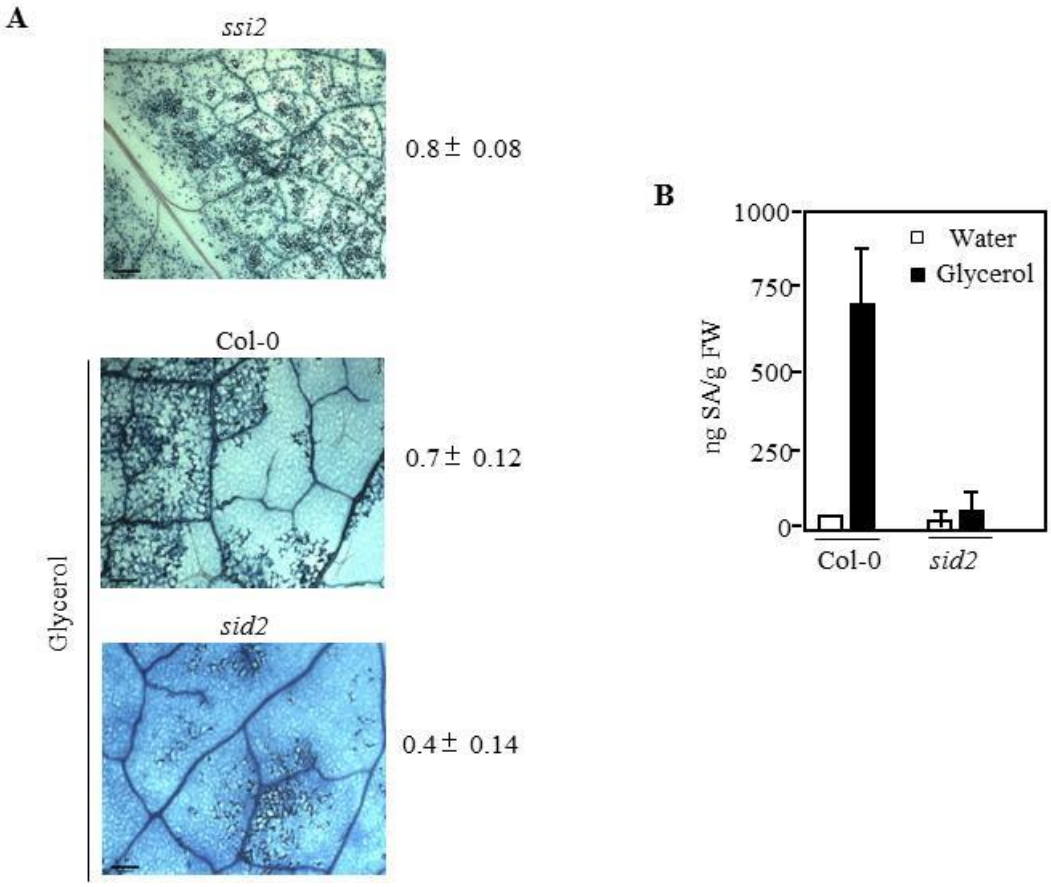

Figure 3.3. (A) Microscopy of trypan blue-stained leaves of indicated genotypes. Scale bars represent 270 microns. Col-0 and *sid2* plants were pre-treated with glycerol. Numbers on the right indicate 18:1 levels (mol%) in the plants used for cell death staining. ± indicates standard deviation where n=5. (**B**) Levels of free salicylic acid (SA) in water- (white bars) or glycerol- (black bars) treated wild-type (Col-0) and *sid2* plants. Bars represent standard deviation of the mean, n=4.

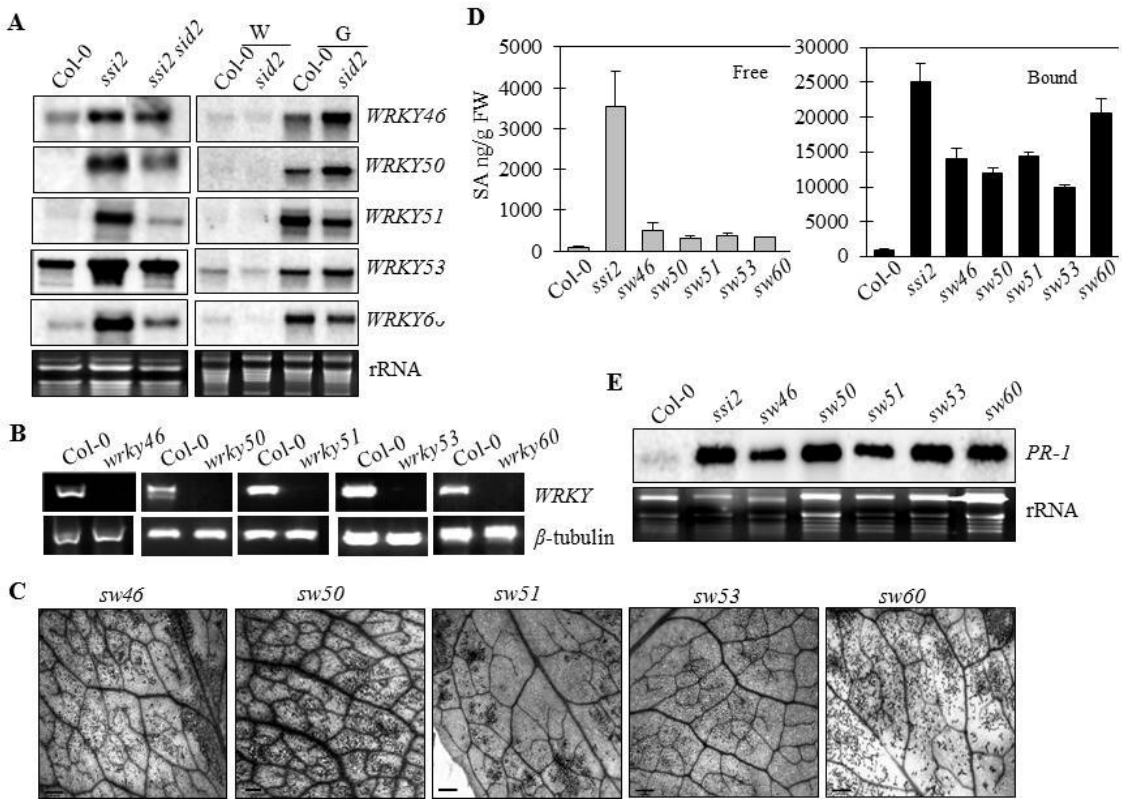

Figure 3.4. SA independent-inducibility and effect of KO mutations in *WRKY46*, *50*, *51*, *53* and *60* in *ssi2* plants. (**A**) Northern blot analysis showing basal (left panel) and water (W)- or glycerol (G)-responsive (right panel) expression of *WRKY* genes in the indicated genotypes. Ethidium bromide staining of rRNA was used as a loading control. (**B**) RT-PCR analysis showing expression of the various *WRKY* genes in wild-type (Col-0) or the respective *WRKY* KO (*wrky*) mutants. *β*–tubulin levels were used as internal control for cDNA amounts. (**C**) Cell death phenotypes of the *ssi2 wrky46* (*sw46*), *ssi2 wrky50* (*sw50*), *ssi2 wrky51* (*sw51*), *ssi2 wrky53* (*sw53*) and *ssi2 wrky60* (*sw60*) double-mutant plants. Microscopy of trypan blue-stained leaves is shown. Scale bars represent 270 microns. (**D**) Endogenous levels of free and bound (SA-glucoside, SAG) SA. Bars represent standard deviation of the mean, n=4. (**E**) Northern blot analysis of basal *PR-1* expression in indicated genotypes. Ethidium bromide staining of rRNA was used as a loading control.

Figure 3.5. (A) Morphological phenotypes of wild-type (Col-0), *ssi2* and the *wrky* single-mutant plants. (B) Morphological phenotypes of *ssi2* and the *ssi2 wrky46* (*sw46*), *ssi2 wrky50* (*sw50*), *ssi2 wrky51* (*sw51*), *ssi2 wrky53* (*sw53*) or *ssi2 wrky60* (*sw60*) double-mutant plants. (C) Morphological phenotypes of *ssi2* and *ssi2 eds1 sid2* plants.

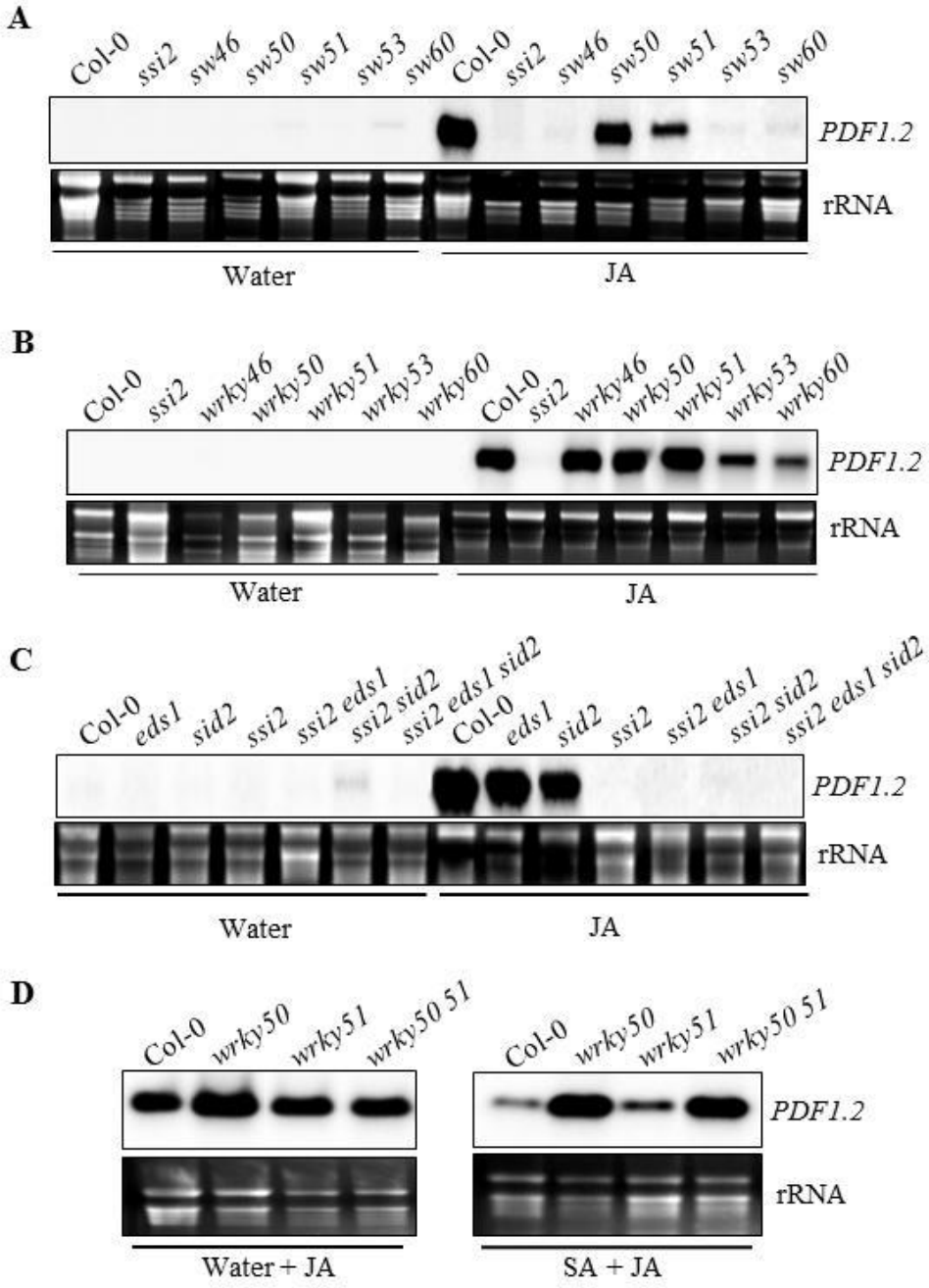

Figure 3.6. Response to jasmonic acid (JA) of various *wrky* mutants. The genotype designations include *ssi2 wrky46* (*sw46*), *ssi2 wrky50* (*sw50*), *ssi2 wrky51* (*sw51*), *ssi2 wrky53* (*sw53*), *ssi2 wrky60* (*sw60*) and *wrky50 wrky51* (*wrky50 51*). SA indicates salicylic acid. (**A-D**) Northern blot analysis of *PDF1.2* expression in indicated genotypes in response to treatment with water or JA. Ethidium bromide staining of rRNA was used as a loading control.

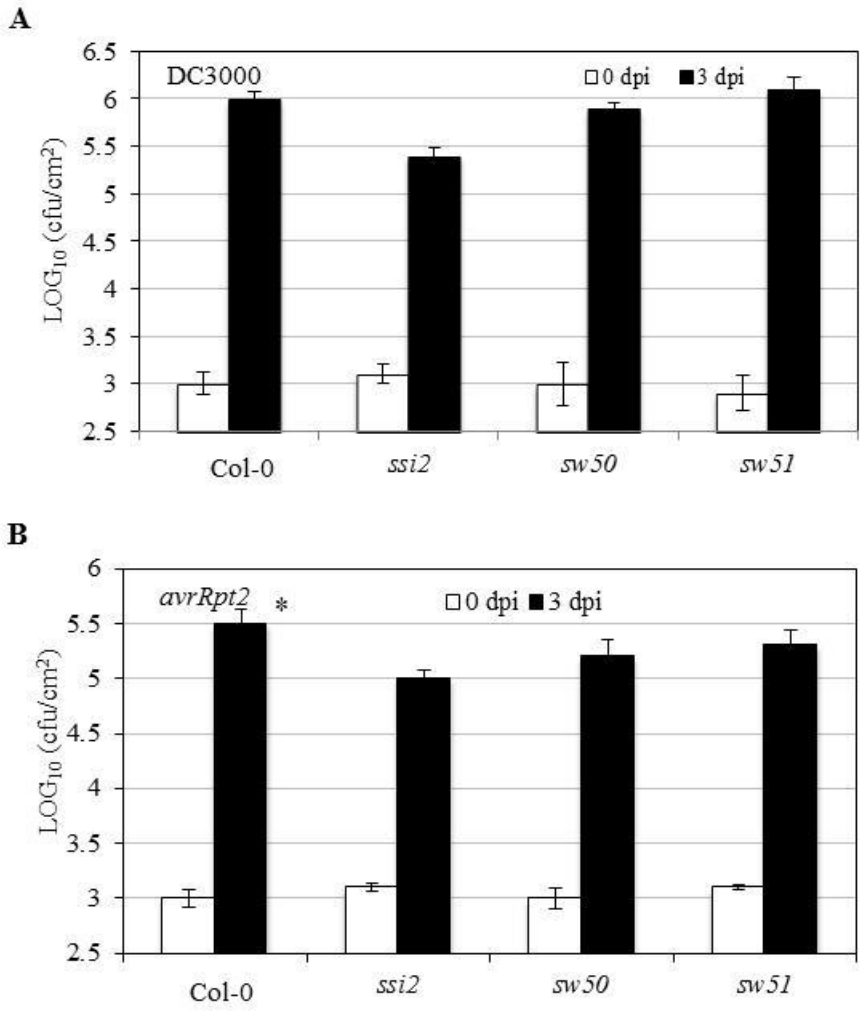

Figure 3.7. Response of *ssi2 wrky50* (*sw50*) and *ssi2 wrky51* (*sw51*) double-mutant plants to *Pseudomonas syringae* (**A & B**) Bacterial counts in wild-type (ecotype Col-0) and the various mutants infiltrated with (**A**) virulent (DC3000) or (**B**) avirulent (*avrRPT2*) strains of *P. syringae*. Bacterial numbers determined at 0 (white bars) or 3 (black bars) days post-inoculation, and presented as a LOG_{10} value of colony forming units (cfu) per cm^2. Error bars indicate standard deviation, n=4. Statistical significance was determined using Students *t*-test. Asterisk denotes data significantly different from all others, $P<0.05$.

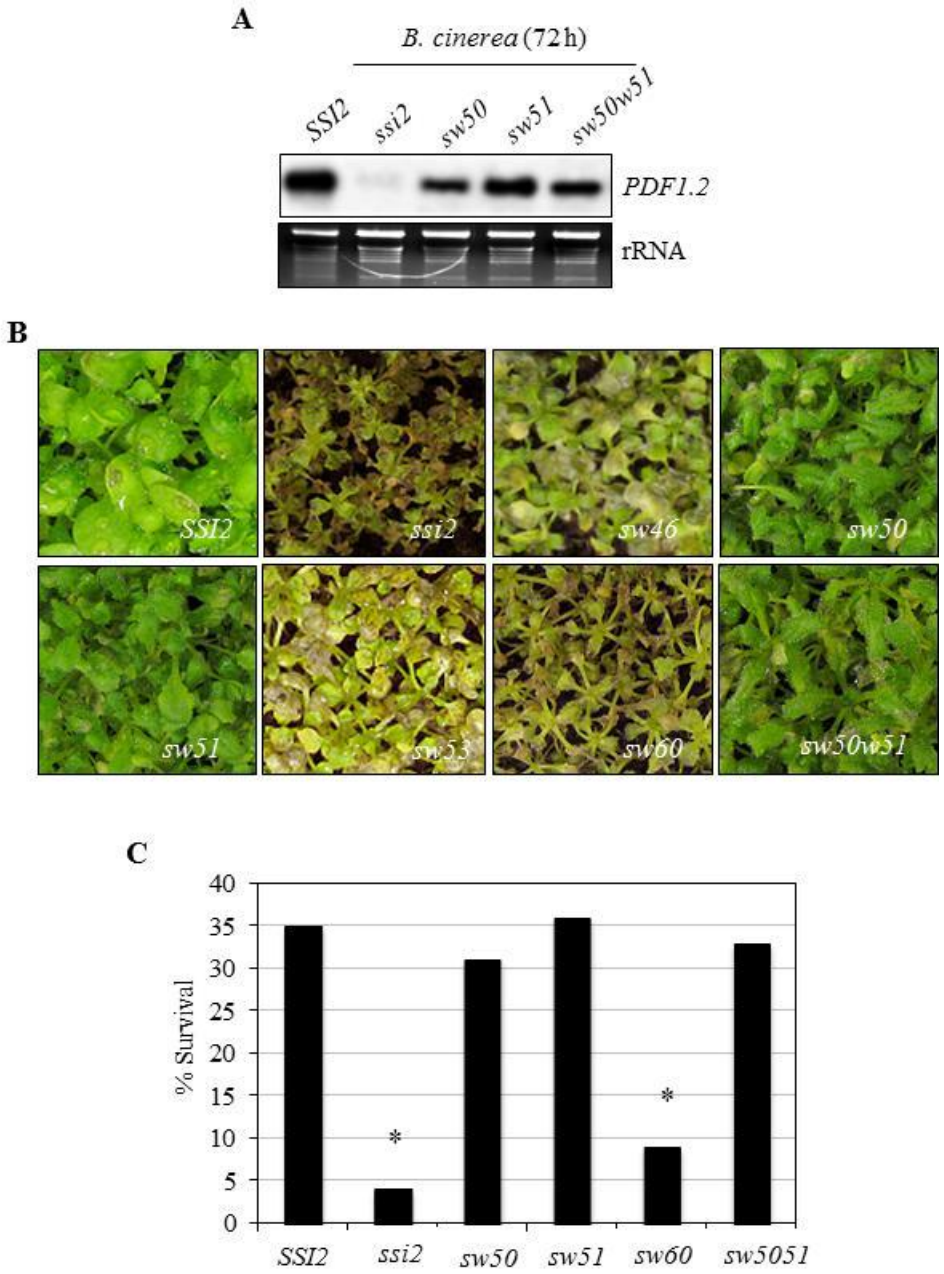

Figure 3.8. Response to *Botrytis cinerea* in wild-type (*SSI2*, ecotype No), *ssi2*, *ssi2 wrky46* (*sw46*), *ssi2 wrky50* (*sw50*), *ssi2 wrky51* (*sw51*), *ssi2 wrky53* (*sw53*), *ssi2 wrky60* (*sw60*) or *ssi2 wrky50 wrky51* (*sw50w51)* plants. (**A**) Northern blot analysis of *PDF1.2* expression in indicated genotypes at 72 h post inoculation with *B. cinerea.* Ethidium bromide staining of rRNA was used as a loading control. (**B**) Morphological phenotype of wild-type or mutant plants 6 days post-inoculation (dpi) with *B. cinerea*. (**C**) Percentage survival of wild-type (*SSI2*), *ssi2*, *sw50*, *sw51*, *sw60* and *sw50w51* plants at 9

days post-inoculation (dpi) with *B. cinerea*. Results representative of five separate experiments. Statistical significance was determined using Students *t*-test. Asterisks denote data significantly different from *SSI2*, where P<0.001.

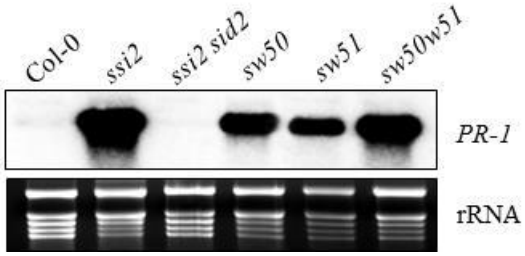

Figure 3.9. Pathogenesis-related (*PR-1*) gene expression in wild-type (Col-0), *ssi2*, *ssi2 sid2*, *ssi2 wrky50* (*sw50*), *ssi2 wrky51* (*sw51*) and *ssi2 wrky50 wrky51* (*sw50w51*) mutants. Ethidium bromide staining of rRNA was used as a loading control.

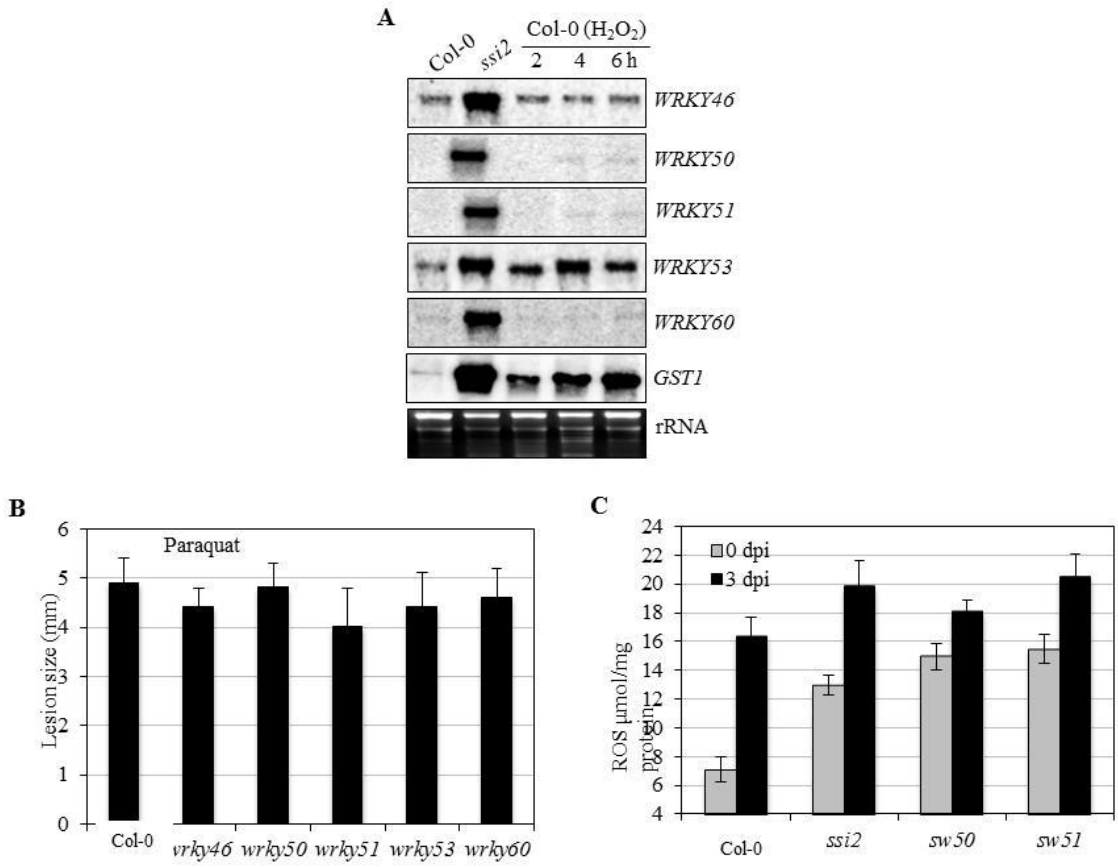

Figure 3.10. Role of *WRKY* genes in sensitivity to, and/or production of, reactive oxygen species (ROS). (**A**) Northern blot analysis showing basal expression of the various *WRKY* genes in wild-type (Col-0), *ssi2*, or H_2O_2-responsive expression in wild-type plants. Induction of glutathione-S-transferase 1 (*GST1*) was used as a positive control for the efficacy of H_2O_2 treatment. Ethidium bromide staining of rRNA was used as a loading control. (**B**) Mean lesion size on wild-type (Col-0) or the various *wrky* single-mutant leaves spot-inoculated with 15 µ M paraquat. (**C**) ROS levels, basal (0 dpi, grey bars) or at 3 day post inoculation (dpi) with *B. cinerea* (3 dpi, black bars), in wild-type (Col-0), *ssi2*, *ssi2 wrky50* (s*w50*) or *ssi2 wrky51* (*sw51*) mutant plants.

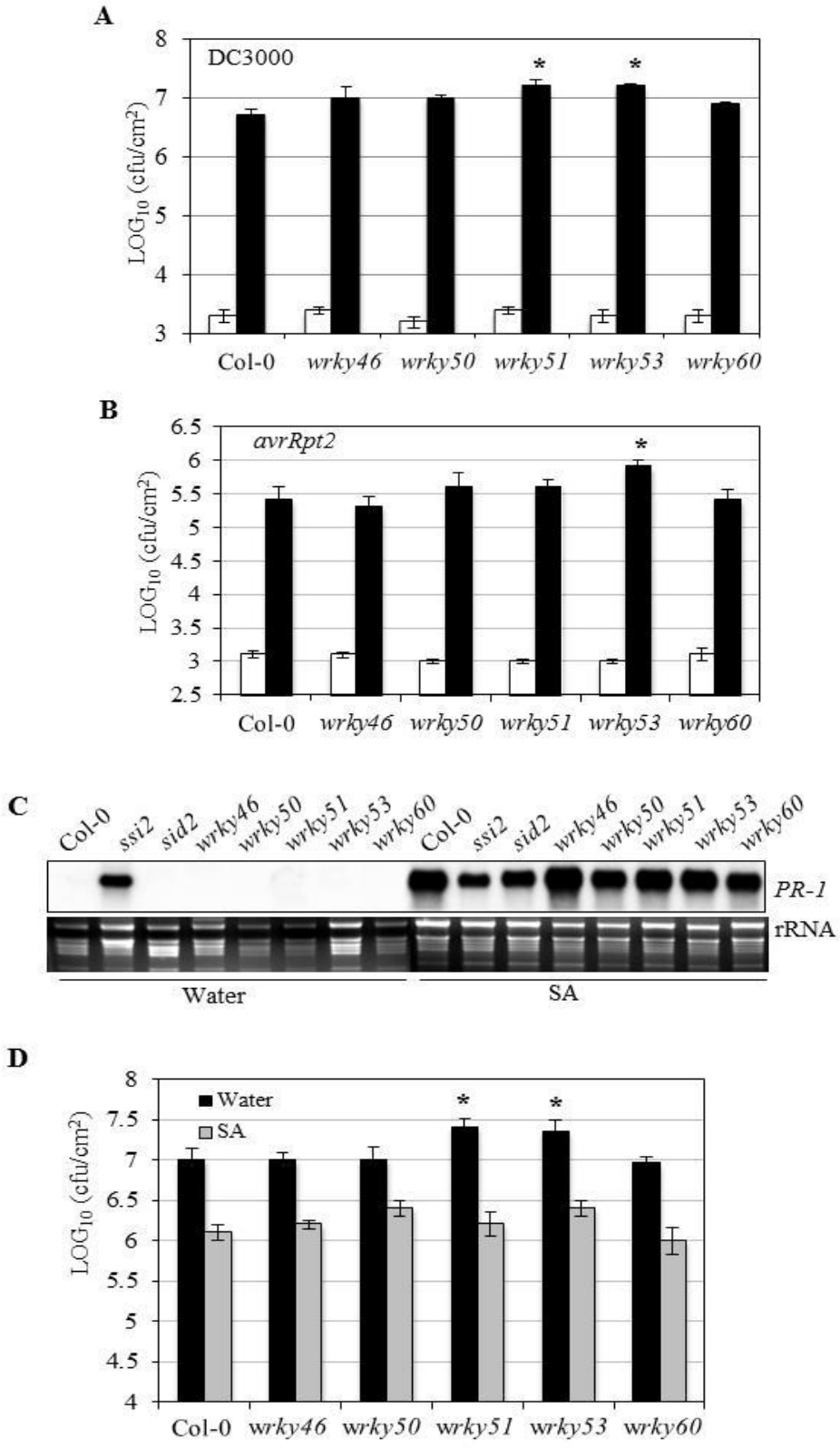
A
DC3000
LOG10 (cfu/cm2)
Col-0
wrky46
wrky50
wrky51
wrky53
wrky60
B
avrRpt2
C
Col-0
ssi2
sid2
wrky46
wrky50
wrky51
wrky53
wrky60
PR-1
rRNA
Water
SA
D
Water
SA

Figure 3.11

Figure 3.11. Salicylic acid (SA)-responsive changes in gene expression and defense to *Pseudomonas syringae* in the *wrky46*, *50*, *51*, *53* and *60* plants. (**A, B & D**) Response to DC3000 (**A & D**) or *avrRPT2*(**B**) strains of *P. syringae* in wild-type (Col-0) and *wrky* mutants. Bacterial counts are presented as LOG_{10} values of colony forming units (CFU) per cm^2 at 0 (white bars) and 3 (black bars) days post inoculation. Error bars indicate standard deviation (n=4). Statistical significance was determined using Student's *t*-test. Asterisks denote data significantly different from Col-0, $P<0.05$ for *wrky51* and *wrky53* in (**A**), $P<0.05$ for *wrky51* in (**B**) and $P<0.01$ for *wrky51* and *wrky53* in (**D**) Black and grey bars indicate water- or SA-treated plants at 3 dpi, respectively. (**C**) Northern blot analysis showing *PR-1* expression in water- and SA-treated plants.

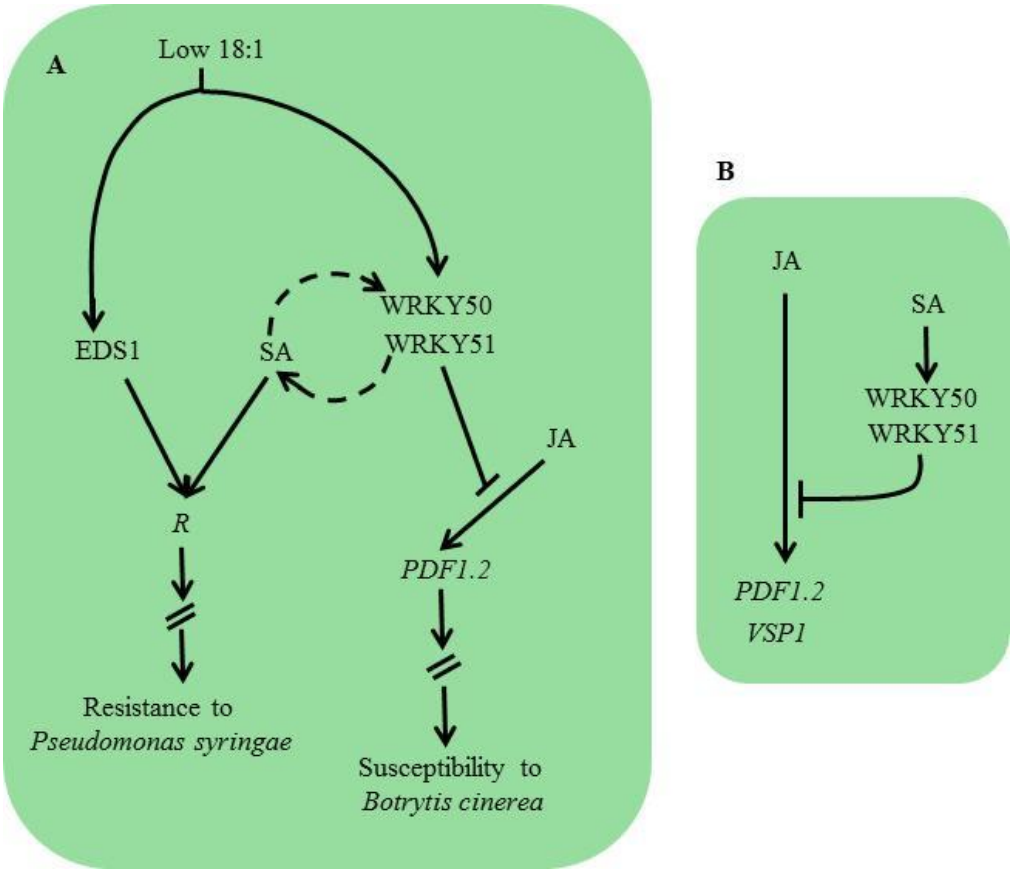

Figure 3.12. Role of WRKY50 and WRKY51 in repression of JA-derived defense responses. (**A**) Signaling induced upon reduction in 18:1 levels requires the functions of EDS1 and SA to upregulate the expression of multiple *R* genes, resulting in enhanced resistance to biotrophic pathogens such as *Pseudomonas syringae*. The low 18:1-mediated signaling requires the WRKY50 and WRKY51 proteins for suppression of JA-responsive induction of *PDF1.2* and resistance to necrotrophs such as *Botrytis cinerea*. WRKY50 and WRKY51 are also required for the accumulation of SA in low 18:1-containing plants. (**B**) WRKY50 and WRKY51 mediate the SA-derived suppression of JA-dependent *PDF1.2* expression in wild-type plants.

CHAPTER FOUR

LONG-CHAIN ACYL-COA SYNTHETASES (LACS) ARE REQUIRED FOR BASAL DEFENSE AND SYSTEMIC IMMUNITY IN ARABIDOPSIS

INTRODUCTION

De novo fatty acid (FA) synthesis occurs exclusively in the plastids and leads to the synthesis of palmitic acid (16:0)-acyl carrier protein (ACP) and oleic acid (18:1)-ACP (reviewed in Kachroo and Kachroo, 2009). The FAs enter glycerolipid synthesis either via the prokaryotic pathway in the chloroplasts or are exported out of plastids as CoA thioesters to enter the eukaryotic glycerolipid synthesis pathway. Desaturation of stearic acid (18:0)-ACP to 18:1-ACP is catalyzed by the *SSI2*/*FAB2*-encoded stearoyl-ACP desaturase (SACPD and is one of the key steps in the FA biosynthesis pathway that regulates levels of unsaturated FAs in the cell. The 18:1-ACP generated in this reaction enters the prokaryotic pathway through acylation of glycerol-3-phosphate (G3P). A loss-of-function mutation in the *SSI2*-encoded SACPD results in the induction of a variety of resistance (*R*) genes (Chandra-Shekara et al., 2007; Venugopal et al., 2009), which, in turn, confers broad-spectrum disease resistance to multiple pathogens in Arabidopsis, soybean and rice (Chandra-Shekara et al., 2007; Venugopal et al., 2009; Kachroo et al., 2007; Jiang et al., 2009; Mandal et al., 2012). The altered morphology, as well as defense-related phenotypes, in *ssi2* can be restored by elevating the endogenous 18:1 levels via second-site mutations in the *ACT1* (Kachroo et al., 2003) or *GLY1* genes (Kachroo et al., 2004), which encode enzymes with G3P acyltransferase (Kunst et al., 1988) and G3P dehydrogenase activities (Kachroo et al., 2004), respectively. The 18:1 levels and *ssi2* phenotypes are also restored by a second site mutation in *ACP4*, which encodes one of the isoforms of acyl carrier proteins (Xia et al., 2009). ACP4 is required for normal FA biosynthesis in leaves and a mutation in *ACP4* is thought to increase 18:1 levels by affecting the ACT1-catalyzed acylation of G3P. Recent studies have shown that 18:1 regulates levels of nitric oxide-associated 1 (NOA1) protein by binding to it and subjecting it to protease-mediated degradation (Mandal et al., 2012). A reduction in 18:1

levels results in increased accumulation of NOA1 and thereby nitric oxide (NO), which via a direct and/or indirect process triggers *R* gene expression. Similar to the *ssi2* mutation, inoculation with an avirulent pathogen also results in the accumulation of NOA1 protein and induction of NO levels. This pathogen inoculation either modulates 18:1 flux and/or a downstream step leading to NOA1 accumulation.

In addition to 18:1, other FAs and/or lipids are also known to participate in various biotic and abiotic responses (Savchenko et al., 2010; reviewed in Kachroo and Kachroo 2009). Compromised systemic acquired resistance (SAR) in mutants defective in certain plastidal fatty acid (FA)/lipid pathways has prompted the suggestion that plastidal FA/lipids participate in SAR (Chaturvedi et al., 2008). SAR involves the generation of a mobile signal in the primary leaves which, upon translocation to the distal tissues, activates defense responses resulting in broad-spectrum resistance. Mutations in genes encoding FA desaturase (FAD) 7 and mono galactosyl diacylglycerol synthase (MGD) 1 were shown to compromise SAR (Chaturvedi et al., 2008). FAD7 catalyzes the desaturation of 16:2 and 18:2 FA species present on plastidal lipids to 16:3 and 18:3, respectively. The MGD1 enzyme transfers a galactosyl residue from uridine diphosphate (UDP)-galactose to diacylglycerol to initiate galactolipid biosynthesis (Jarvis et al., 2000). Mutations in both *FAD7* and *MGD1* affect plastidal membrane lipids. However, detailed characterization of plants defective in *FAD7* have shown that the impaired SAR in *fad7* plants is due to a second site mutation in the *GLABROUS* (*GL*) *1* gene (Xia et al., 2010). Similarly, *act1* plants, which are affected in acylation of G3P with 18:1 and thereby plastidal lipid levels, show normal SAR (Chanda et al., 2011). Defective SAR in *gl1* plants is thought to be associated with their impaired cuticle, a hydrophobic layer that covers the aerial surface of plants. The plant cuticle is composed of cutin and cuticular wax and is made up of complex mixtures of FAs, alcohols, aldehydes, alkanes and ketones (reviewed in Samuels et al., 2008; Kachroo and Kachroo, 2009). The plant cuticle has long been thought to mediate passive resistance against various biotic and abiotic stresses. However, the result that a mutation in long chain acyl-CoA synthetase *(LACS) 2* confers resistance to the necrotrophic fungal pathogen *B. cinerea* suggests that cuticle and/or its components might be required for proper induction of plant defense

responses (Bessire et al., 2007).

This study was undertaken to characterize the role of cuticle in plant defense against fungal and bacterial pathogens. Mutations in *ACP4* and several isoforms of *LACS* impaired normal development of the cuticle and compromised SAR. In contrast, *acp4* or *lacs* plants showed very distinct responses to two necrotrophic fungal pathogens, *Colletotrichum higginsiasum* and *B. cinerea*. The requirement for intact cuticle during SAR was further confirmed by mechanical abrasion of cuticles in wild-type plants. The SAR-disruptive effect of cuticle abrasion was highly specific because it did not alter local defenses and hindered SAR only during the time-frame during which the mobile signal is translocated to distal tissues.

RESULTS

A mutation in *ACP4* compromises SAR

The *acp4* plant was isolated as a genetic suppressor of the *ssi2* mutation (Xia et al., 2009). Interestingly, the *acp4* single mutant showed enhanced susceptibility to virulent and avirulent bacterial pathogens (Xia et al., 2009). To determine if these plants were compromised in SAR, I first inoculated wild-type and *acp4* plants with $MgCl_2$ or an avirulent strain of *P. syringae* expressing *avrRpt2*. Then, 48 hr later systemic leaves of all plants were challenged with a virulent strain of *P. syringae* (DC3000). The proliferation of virulent bacteria was monitored at 0 and 3 days post inoculation (dpi). The wild-type plants, inoculated first with an avirulent strain, showed ~10-fold reduced growth of virulent bacteria compared to plants whose primary leaves were infiltrated with $MgCl_2$ (Figure 4.1A). In contrast, the *acp4* plants showed no reduction in the growth of virulent bacteria at 3 dpi, when pre-exposed to avirulent bacteria. Similar results were obtained when wild-type and *acp4* plants were inoculated with an avirulent stain expressing *avrRps4* followed by inoculation with virulent bacteria (Figure 4.1B).

The defective SAR in *acp4* plants was not due to impairments in SA- or JA-mediated

signaling, since *acp4* plants accumulated wild-type-like levels of SA and JA in response to pathogen infection and showed wild-type-like responsiveness to these phytohormones (Xia et al., 2009). To determine if *acp4* plants were affected in methyl SA (MeSA) response, which is required for SAR in tobacco (Park et al., 2007), I tested MeSA responsiveness of *acp4* plants. The acp4 plants were also responsive to methyl SA (MeSA) and induced wild-type-levels of *PR-1* in response to MeSA (Figure 4.1C). Since MeSA is biologically inactive (Seskar et al., 1998), it appears that *acp4* plants are not impaired in the conversion of MeSA to SA, a reaction essential for the onset of SAR in systemic leaves (Park et al., 2007). Together, these results suggest that defective SAR in *acp4* plants is associated with a factor other than SA, JA or MeSA.

To test if ACP4 participated in mobile signal generation, I next evaluated the response of wild-type and *acp4* plants to phloem exudates collected from wild-type or *acp4* petioles. However, since the time-frame for mobile signal translocation was not known for Arabidopsis I first used a "detached leaf approach" to evaluate the time period during which mobile signal moved from local to distal tissues. The wild-type Arabidopsis plants were inoculated with $MgCl_2$ or an avirulent strain of *P. syringae* expressing *avrRpt2* and 48 hr later systemic leaves of all plants were challenged with a virulent strain of *P. syringae* (DC3000). The *avr*-inoculated leaves were detached at 2, 4, 6 and 24 h post treatment and the growth of virulent bacteria was quantified at 3 dpi. Detachment of *avr*-inoculated leaves prior to 6 h compromised SAR, suggesting that the translocation of mobile signal initiated between 4-6 h after inoculation of *avr* bacteria (Figure 4.2A). Furthermore, SAR was significantly better when *avr*-inoculated leaves were detached at 24 h compared to 6h. This suggested continuous build-up of the mobile signal and/or downstream signaling occurring within initial 24 h period was essential for SAR. Interestingly, initiation and/or establishment of SAR did not correlate with induction of the SAR marker gene *PR-1* (Figure 4.2B), which was induced at 48 h post inoculation of *avr* bacteria, long after SAR had already established. With these observations in mind, I infiltrated the wild-type and *acp4* leaves with $MgCl_2$ or *P. syringae* expressing *avrRpt2* and the petiole exudates collected from the inoculated leaves were injected into the leaves of fresh wild-type or acp4 plants. The exudate-injected leaves were then analyzed for the

expression of the SAR marker gene, *PR-1*. Interestingly, petiole exudates from pathogen-inoculated wild-type as well as *acp4* plants induced *PR-1* gene expression in wild-type leaves but not in *acp4* leaves (Figure 4.2C). Together, these results suggest that *acp4* plants are competent in generating the mobile SAR signal but they are incapable of responding to this signal.

To test if the altered leaf phenotype of *acp4* plants was due to a defect in the cuticle, which forms the outermost structure of the leaves (Samuels et al., 2008), I stained wild-type and *acp4* leaves with toluidine blue, a hydrophilic dye that only penetrates leaves with permeable cuticles (Tanaka et al., 2004). Toluidine blue rapidly penetrated *acp4* leaves, staining these blue, suggesting cuticular permeability (Figure 4.3A). The cuticular defect was further confirmed by detailed biochemical and microscopic analysis (Xia et al., 2009). To determine if a defect in cuticle correlated with cell-type specific expression of ACP4 in the leaf tissue, I performed histochemical analysis of transgenic lines expressing β-glucuronidase (GUS) under the control of the *ACP4* promoter. The histochemically-stained leaves were fixed, sectioned, and examined by light microscopy. GUS activity was detected throughout the leaf, although maximum activity was detected in vascular tissues and trichomes (Figure 4.3B). This result suggests that ACP4 functions are likely not restricted to the synthesis of cuticular components in the epidermal layer and that ACP4 is likely involved in general FA and lipid synthesis, which is highest in the leaf mesophyll tissues.

Intact cuticle is specifically required for SAR and not for local responses

To further verify if cuticle was required for SAR in wild-type plants, I damaged the cuticle of wild-type leaves by mechanical abrasion and tested their ability to induce SAR. Among several methods described for the removal of cuticle (Campbell and McInnes, 1999), it was determined that gentle rubbing with a buffered solution containing celite and bentonite was sufficient to damage the cuticle and such leaves stained intensely with toluidine blue (Figure 4.4A). However, leaves stained 24 hr after mechanical abrasion imbibed significantly less stain, suggesting that the leaves were capable of restoring

their damaged cuticle (Figure 4.4A). These results were further confirmed by TEM analysis; leaves analyzed 1 and 24 h post abrasion showed electron-opaque and electron-dense cuticles, respectively (Figure 4.4B). Interestingly, there was a 2.4 fold increase in the thickness of cell wall 1 hr post abrasion (681.75 ± 24.63 nm). In comparison, leaves analyzed 24 hr post abrasion showed normal thickness of cell wall (277.3 ± 13.3 nm). Analysis of cutin monomers and wax contents did not show a significant difference between treated and untreated leaves (Figures 4.4C, 4.4D), suggesting that abrasion was not associated with changes in the composition of cuticular wax or cutin monomers.

To test the requirement of cuticle in SAR, the cuticle was mechanically damaged from the distal leaves at 0, 12, 24 or 42 hr after infiltrating the primary leaves with $MgCl_2$ or an avirulent pathogen. Both control and damaged distal leaves were then inoculated with virulent bacteria 48 hr after infiltration of the primary leaves. The growth of the virulent bacteria was monitored at 0 (white bars) and 3 dpi (blue bars) (Figure 4.4E). Control plants preinfiltrated with $MgCl_2$ (with intact cuticle) supported more growth of the secondary virulent pathogen than plants that were preinfected with an avirulent strain, indicating the appropriate induction of SAR (Figure 4.4E). In contrast, distal leaves damaged at 0 or 12 hr after avirulent inoculation supported increased growth of the virulent pathogen (virulent bacteria inoculated 36 and 48 h post abrasion, respectively) indicating that these were compromised in SAR. On the other hand, distal leaves that were damaged 24 or 42 hr after avirulent inoculation exhibited normal SAR induction (virulent bacteria inoculated 6 and 24 hr post abrasion, respectively). The mechanical abrasion of leaves did not induce the expression of marker genes normally associated with accumulation of reactive oxygen species, SA or JA (Figure 4.4F), which suggests that abrasion was unlikely to have an effect on SAR response. These results confirmed that an intact cuticle is essential for SAR and showed that the proper onset of SAR requires a cuticle-derived component(s) within 12–24 hr of primary infection.

To determine if cuticle was also required for local responses, I tested the response of wild-type plants with damaged cuticles to virulent and avirulent (*avrRpt2*) pathogens. Unlike SAR, cuticular damage did not cause increased susceptibility to either virulent (Figure 4.4G) or avirulent (Figure 4.4H) pathogens. Together, these data suggest that

cuticle is specifically required for SAR and not for local responses.

A mutation in multiple *LACS* isoforms compromises SAR

To test the possibility that an intact cuticle was essential for SAR signal perception, I examined the SAR response in *lacs1*, *lacs2* and *lacs9* mutants, which are known to have defective cuticles (Schnurr et al., 2004; Bessire et al., 2007; Lu et al., 2009; Xia et al., 2009; Wang et al., 2010). The LACS encoded acyl CoA synthetases are enzymes synthesizing the CoA ester formation of FAs (Browse and Somerville, 1991; Schnurr et al., 2004). The Arabidopsis genome encodes nine *LACS* isoforms (Shockey et al., 2002), and, of these, only *lacs2* has been studied for its response to bacterial and fungal pathogens (Bessire et al., 2007; Tang et al., 2007). Intriguingly, a mutation in *lacs2* confers enhanced resistance to *B. cinerea* (Bessire et al., 2007; Tang et al., 2007) which, together with my results on SAR, suggest that cuticle and/or its components play contrasting roles during host-pathogen interactions. Additive effects seen in certain *lacs* double-mutant plants suggest redundant functions, justifying detailed analysis of all the *LACS* isoforms for their role in SAR and defense against necrotrophic pathogens.

The *lacs1*, *lacs2* and *lacs9* mutants were obtained from the laboratories of Drs. Jenks and Browse. For the remaining *LACS* isoforms, I screened SALK T-DNA knockout (KO) lines available at the Arabidopsis database (Figure 4.5A). Homozygous T-DNA lines were obtained for *LACS3*, *LACS4*, *LACS6*, *LACS7* and *LACS8*, and these were confirmed by RT-PCR analysis; the KO plants did not show any detectable expression of the *LACS* genes (Figure 4.5B). Analysis of individual lipid profiles showed reduced levels of MGDG and DGDG lipids in *lacs2*, *lacs3* and *lacs4* plants (Figure 4.6A), which correlated with a reduction in total lipid levels (Figure 4.6B). However, this reduction in lipid levels did not translate into a corresponding decrease in the levels of FA species (Figure 4.6C).

Next, I tested the response of various *lacs* mutants to the necrotrophic pathogens *C. higginsianum* and *B. cinerea*. As shown earlier, *lacs2* plants showed significant resistance to *B. cinerea* (Figure 4.7A). In contrast, mutations in *lacs1*, *lacs3*, *lacs4*, *lacs6*, *lacs7*,

lacs8 or *lacs9* showed a wild-type-like response. To determine if enhanced resistance in *lacs2* was due to increased permeability of the cuticle, I assayed the response of *acp4* plants to *B. cinerea* (Figure 4.7A, right panel). Interestingly, *acp4* plants showed enhanced susceptibility to *B. cinerea*. Furthermore, all the *lacs* mutants, including *lacs2*, showed a wild-type-like response to *C. higginsianum* while, in contrast, *acp4* showed enhanced susceptibility (Figure 4.7B). Together, these results suggest that cuticular permeability does not correlate with enhanced resistance to necrotrophic pathogens and that basal resistance to different necrotrophs might depend on the extent of the cuticular damage.

In contrast to their response to necrotrophic pathogens, *LACS1*, *LACS2*, *LACS3*, *LACS7*, *LACS8* and *LACS9* were required for normal SAR; unlike wild-type, *lacs4* and *lacs6* plants, which showed ~10-fold reduced growth of virulent bacteria, the *lacs1, lacs2*, *lacs3*, *lacs7*, *lacs8* and *lacs9* mutants showed comparable growth of virulent bacteria in mock- or *avrRpt2*- inoculated plants (Figure 4.8A). Since G3P levels play a critical role in SAR (Chanda et al., 2011), I quantified G3P levels in petiole exudates collected from wild-type and *lacs* mutants inoculated with $MgCl_2$ or *avrRpt2* bacteria. The *lacs1*, *lacs2* and *lacs3* plants accumulated wild-type-like or higher levels of G3P, suggesting that the particular SAR defect in these is not associated with G3P metabolism (Figure 4.8B). In contrast, *lacs7*, *lacs8* and *lacs9* accumulated reduced levels of G3P after pathogen inoculation. To determine if, like *acp4*, a mutation in *lacs* compromised perception of the mobile signal in the distal tissues, I assayed SAR in response to petiole exudate collected from wild-type plants challenged with $MgCl_2$ or *avrRpt2* bacteria. Intriguingly, SAR was normal in *lacs2* and *lacs9* mutants, partial in *lacs1*, *lacs3* and *lacs7* but remained compromised in *lacs8* plants (Figure 4.8C). Together, these results suggest that LACS3, LACS7 and LACS8 are involved in the perception of G3P and/or other SAR signals and that perception of SAR signal(s) in the distal tissue is either dependent on the severity of cuticular defect and/or specific compositional changes in the cuticle.

To determine if compromised SAR in *lacs1, lacs3*, *lacs7* and *lacs8* mutants correlates with a defective cuticle, I monitored leaching of chlorophyll from the wild-type and

mutant plants. As shown earlier, *lacs2* leaves leached chlorophyll rapidly as compared to wild-type leaves (Bessire et al., 2007; Xia et al., 2009; Wang et al., 2010). In comparison, *lacs1, lacs3, lacs4, lacs6, lacs7* and *lacs8* leaves leached chlorophyll faster than wild-type but slower than *lacs2* plants (Figure 4.9A). These results suggest that mutation in *lacs* isoforms causes increased cuticular permeability. To ascertain this further, I analyzed the outermost cell wall of the epidermis by transmission electron microscopy (TEM). As expected, the cuticle of the wild-type leaf appeared as a continuous and regular electron-dense osmiophilic layer outside the cell wall (Figure 4.9B). Consistent with their increased chlorophyll leaching, *lacs* mutants showed varying levels of electron opaque cuticle, suggesting that *LACS* isoforms contribute to normal development of cuticle.

Discussion

The results presented in this chapter suggest that the plant cuticle, in addition to serving as a physical barrier, participates in specific responses leading to proper induction of SAR and basal defenses. Interestingly, several plant mutants defective in SAR show a normal response to necrotrophic pathogens. This suggests that components required for induction and/or establishment of SAR and basal defenses are mutually exclusive. Intriguingly, although the *lacs2* and *acp4* plants produced contrasting phenotypes in response to *B. cinerea*, they both showed compromised SAR. Clearly, increased resistance of *lacs2* to *B. cinerea* does not correlate with cuticular permeability since *acp4* shows susceptibility even though it contains a permeable cuticle. Likewise, the *gpat4 gpat 8* double-mutant plants contain a permeable cuticle but show increased susceptibility to the necrotrophic pathogen *Alternaria* (Li et al., 2007). Notably, *lacs2* plants show normal responses to *Alternaria* and several other necrotrophs. The enhanced resistance to *B. cinerea* can also be induced upon overexpression of fungal cutinase, which disrupts normal development of cuticle (Bessire et al., 2007; Sieber et al., 2000). These results suggest that levels of certain cuticular components, rather than cuticular permeability, might be required for resistance/susceptibility phenotypes against necrotrophic pathogens.

Unlike basal defense against necrotrophic pathogens, induction of normal SAR appears to correlate with cuticle permeability. In addition to *lacs* mutants, a mutation in *GL1*, *GL3*, *TTG3*, *CER1*, *CER3* and *CER4* also lead to increased cuticle permeability and compromised SAR (Xia et al., 2009; Xia et al., 2010). The variable extent of cuticular damage in *lacs*, *gl*, *cer* and *ttg3* mutants suggest that SAR is likely sensitive to minor alterations in the cuticle. This is further supported by the result that mechanical removal of cuticle compromised SAR without causing any major alterations in cutin monomer or wax compositions. While it is likely that the mechanical removal of cuticle produces effects that are separate from that of genetic mutations affecting cuticle development, it is important to note that SAR was impaired only if the cuticle was removed within 24 hr of primary infection but not later. This is further consistent with the time frame for transport of mobile signal to the distal tissues, both in Arabidopsis as well cucumber (this study and Rasmussen et al., 1991; Smith-Becker et al., 1998), and suggests that perception of the mobile signal by the cuticle of distal tissues is only relevant during the time frame of signal generation in response to primary infection.

Although *acp4* plants induced SAR in response to exudates collected from *avr*-infected *acp4* plants, it was not exactly comparable to that from wild-type plants (Xia et al., 2009). This suggests that ACP4- and/or cuticle-derived factor might participate in mobile signal generation. This is further supported by the observation that cuticle defective *lacs7*, *lacs7* and *lacs8* mutants showed reduced accumulation of G3P, a critical mobile inducer of SAR (Chanda et al., 2011). However, normal induction of G3P in *avr*-inoculated *lacs1*, *lacs2* and *lacs3* mutants suggests that induction of G3P might be regulated by one or more cuticular component(s) rather than cuticular permeability. Partial or no restoration of SAR when *lacs7* and *lacs8* mutants were treated with exudate collected from *avr*-inoculated wild-type plants, respectively, suggest that perception likely require factor(s) other than G3P.

At this stage the exact role of various LACS isoforms in cuticle formation remains unclear. The cuticular defect in *acp4* plants may be related to their reduced 16:0 levels. Indeed, 16:0 and 18:0 FAs serve as precursors for the synthesis of very long-chain FAs,

which in turn contribute to the synthesis of long-chain aliphatic compounds, the major components of cuticular wax (Samuels et al., 2008). In addition to serving as precursors for glycerolipid synthesis, short-chain FAs produced in plastids also act as precursors for the synthesis of hydroxy FAs, which form major components of the cutin polyester. Thus, reduced overall FA flux in acp4 plants is likely responsible for their defective cuticle. More work will be needed to determine the role of LACS isoforms in induction, establishment and perception of SAR.

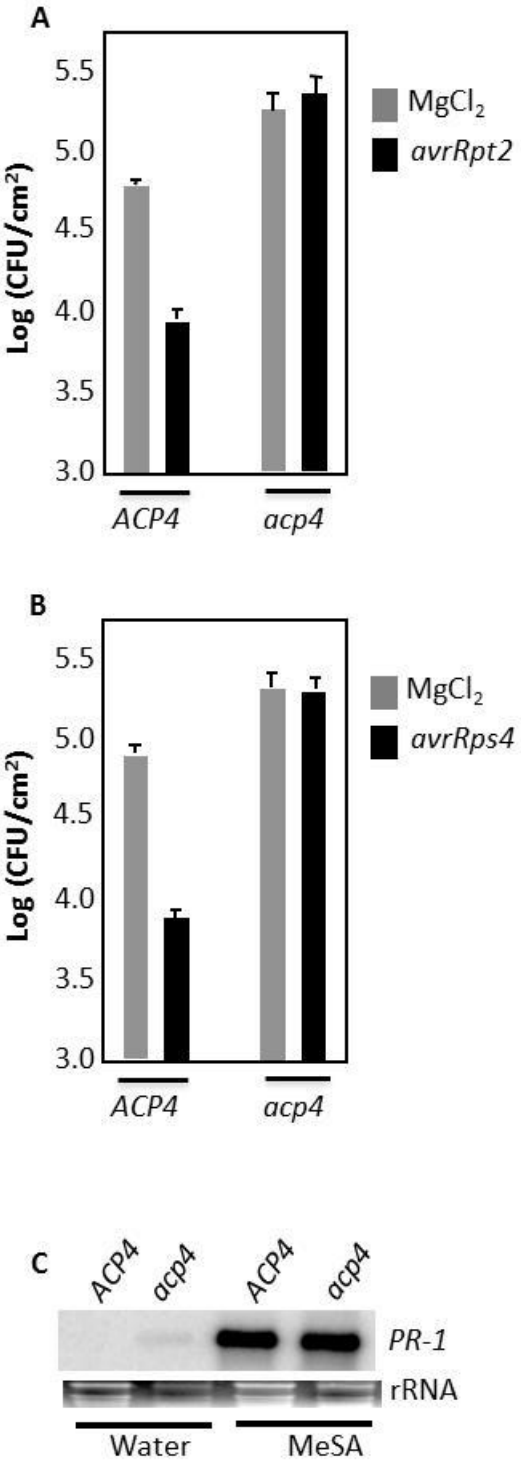

Figure 4.1. The *acp4* plants are compromised in SAR.

(**A and B**) SAR response in wild-type (*ACP4*; Nössen ecotype) and *acp4* plants. Primary leaves were inoculated with $MgCl_2$ (gray bars) or *P. syringae* expressing *avrRpt2* (black bars; **A**) or *avrRps4* (black bars; **B**) and the systemic leaves were inoculated 48 h later

with a virulent strain of *P. syringae*. The leaves inoculated with virulent bacteria were sampled at 3 dpi. The error bars represent SD. (**C**) RNA gel blot showing transcript levels of *PR-1* gene in plants treated with water or MeSA for 48 hr. Ethidium bromide staining of rRNA was used as a loading control.

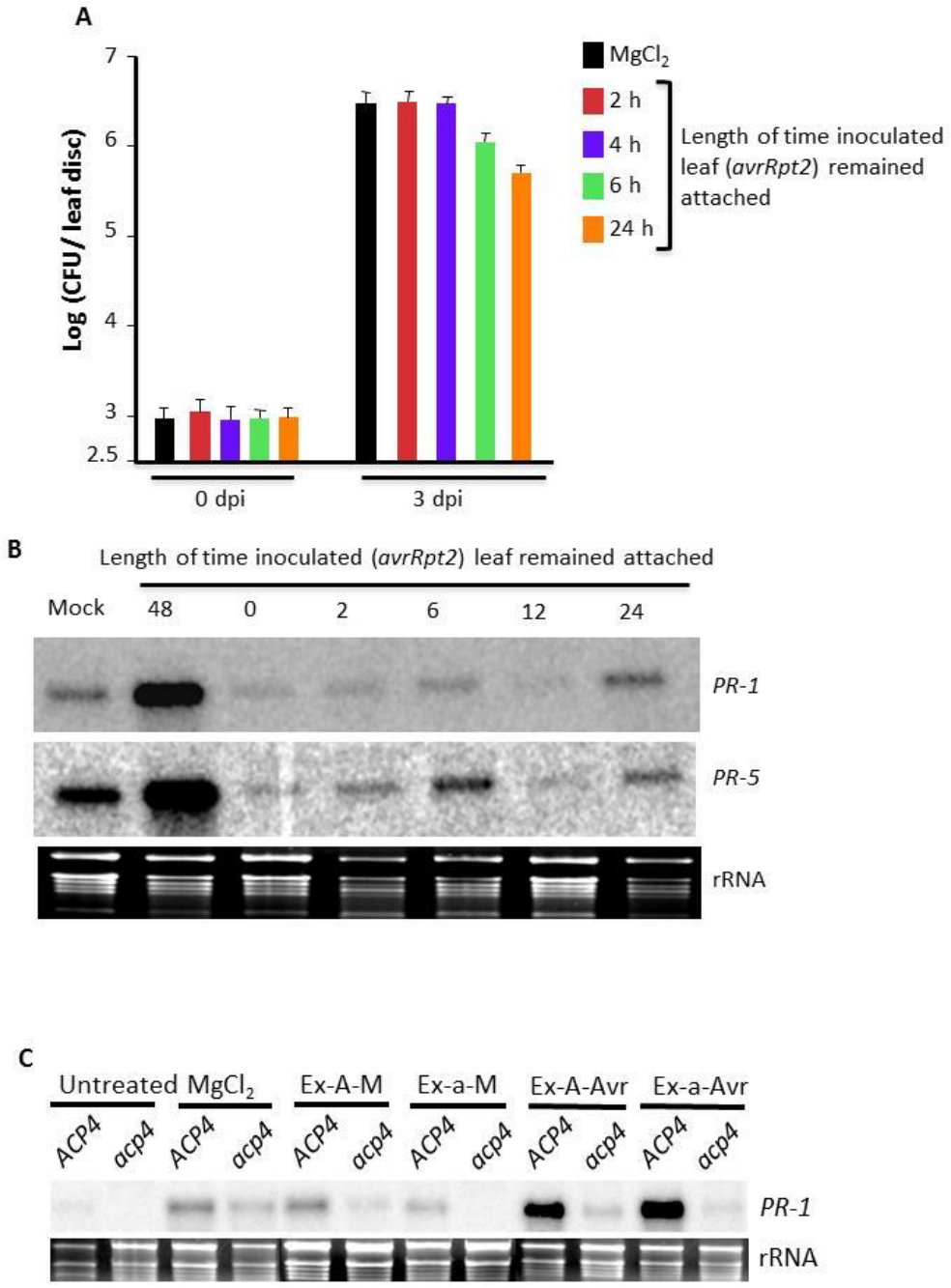

Figure 4.2. The *acp4* plants are unable to perceive SAR signal(s).

(**A**) Leaf detachment assay showing time-frame of SAR induction. SAR in wild-type plants (Col-0) inoculated with $MgCl_2$ or *avrRpt2*. The local leaves inoculated with *avrRpt2* were removed 2, 4, 6 or 24 h post inoculation. Two days later, the distal leaves were inoculated with virulent bacteria and growth of virulent bacteria was monitored at 0 and 3 dpi. The error bars represent SD. (**B**) Expression of *PR-1* and *PR-5* genes in distal tissues of mock- or *avrRpt2*-inoculated plants shown in A. Ethidium bromide staining of

rRNA was used as a loading control. (**C**) RNA gel blot showing transcript levels of *PR-1* gene in untreated or treated leaves of *ACP4* (A) and *acp4* (a). Leaves were infiltrated either with $MgCl_2$ or petiole exudates (Ex) and analyzed for *PR-1* transcript levels 48 hr after treatments. M and Avr indicate petiole exudates collected from leaves infiltrated with $MgCl_2$ or *P. syringae* expressing *avrRpt2*.

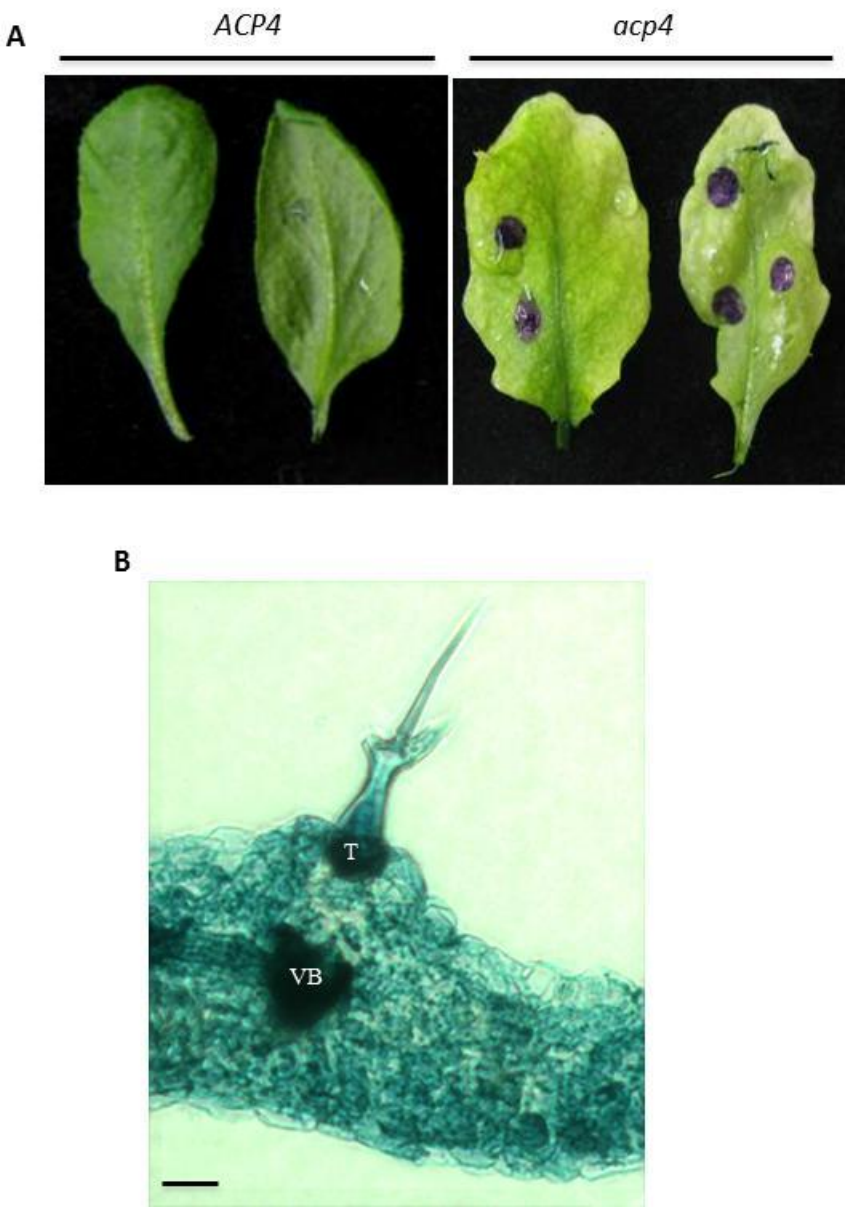

Figure 4.3. The *acp4* plants show permeable cuticle.

(**A**) Toluidine blue staining of wild-type (*ACP4*) and *acp4* leaves. Leaves were stained for 30 min and rinsed with distilled water. (**B**) Cross section of a leaf from *ACP4-GUS* transgenic line that was stained for GUS activity prior to sectioning. T and VB indicate trichome and vascular bundle, respectively (scale bar, 270 microns).

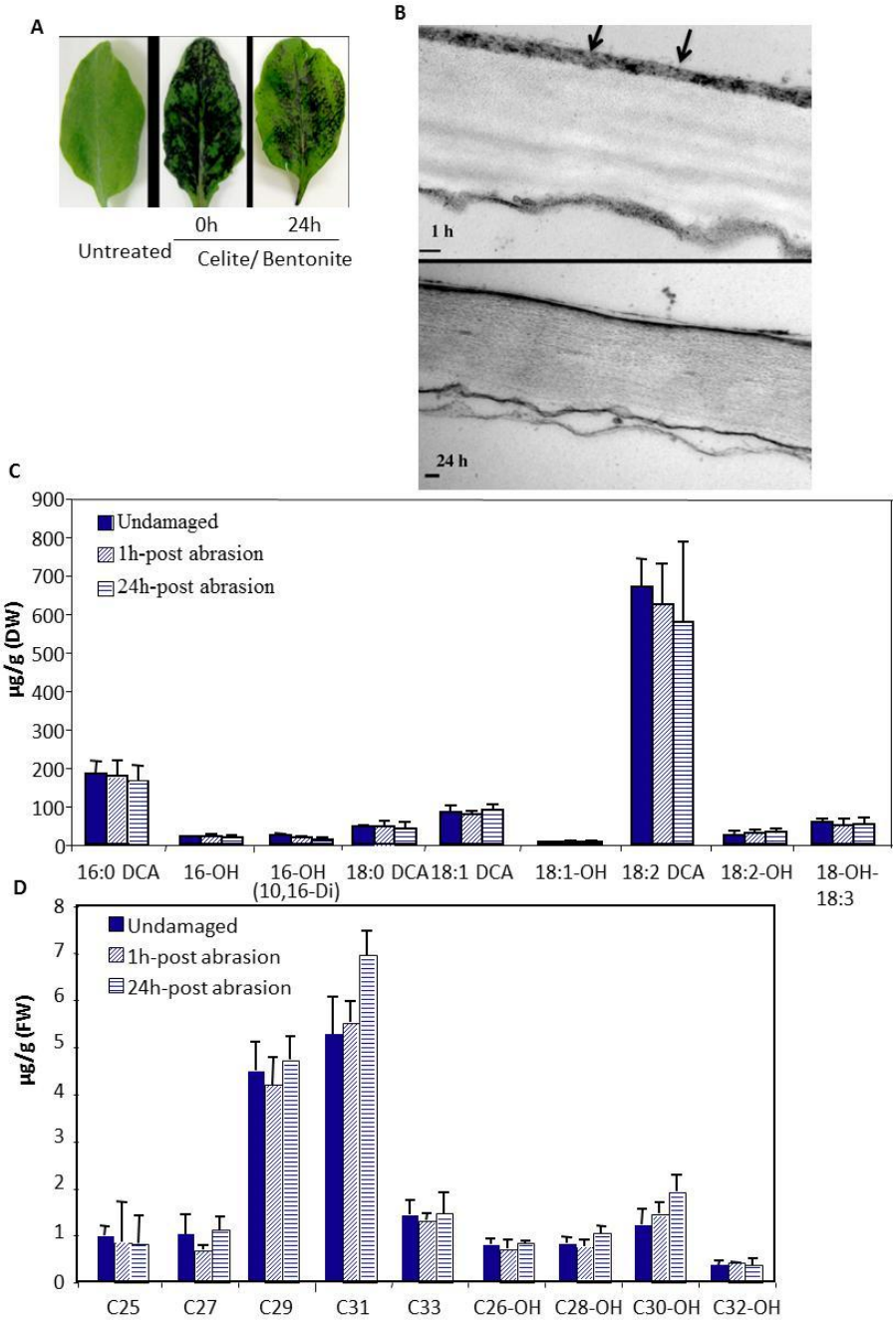

Figure 4.4. Cuticle phenotypes, SAR, and basal resistance in wild-type plants subjected to mechanical abrasion.

(**A**) Toluidine blue-stained leaves from intact or treated plants.

(**B**) Transmission electron micrographs showing cuticle layer on adaxial surface of wild-type (Nössen) plants 1 and 24 hr post abrasion. Arrows indicate electron-opaque regions [scale bars, 100 nm (1 hr) and 50 nm (24 hr)]. (**C**) Analysis of lipid polyester monomer content of wild-type plants before and after 1 and 24 h abrasion. Error bars represent SD.

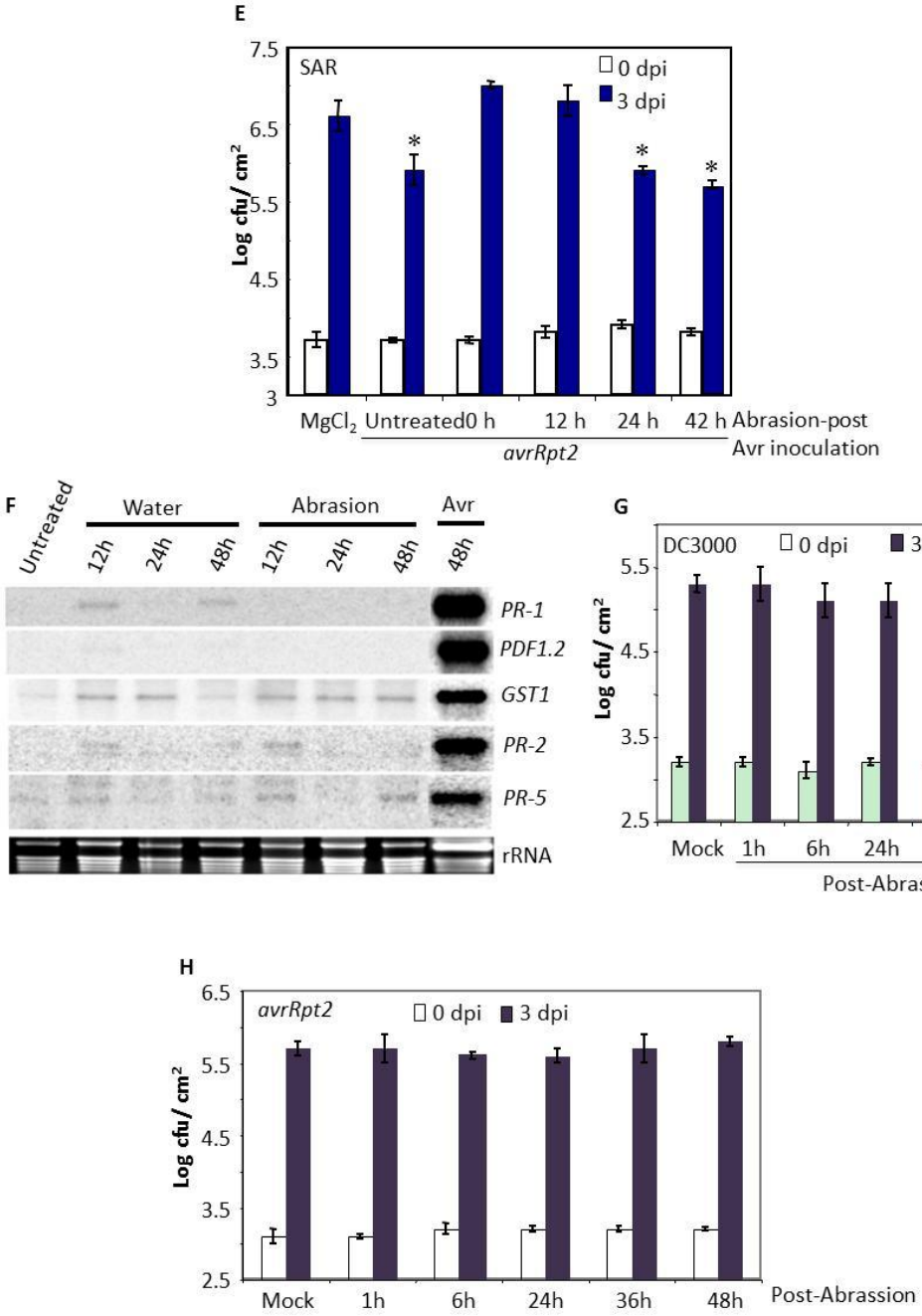

(**D**) Analysis of wax components from leaves of four-week old control and abraded plants 1 and 24 h post abrasion. C25-C33 are alkanes, C26-OH-C32-OH are primary alcohols.

(**E**) SAR in wild-type plants inoculated with $MgCl_2$ (mock) or *P. syringae* expressing *avrRpt2*. The distal leaves of a subset of plants were subjected to mechanical abrasion at 0, 12, 24 or 42 hr after inoculation of the avirulent pathogen in the primary leaves. The distal leaves in all plants were infiltrated with the virulent pathogen 48 hr after inoculation of the avirulent pathogen. Asterisks denote a significant difference with

$MgCl_2$, 0 or 12 hr infiltrated leaves (t test, $p < 0.05$). (**F**) (**G**) Basal resistance in wild-type plants subjected to mechanical abrasion. (**H**) *R*-mediated resistance response in wild-type plants subjected to mechanical abrasion. Plants in G and H were inoculated with virulent (**G**) or aviruent (**H**) bacteria and the leaves were sampled at 3 dpi. Error bars represent SD.

A

Gene	ID	Salk Line	Mutant Designation
LACS1(CER8)	At2g47240	Salk_127191	*lacs1-1* (Lu, 2009)
LACS2 (BRE1)	AT1G49430	GABI368C02	*lacs2-3* (Bessire, 2007)
LACS3	At1g64400	Slak_027707	*lacs3-1*
LACS4	At4g23850	Salk_101543	*lacs4-1*
LACS6	At3g05970	Salk_130541	*lacs6-1*
LACS7	At5g27600	Salk_146444	*lacs7-1*
LACS8	At2g04350	Salk_105118	*lacs8-1*
LACS9	At1g77590	CS2597	*lacs9-1* (Schnurr, 2002)

B

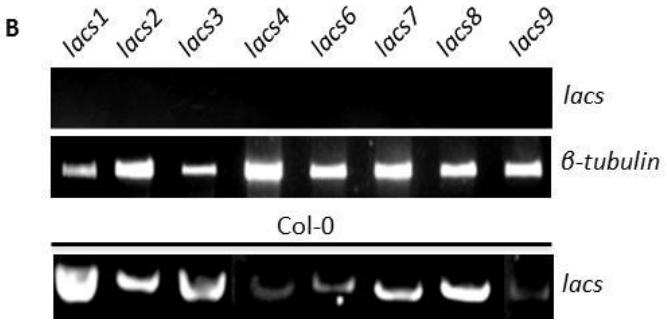

Figure 4.5. Isolation of *lacs* mutants.

(**A**) List of *LACS* genes and the respective SALK lines characterized in this study. (**B**) RT-PCR analysis showing expression levels of indicated *LACS* genes in the KO plants. Levels of *β-tubulin* were used as a loading control. The bottom panel shows expression levels of respective *LACS* genes in the RNA prepared from wild-type Col-0 plants.

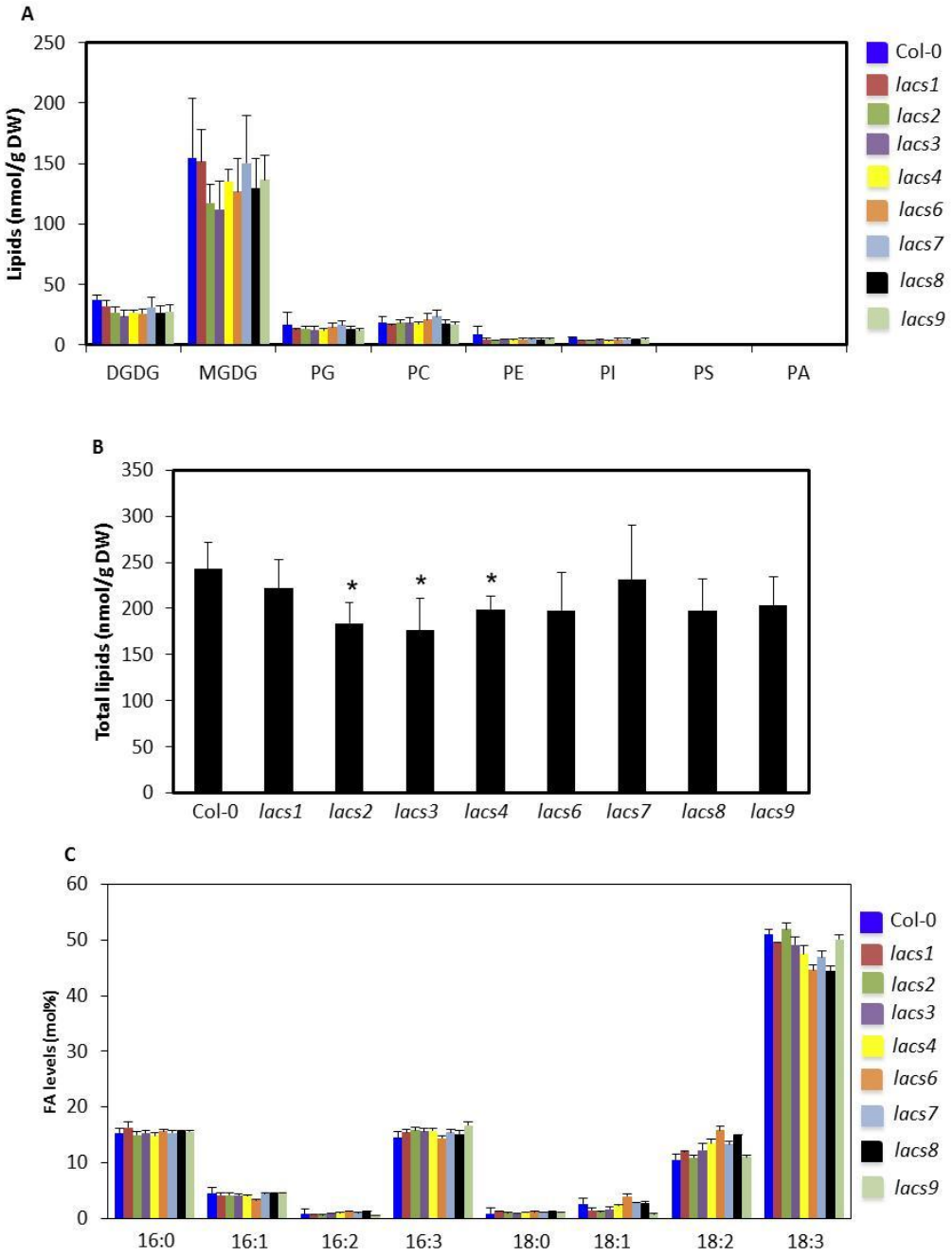

Figure 4.6. (**A**) Profile of total lipids extracted from wild-type (Col-0) and *lacs* plants. The values are presented as a mean of five replicates. The error bars represent SD. Symbols for various components are the following: DGD, digalactosyldiacylglycerol; MGD, monogalactosyldiacylglycerol; PG, phosphatidylglycerol; PC, phosphatidylcholine; PE, phosphatidylethaloamine; PI, phosphatidylinositol; PS, phosphatidylserine. (**B**) Total lipid levels in indicated genotypes. DW indicates dry weight. Asterisks denote a significant difference with wild-type (t test, $p < 0.05$). (**C**)

Levels of FAs in 4-week-old wild-type Col-0 or indicated *lacs* genotypes. The error bars represent SD.

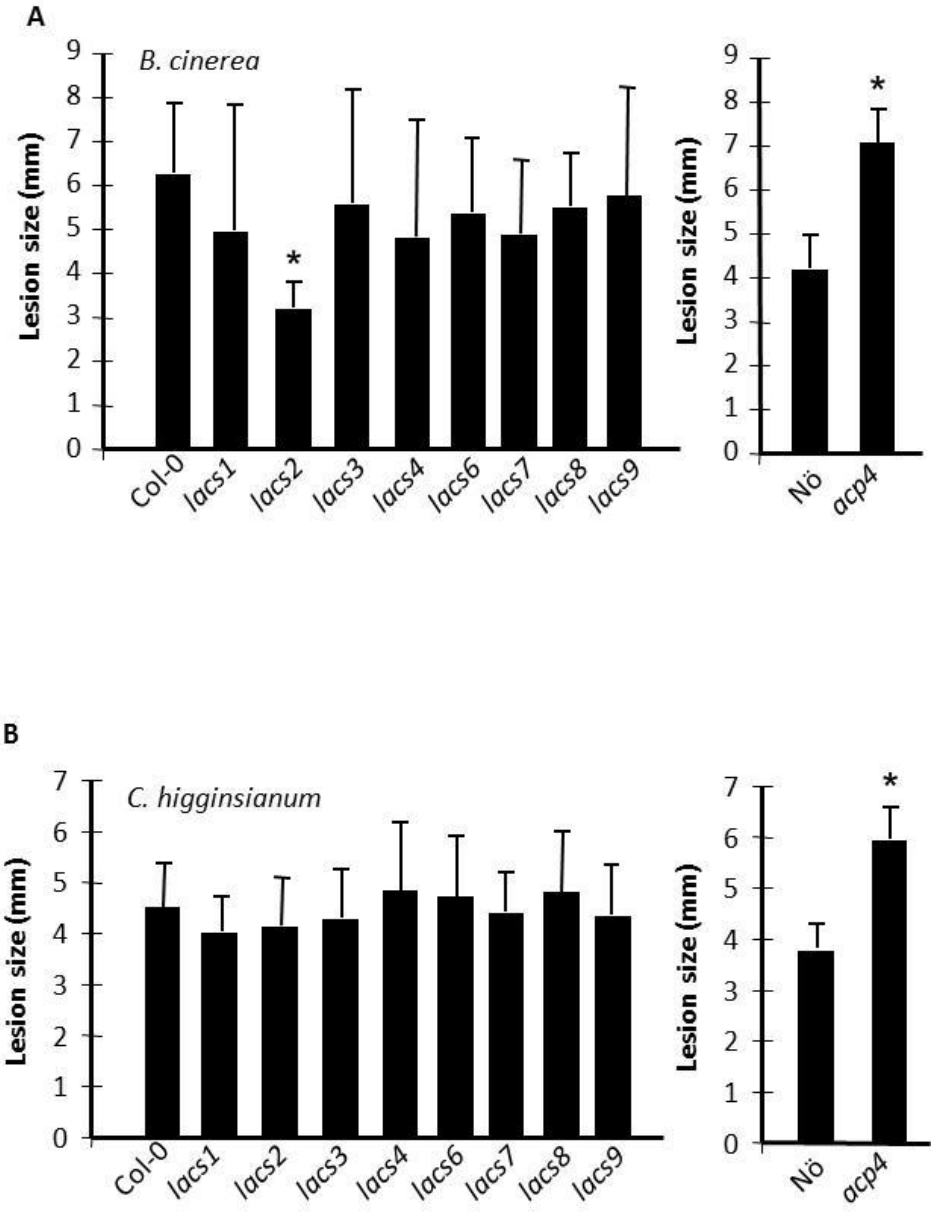

Figure 4.7. A mutation in majority of *LACS* gene does not impair resistance to necrotrophic pathogens.

(**A and B**) Lesion size in spot-inoculated genotypes. The plants were spot-inoculated with 10^6 spores/ml of *C. higginsianum* (**A**) or *B. cinerea* (**B**) and the lesion size was measured from 20-30 independent leaves at 6 dpi. Statistical significance was determined using Students *t*-test. Asterisks indicate data statistically significant from that of control (Col-0 or Nossen) ($P<0.05$). Error bars indicate SD.

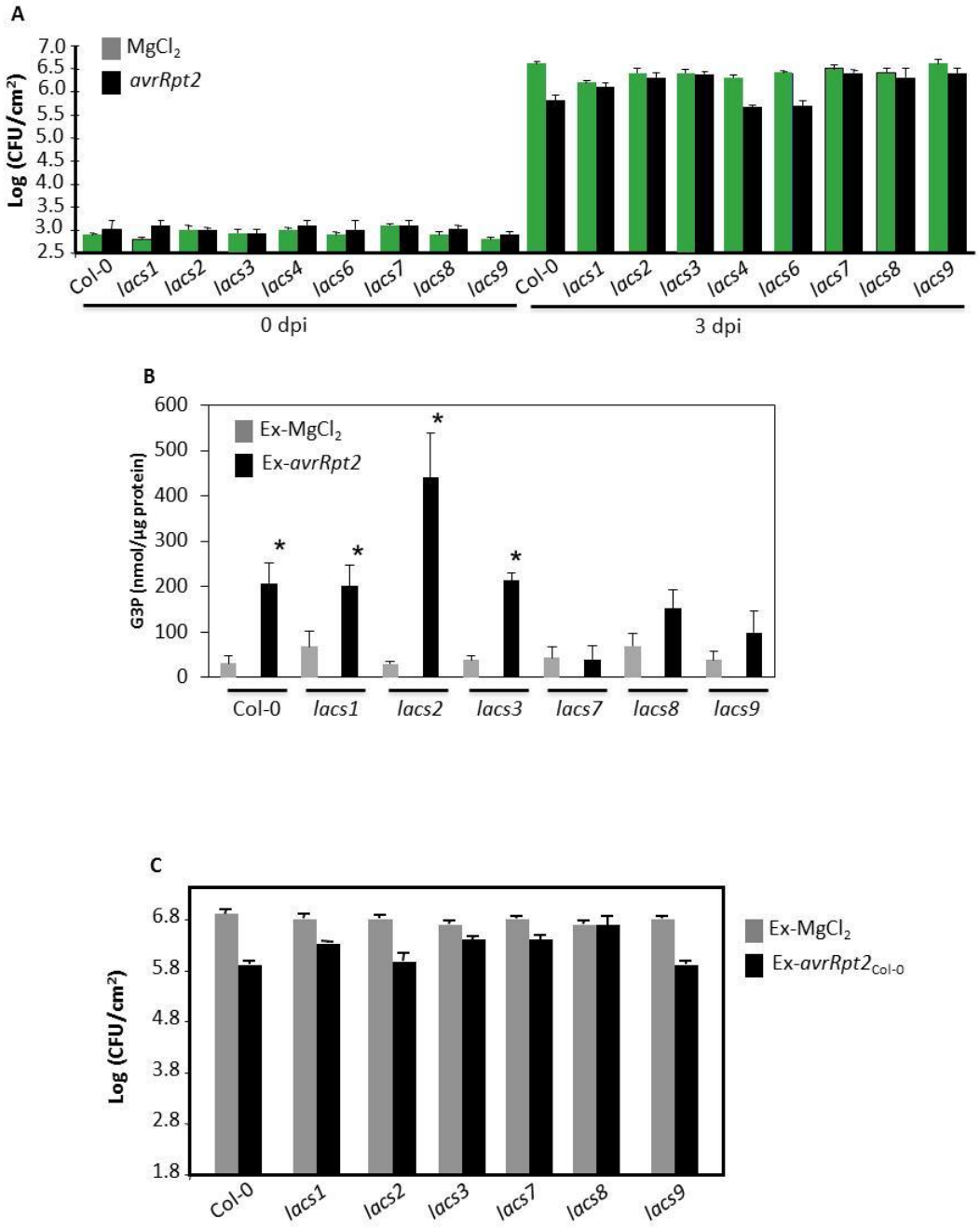

Figure 4.8. A mutation in majority of *LACS* genes compromises SAR.

(**A**) SAR response in indicated genotypes. The leaves were infiltrated with $MgCl_2$ or an avirulent strain of *P. syringae* expressing *avrRpt2* and 48 hr later systemic leaves of all plants were challenged with a virulent strain of *P. syringae* (DC3000). The proliferation of virulent bacteria was monitored at 0 and 3 days post inoculation (dpi). (**B**) Levels of G3P in petiole exudates collected from leaves infiltrated with $MgCl_2$ or an avirulent strain of *P. syringae* expressing *avrRpt2*. Asterisks indicate data statistically significant

from that of $MgCl_2$ infiltrated leaves ($P<0.05$). Error bars indicate SD. (**C**) SAR response in Col-0 and indicated *lacs* genotypes infiltrated with exudates collected from Col-0 plants that were treated either with $MgCl_2$ or *avrRpt2* bacteria. Error bars indicate SD.

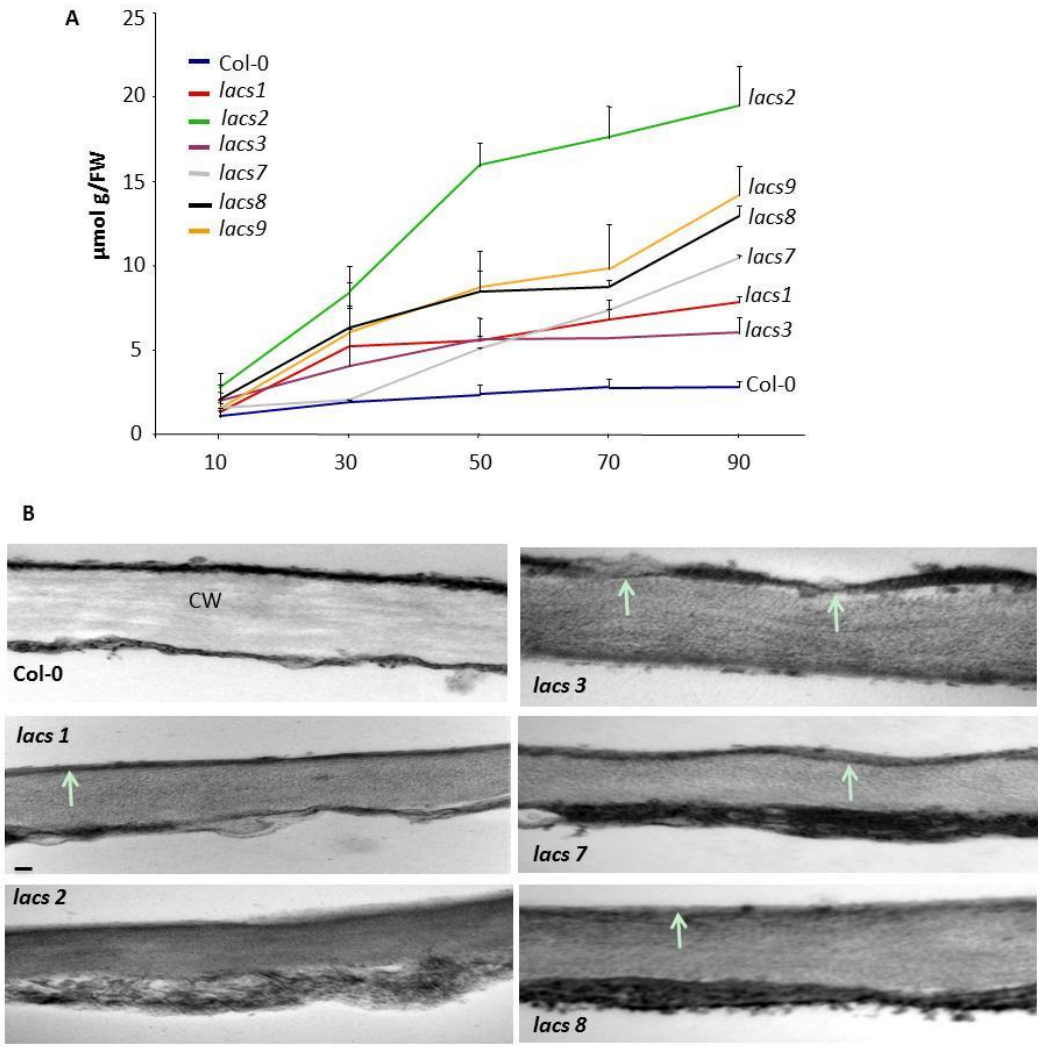

Figure 4.9. A mutation in *lacs3, lacs7* and *lacs8* affects normal development of cuticle.

(**A**) A time-course measurement of chlorophyll leaching in indicated genotypes. Error bars indicate SD. (**B**) Transmission electron micrographs showing the cuticle layer on the adaxial surface of leaves from indicated genotypes. Arrows indicate electron-opaque regions. CW indicates cell wall (scale bars, 50 nm).

CHAPTER FIVE

GLYCEROL-3-PHOSPHATE MEDIATES BASAL DEFENSE AGAINST NECROTROPHIC PATHOGENS

INTRODUCTION

Plant fungal pathogens have evolved different types of lifecycles, such as those of obligate biotrophy, hemibiotrophy and necrotrophy, to adapt to their hosts (Glazebrook J., 2005). Obligate biotrophic pathogens only infect, colonize and grow on the living host tissues, whereas necrotrophic pathogens infect and kill the living host tissues and obtain nutrients from the dead tissues. Hemibiotrophic pathogens have combined strategies; they initiate infection on living tissues then switch to a necrotrophic growth stage at a later time point to feed on dead tissues. The mechanisms underlying in these varied strategies for infection are largely unknown.

Botrytis cinerea (teleomorph: *Botryotinia fuckeliana*), the causal agent of grey mold disease, is the most destructive necrotrophic phytopathogen worldwide. Recent phylogenetic studies showed that there are 22 species in the genus *Botrytis*, and most of them have a narrow host range except *Botrytis cinerea* (Staats et al., 2005). This ascomycete pathogen can infect more than 200 crop species, including vegetables, fruits, oil crops and forages, and cause heavy losses during the growing season and post-harvest (Choquer et al., 2007). In nature, sclerotia, the survival structures which produce conidiophores, together with mycelia that survived in the dead infected tissues of the host, serve as the primary inoculum for subsequent infections (Beever and Weeds, 2004). Typically, conidia generated by conidiophores are transmitted to the host surface by air currents or water splash. Under proper conditions, conidia start the penetration, followed by primary lesion formation, lesion expansion and sporulation, and complete the infection cycle (Van Kan, 2006). The infections can start from seeds, wounded tissues, senescent leaves, or ripen fruits, and the symptoms caused by *B. cinerea* are quite variable depending on the tissues types and environmental conditions (Williamson et al.,

1995). The most typical symptom is grey mold, indicating masses of grey colored conidia in the infection sites.

The success of this very important fungal pathogen, *B. cinerea*, is largely attributed to its powerful arsenal of weapons. During the infection process, *B. cinerea* can secrete a combination of cell wall degrading enzymes, peptidases, effector proteins and toxins, and these compounds effectively contribute to its virulence (Williamson et al., 2007; Amselem et al., 2011). For penetrating the host surface, the first step of the infection cycle, might not require physical pressure (Tenberge, 2004). To break the plant cuticle layer, *B. cinerea* appressoria secrete many degrading enzymes such as cutinase and lipase (Reis et al., 2005), and induce an apoplastic oxidative burst with reactive oxygen species (ROS)-generating enzymes such as superoxide dismutase (Rolke et al., 2004). Upon breaking the cuticle layer, appressoria secrete hundreds of cell wall degrading enzymes, such as pectinases and cellulases, to breakdown the host cell wall complex (Wubben et al., 1999; Kars et al., 2005; Brito et al., 2006). Besides these degrading enzymes, *in planta*, *B. cinerea* produces an important cofactor, oxalic acid (Verhoeff et al., 1988). Oxalic acid can create a low pH environment and optimize the activities of many secreted enzymes around the infection site, especially for the cell wall degrading enzymes (Deighton et al., 2001; Manteau et al., 2003). In addition, *B. cinerea* also produces many phytotoxic compounds that lead to host cell death; for example, botrydial, which can facilitate the penetration and colonization in a light-dependent manner (Colmenares et al., 2002).

B. cinerea poses special challenges to pathologists, breeders and growers due to its long-lived survival structures, wide host range, and high variability in strains and populations. In the last twenty years, considerable efforts were invested to study this necrotrophic pathogen in various aspects, including biology, epidemiology and disease management, especially related to its pathogenicity (Backhouse et al., 1984; Beever et al., 1989; Beever and Weeds, 2004; Berrie et al., 2002; Broome et al., 1995; Catlett et al, 2003; Leroux, 2004; Rolland et al., 2003). Recently, two *B. cinerea* strains, B05.10 and T4, were sequenced by the Broad Institute (http://www.broadinstitute.org) and Genoscope (http://www.cns.fr/externe/English/corps_anglais.html), respectively, and a

comprehensive genomic analysis of *B. cinerea* and *Sclerotinia sclerotiorum* revealed a clear picture of gene organization, gene content and predictive gene function in these two closely related necrotrophic pathogens (Amselem et al., 2011). Together, all these studies will help us to better understand the phytopathology of this successful fungal pathogen in the future.

Another aspect of this interaction is the host defense mechanisms utilized to defend against this pathogen. Plant hosts actively defend themselves at various levels. Besides the performed physical barriers, one of the early events in defense responses is cell wall modifications, which can prevent or slow down primary infection (Dixon and Pavia, 1995; van Baarlen et al., 2004). The infection can also trigger an oxidative burst in the host cells, and the plant plasma membrane-associated NADPH-dependent oxidases are required in this progress (Muckenschnabel et al., 2003; Lyon et al., 2004). The generation of ROS by plant cells is thought to induce the hypersensitive response (HR) and limit the colonization of biotrophs. Conversely, *B. cinerea* triggers HR leading to host cell death, which further facilitates fungal colonization. In Arabidopsis, the mutants which have changes in sensitivity to ROS or ability to develop HR showed different response to *B. cinerea* (Govrin and Levine, 2000; Hoeberichts et al., 2003; van Baarlen et al., 2007). In addition, plants also produce some antifungal compounds that inhibit fungal growth. One example is camalexin (3-thiazol-20-yl-indole) (Glawischnig, 2007). Originating from tryptophan, the biosynthesis of camalexin is induced by *B. cinerea* infection and several genes, including *PAD3* (phytoalexin deficient mutant 3), involved in camalexin biosynthesis were identified (Glazebrook and Ausubel, 1994; Glazebrook et al., 1996; Glawischnig et al., 2004; Hull et al., 2000; Mikkelsen et al., 2000). The toxic activity of camalexin is associated with disruption of fungal membrane integrity (Rogers et al., 1996). Meanwhile, many studies have showed that phytohormone-mediated pathways, such as salicylic acid (SA), jasmonic acid (JA) and ethylene, are required in basal defense to *B. cinerea* (Thomma et al., 1998, 1999, 2001; Alonso et al., 2003; Ferrari et al., 2003). In Arabidopsis, after *B. cinerea* infection, ~ 200 of 621 up-regulated genes are related to SA-, JA- and ethylene-mediated signaling pathways (AbuQamar et al., 2006).

Classical studies in plant pathology implied defense-signaling pathways as separate from primary metabolism in plants. However, recent evidence implicates a number of primary metabolic pathways and their components as interfacing with plant defense. Studies in Dr. Aardra kachroo's laboratory have demonstrated novel roles for primary metabolites, such as fatty acids and components of glycerolipid metabolism, in mediating plant defense against a variety of pathogens. Characterizing the roles of various primary metabolic components is particularly attractive as it will enable the development of novel and sustainable strategies for crop improvement.

G3P is a conserved metabolite in many organisms. In plants, G3P is generated through glycerol via glycerol kinase (*GK*), or the reduction of dihydroxyacetone phosphate (DHAP) via G3P dehydrogenase (*G3Pdh*) (Figure 5.1). The plastidal G3P acyltransferase (*ACT1*) is another enzyme tightly associated with G3P metabolism because it acylates G3P with the fatty acid oleic acid (18:1) to form lyso-phosphatidic acid. This is the first committed step for lipid biosynthesis via the prokaryotic pathway in plants. G3P metabolism is important also for maintaining the homeostasis of other primary metabolites, such as fatty acids, lipids and sugars. Previously, our laboratory reported that cellular G3P levels were induced in *Arabidopsis* in response to the hemibiotrophic pathogen, *Colletotrichum higginsianum,* and increased accumulation of G3P enhanced resistance to this pathogen. This G3P-mediated induction of basal defense is independent of signaling induced by the defense-related phytohormones SA, JA, and ethylene (Chanda et al., 2008). Although different pathogens evolve specific features contributing to pathogenicity, many of them also share conserved mechanisms (Choquer *et al.* 2007). Therefore, it is reasonable to speculate that this G3P-mediated basal defense might also protect against true necrotrophs. In this study, I have shown the role of G3P and its metabolizing enzymes in mediating defense against the necrotrophic pathogens, *B. cinerea.*

RESULTS/DISCUSSION

Mutations in Arabidopsis G3P synthesizing enzymes are associated with increased susceptibility to *Botrytis*

Previous research work in Dr. Pradeep Kachroo's laboratory showed that G3P level is important for basal defense to hemibiotrophic fungal pathogen, *C. higginsianum*, in *Arabidopsis*. Here, I evaluated whether G3P contributes to defense against the important necrotrophic pathogen, *B. cinerea*. I evaluated the response of different Arabidopsis mutants defective in G3P biosynthesis. Compared with wild-type (Col-0), the *gly1* and *gli1* mutants showed more severe symptoms when spray-inoculated (whole plant spray with spores) with *B. cinerea*, and the *act1* mutant showed increased resistance to the infection (Figure 5.2 A). In spot-inoculation (localized application of spores), the lesion sizes in the *gly1* and *gli1* mutants were significantly different than with wild type (Figure 5.2 B). Proliferation of the fungus was facilitated in the *gly1* and *gli1* mutants, but was comparatively limited in the *act1* mutant. To estimate the extent of fungal growth in the different genotypes, I amplified the actin gene of *B. cinerea* from RNA of infected plant tissue at 0 and 3 dpi. Amplification of the Arabidopsis β-tubulin gene was used as control for RNA levels (Figure 5.2 C). In comparison to wild type, the *gly1* and *gli1* mutants supported more fungal growth, but not the *act1* mutant. Interestingly, the *gli1* mutant showed more susceptibility to *B. cinerea* than the *gly1* mutant (Figure 5.2 A and B). Since both GLY1 and GLI1 are involved in G3P generation, I generated the *gly1 gli1* double mutant and challenged the double mutant with *B. cinerea* (Figure 5.2 D and E). Compared to the wild type and the single *gli1* and *gly1* mutants, the *gly1 gli1* double mutant showed significantly more severe symptoms in spray inoculation and developed larger-sized lesions after spot inoculation. Together, these results suggest that, although the relative contribution of the GLI1-catalyzed reaction was more in defense against *B. cinerea*, both GLI1 and GLY1 contributed additively to defense against this fungus. Furthermore, as in the case of *C. higginsianum*, a mutation in *ACT1* enhanced resistance to *B. cinerea* in Arabidopsis.

To test whether changes in host G3P metabolism affected pathogen entry or pathogen proliferation, I monitored fungal growth on leaf petioles at 12 h, 24 h and 48 h post inoculation (hpi). Both germination and growth of primary fungal mycelia were facilitated in the *gly1 gli1* mutant (Figure 5.2 F). These results strongly support the assumption that G3P levels are important for basal defense to *B. cinerea*, since both GLY1 and GLI1 are required for G3P synthesis in Arabidopsis.

Exogenous application of G3P rescues the enhanced susceptibility phenotype of the *gli1* and *gly1* mutants

To investigate further the above assumption, I estimated G3P levels in the Col-0, *act1*, *gly1* and *gli1* plants at 0 h and 72 hpi with *B. cinerea* (Figure 5.3 A). The G3P levels increased ~ 4- and 5- fold at 72 hpi in Col-0 and the *act1* mutant, respectively. In contrast, induced G3P levels were significantly lower in both *gly1* and *gli1* mutant plants. This result indicated that *B. cinerea* infection induced the accumulation of G3P in *Arabidopsis*. This result also indicated that the pathogen-induced accumulation of G3P was impaired in the *gly1* and *gli1* mutants, which lack enzymes responsible for G3P biosynthesis.

Another possibility was that in the *gli1* mutant, increased basal levels of glycerol (Chanda B. et al., 2008) contributed to enhanced susceptibility. A mutation in *GLI1* results in the accumulation of glycerol because GLI1 utilizes glycerol to generate G3P. To distinguish whether the reduced G3P or increased glycerol in the gli1 mutant contributed to its enhanced susceptibility to *B. cinerea,* I used exogenous glycerol application to study the effect on pathogen resistance in various mutant backgrounds. I sprayed Col-0, *act1*, *gly1,* and *gli1* plants with 50 mM glycerol followed by inoculation with *B. cinerea* 24 h after the glycerol application. If high glycerol enhanced susceptibility, it would do so in the wild type and all the mutant backgrounds. On the other hand, if G3P contributed to defense, gli1 mutant plants would not be altered in their response, since GLI1 is required to convert the exogenously applied glycerol into G3P (Aubert et al., 1994). Interestingly, Col-0 and *gly1,* but not *act1,* plants showed enhanced resistance to *B. cinerea* when

pretreated with glycerol (Figure 5.3 B and C). In contrast, the glycerol-treated *gli1* plants were as susceptible to *B. cinerea* as their water-treated counterparts. This result supported the notion that exogenous glycerol was converted to G3P and the increased G3P conferred enhanced resistance to *B. cinerea* in wild type and *gly1* plants. The increased susceptibility of the *gli1* mutant was caused by the failure to convert glycerol to G3P, not its high endogenous glycerol levels. To further test the role of G3P in basal defense to *B. cinerea*, I infiltrated 100 µM G3P into the Col-0, *act1*, *gly1* and *gli1* plants and inoculated *B. cinerea* 24 h later. The exogenous application of G3P enhanced the resistance in all four genotypes, especially in the *gly1* and *gli1* mutants (Figure 5.3 D). Meanwhile, the exogenous application of glucose, which is a good carbon source for *B. cinerea*, on Col-0 plants supported fungal growth (Figure 5.3 E). Infiltration of water or G3P did not induce the expression of pathogenesis-related genes such as *PR-1* or *PDF1.2* in Arabidopsis (Figure 5.3 F) indicating that these treatments did not affect resistance due to induction of the SA- or JA-mediated pathways.

Overexpression of *GLY1* and *GLI1* genes confer enhanced resistance to *B. cinerea*

To further test the hypothesis that increased G3P levels are associated with enhanced resistance to *B. cinerea*, I cloned the *GLY1* and *GLI1* genes into the *pBAR1* vector, under control of the cauliflower mosaic virus 35S promoter. Each construct was transformed into wild-type (Col-0) plants. The transgenic plants overexpressing *GLY1* or *GLI1* showed similar morphology as wild type. The T2 plants showing high expression level of *GLY1* or *GLI1* gene were selected for further experiments. In spray inoculation, compared with the wild type, the 35S *GLY1* or 35S *GLI1* plants supported much reduced fungal colonization and growth (Figure 5.4 A). After spot inoculations, the fungal growth and proliferation were significantly reduced in the 35S *GLY1* or 35S *GLI1* plants in comparison to Col-0, *gly1* or *gli1* plants (Figure 5.4 B). To test whether overexpression of the *GLY1* gene could rescue resistance in the absence of *GLI1* function, I generated *gli1* 35S *GLY1* lines and estimated pathogen response in these plants. Interestingly, in spray inoculation, the *gli1* 35S *GLY1* lines still showed better resistance than the *gli1* mutant and performed similar to wild-type plants. This result was further confirmed in

spot-inoculation tests on leaf petioles in different genotypes (Figure 5.4 C). This indicated that the *GLY1* and *GLI1* genes have additive effects in contributing to G3P accumulation after *B. cinerea* infection and that *GLI1* has a more significant contribution than *GLY1*.

Exogenous G3P affects *Botrytis cinerea* growth

Some fungal pathogens could obtain primary metabolites from host cells as carbon sources and support their growth (Wei et al., 2004). This suggested that pathogens can uptake metabolites from the plant host actively or inactively. Since the G3P levels were induced in plants after *B. cinerea* infection and the accumulation of G3P was associated with enhanced resistance, there was the possibility that the influx of host-generated G3P into the fungal pathogen affected its pathogenicity. To test this, I performed an *in vitro* G3P assimilation assay (Figure 5.4 A). The spores of *B. cinerea* (10^5 /mL) were cultured in 20 mL liquid CD (Czapek-Dox) minimal medium for 7 days and different amounts of [^{14}C]-G3P (55 μCi/ umol) were added to the liquid culture. The DPM values (disintegrations per minute) of fungal extracts indicated that labeled G3P in the medium was utilized by *B. cinerea*. Next, I separated the extracts on TLC plates together with [^{14}C]-G3P as standard (Figure 5.5 B). Along with the [^{14}C]-G3P band, G3P derivatives in the fungus also showed on the TLC plate. Furthermore, I tested the effect of G3P on fungal growth *in vitro* assay (Figure 5.5 C). In liquid culture, the fungal growth was inhibited when G3P or G3P plus sucrose were supplied as carbon sources. Together, these results suggest that exogenous G3P could affect growth of *B. cinerea*.

Increased G3P restores basal resistance to *Botrytis* in camalexin-deficient plants

Camalexin, a well-known phytoalexin, contributes to resistance against *B. cinerea* (Glazebrook and Ausubel, 1994; Veronese et al., 2004). To test whether the G3P-metabolic mutants *act1*, *gly1* and *gli1* were altered in camalexin accumulation after pathogen infection, I measured the camalexin levels in these plants at 0 h and 72 hpi and compared them to those in wild-type plants (Figure 5.6 A). In comparison to their basal

levels, camalexin levels were significantly induced in wild type as well as mutant plants after infection. Moreover, induced camalexin levels were highest in the *gli1* mutant compared to other genotypes, even though these plants were the most susceptible to *B. cinerea*. These results implied that camalexin biosynthesis was not reduced in the *act1*, *gly1* or *gli1* mutants, and that the enhanced resistance of the *act1* plants, or the increased susceptibility of the *gly1* and *gli1* plants to *B. cinerea*, was unlikely to be due to changes in camalexin biosynthesis.

Next, to determine the relationship between G3P- and camalexin-derived resistances to *B. cinerea*, I generated the *act1 pad3* double mutant and checked pathogen response in these plants (Figure 5.6 B and C). In spot inoculation, the *pad3* mutant showed increased susceptibility to *B. cinerea* as reported previously (Nafisi et al., 2007). In contrast, smaller lesions were detected in the *act1 pad3* mutants and these were comparable to those in wild-type plants. In addition, *PR-1* gene expression was similar in the Col-0, *act1*, *pad3* and *act1 pad3* plants after spray inoculation (Figure 5.6 H). To further confirm this result, I infiltrated water or 100 μM G3P into the *pad3* mutant, followed by spot inoculation 24 h post treatment. As expected, the G3P-infiltrated *pad3* plants showed significantly smaller lesions than water-infiltrated plants (Figure 5.6 D and E). I also challenged the *act1 pad3* double mutant with another important necrotrophic pathogen, *Alternaria brassicae*. In spot inoculation, I found the *act1 pad3* mutants reacted similarly to wild-type plants, developing smaller lesions than those in the *pad3* mutant (Figure 5.6 F and G). These results suggest that the *act1* mutation or exogenous application of G3P could rescue resistance to necrotrophic pathogens in a camalexin-deficient background, and that the G3P-associated resistance to *B. cinerea* acted independent or downstream of the *PAD3*-mediated pathway.

Increased susceptibility in the *gly1* or *gli1* mutants is not due to defect in the SA pathway

Basal resistance to *B. cinerea* is known to require SA-mediated signaling (Ferrari et al., 2003). Therefore, I evaluated whether the increased susceptibility to *B. cinerea* in the

gly1 and *gli1* mutants was due to a defect in the SA pathway. First, I generated *act1 sid2* and *gly1 sid2* double mutants, since SID2/ICS1 (isochorismate synthase) is the key enzyme in SA biosynthesis in Arabidopsis (Nawrath and Métrauxref, et al., 1999). In spot-inoculation assay, compared to wild-type plants, the *sid2* single mutant developed larger sized lesions. Furthermore, the *gly1 sid2* plants developed even larger-sized lesions than the *sid2* single mutant (Figure 5.7 A). Conversely, the *act1* mutation partially rescued resistance to *B. cinerea* in the *sid2* background (Figure 5.7 A). These results suggest that *GLY1* and *SID2* function additively in defense against *B. cinerea*. Next, I checked *PR-1* expression in Col-0, *act1*, *gly1* and *gli1* plants after infection by *B. cienrea*, since *PR-1* is a molecular marker for the SA pathway. In Northern blot analysis, all genotypes showed similar levels of *PR-1* transcript induction in response to spray inoculation with *B. cienrea* (Figure 5.7 B). I also quantified levels of SA and its glucoside, SAG, in Col-0, *act1*, *gly1* and *gli1* plants after spray inoculation. The SA/SAG levels were significantly induced in Col-0, *act1*, *gly1* and *gli1* plants compared to water-treated plants. Induced SA/SAG levels in the *act1*, *gly1* and *gli1* mutants were similar or slightly higher than those in wild type plants (Figure 5.7 C and D). Finally, I pretreated (spray treatment) Col-0, *gly1* and *gli1* plants with water or 500 μM SA, and monitored the effect on pathogen response in these genotypes. After SA treatment, all the genotypes showed enhanced resistance to *B. cinerea* compared to water treated plants. However, SA-treated *gly1* and *gli1* mutants developed larger lesions than the SA-treated wild-type plants. This result indicates that exogenous application of SA could only partially restore basal resistance in the *gly1* and *gli1* mutants.

In summary, my results suggest that the SA pathway, including SA perception, SA accumulation, and SA signaling, are not defective in the *gly1* and *gli1* mutants and G3P-mediated resistance functions independently or downstream of the SA pathway.

Increased susceptibility in the *gly1* or *gli1* mutants is not due to increased sensitivity to reactive oxygen species

It is well known that some necrotrophic pathogens such as *B. cinerea* can generate reactive oxygen species (ROS) themselves, or induce ROS production in the host cells. Increased ROS facilitates hypersensitive response (HR) and cell death, which in turn promote necrotrophic pathogen proliferation (Govrin and Levine, 2000; Mengiste et al., 2003; Rolke et al., 2004). To test whether increased ROS levels or increased sensitivity to ROS contributed to *GLY1*- or *GLI1*-mediated defense against *B. cinerea*, I quantified H_2O_2 levels in Col-0, *act1*, *gly1,* and *gli1* plants upon infection with *B. cinerea*. The basal H_2O_2 levels in water-treated plants were similar in all the genotypes. The induced H_2O_2 levels were slightly higher in the *gly1* and *gli1* mutants, but this increase was not statistically significant (Figure 5.7 F). To test the sensitivity of these plants to ROS, I treated Col-0, *act1*, *gly1,* and *gli1* plants with Paraquat (*N*, *N*′-dimethyl-4, 4′-bipyridinium dichloride), a chemical that promotes ROS accumulation by inhibiting electron transport during photosynthesis (Castello et al., 2007). The leaves were spotted with 10 µL of 10 µM Paraquat and the lesion size was measured 24 h post treatment. The *gly1* and *gli1* mutants showed similar-sized lesions as wild-type plants (Figure 5.7 G). Similar results were obtained when Col-0, *act1*, *gly1* and *gli1* plants were spray-treated with water or H_2O_2 (25 µM). These results indicate that the *gly1* and *gli1* mutants are not more sensitive to ROS than wild-type plants

Increased susceptibility in the *gly1* or *gli1* mutants is not due to a defect in the JA pathway

JA-mediated signaling is also crucial for basal resistance to *B. cinerea* (Ferrari et al., 2003; Méndez-Bravo et al., 2011). Therefore, I tested whether the increased susceptibility to *B. cinerea* in the *gly1* and *gli1* mutants was due to defects in the JA pathway. First, I checked the expression of *PDF1.2*, a molecular marker for the JA-mediated defense pathway in the Col-0, *act1*, *gly1* and *gli1* plants after treatment with water or pathogen. In Northern blot analysis, all the genotypes showed similar transcript levels for *PDF1.2* upon infection with *B. cinerea* (Figure 5.8 A). Next, I pre-treated (spray treatment) Col-0, *gly1* and *gli1* plants with water or 100 µM JA solution, and monitored the pathogen response in these genotypes. The JA treatment significantly enhanced resistance to *B.*

cinerea in all the genotypes compared to water-treated plants. However, exogenous JA application failed to completely restore basal resistance in the *gly1* and *gli1* mutants (Figure 5.8 B and C). These results indicated that exogenous application of JA could only partially rescue the enhanced susceptibility of the *gly1* and *gli1* mutants. In summary, the *gly1* and *gli1* mutants are likely not defective in JA signaling and the G3P-mediated resistance acts independently, or downstream, of the JA pathway.

Mutation in *GLY1* or *GLI1* leads to susceptibility to non-host isolates of *Botrytis*

The *GLI1* gene, also known as *NHO1* (non-host resistance 1), is required for non-host resistance in Arabidopsis (Lu et al., 2001). Therefore, I tested whether *GLY1* or *GLI1* also contributed to defense against non-host species (species that do not normally infect Arabidopsis) of *Botrytis*. Two *Botrytis* spp. were isolated locally in Kentucky, one from grape and the other from strawberry. As expected, both strains showed significantly reduced virulence on wild-type *Arabidopsis* plants as compared to *B. cinerea* (Figure 5.8, lower panel). Inoculation of these strains on *act1*, *gly1* and *gli1* mutant plants showed that, at 9 dpi the *act1* mutant barely developed any symptoms. At this time point, the wild-type plants developed symptoms, albeit much reduced in comparison to *B. cinerea* (Figure 5.8). In contrast, both *gly1* and *gli1* mutants showed severe symptoms. These results suggested that *GLY1*- and *GLI1*-derived G3P also contributes to defense against non-host *Botrytis* species in Arabidopsis.

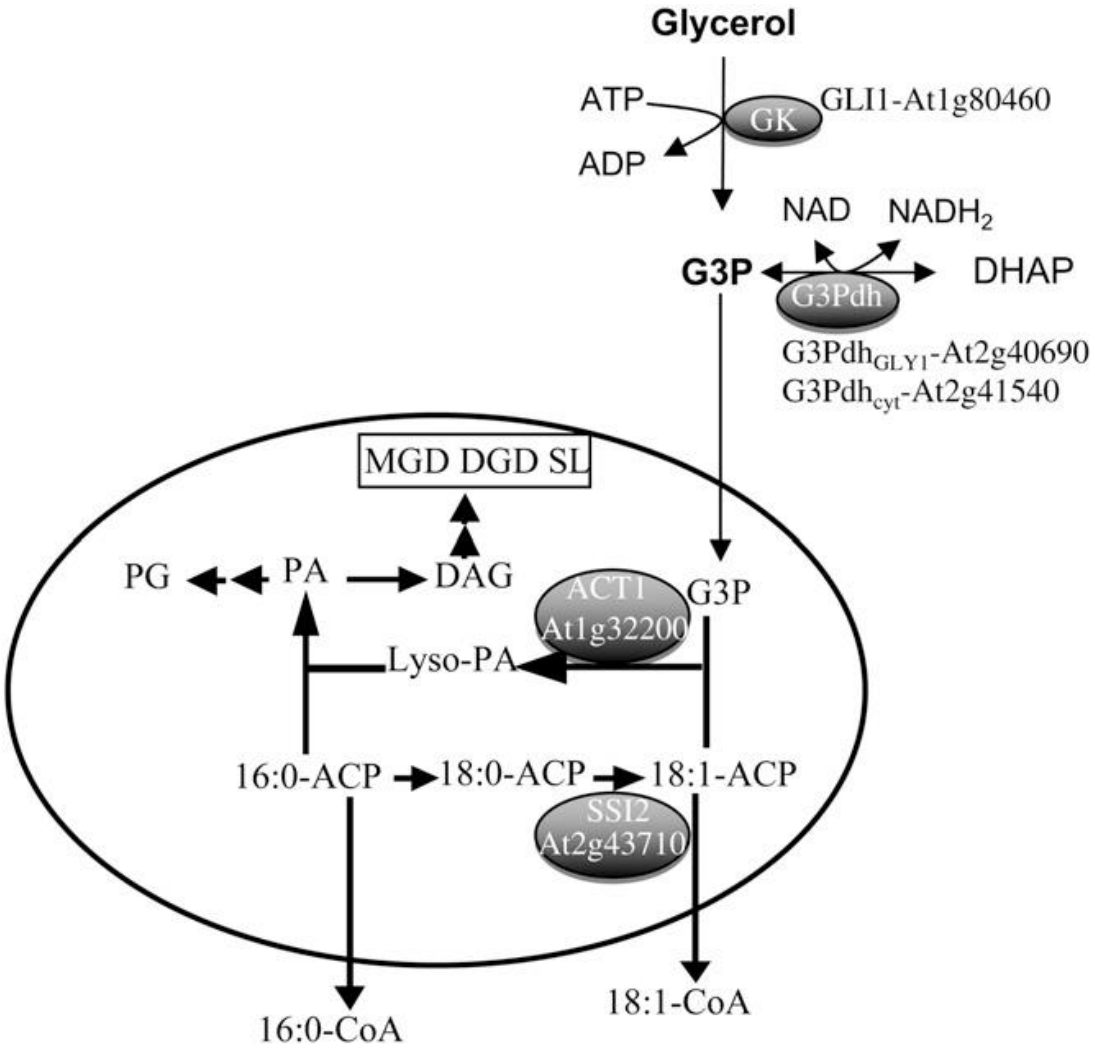

Figure 5.1. A condensed scheme of glycerol metabolism in plants.

Glycerol is phosphorylated to G3P by GK (GLI1). G3P can also be generated by G3Pdh via the reduction of DHAP in both the cytosol and the plastids (represented by the oval). G3P generated by this reaction can be transported between the cytosol and plastidial stroma. In the plastids, G3P is acylated with oleic acid (18:1) by the ACT1-encoded G3P acyltransferase. This ACT1-utilized 18:1 is derived from the stearoyl-acyl carrier protein (ACP)-desaturase (SSI2)-catalyzed desaturation of stearic acid (18:0). The 18:1-ACP generated by ACT1 either enters the prokaryotic lipid biosynthetic pathway through acylation of G3P or is exported out of the plastids as a CoA-thioester to enter the eukaryotic lipid biosynthetic pathway. Lyso-PA, Acyl-G3P; PA, phosphatidic acid; PG, phosphatidylglycerol; MGD, monogalactosyldiacylglycerol; DGD, digalactosyldiacylglycerol; SL, sulfolipid; DAG, diacylglycerol.

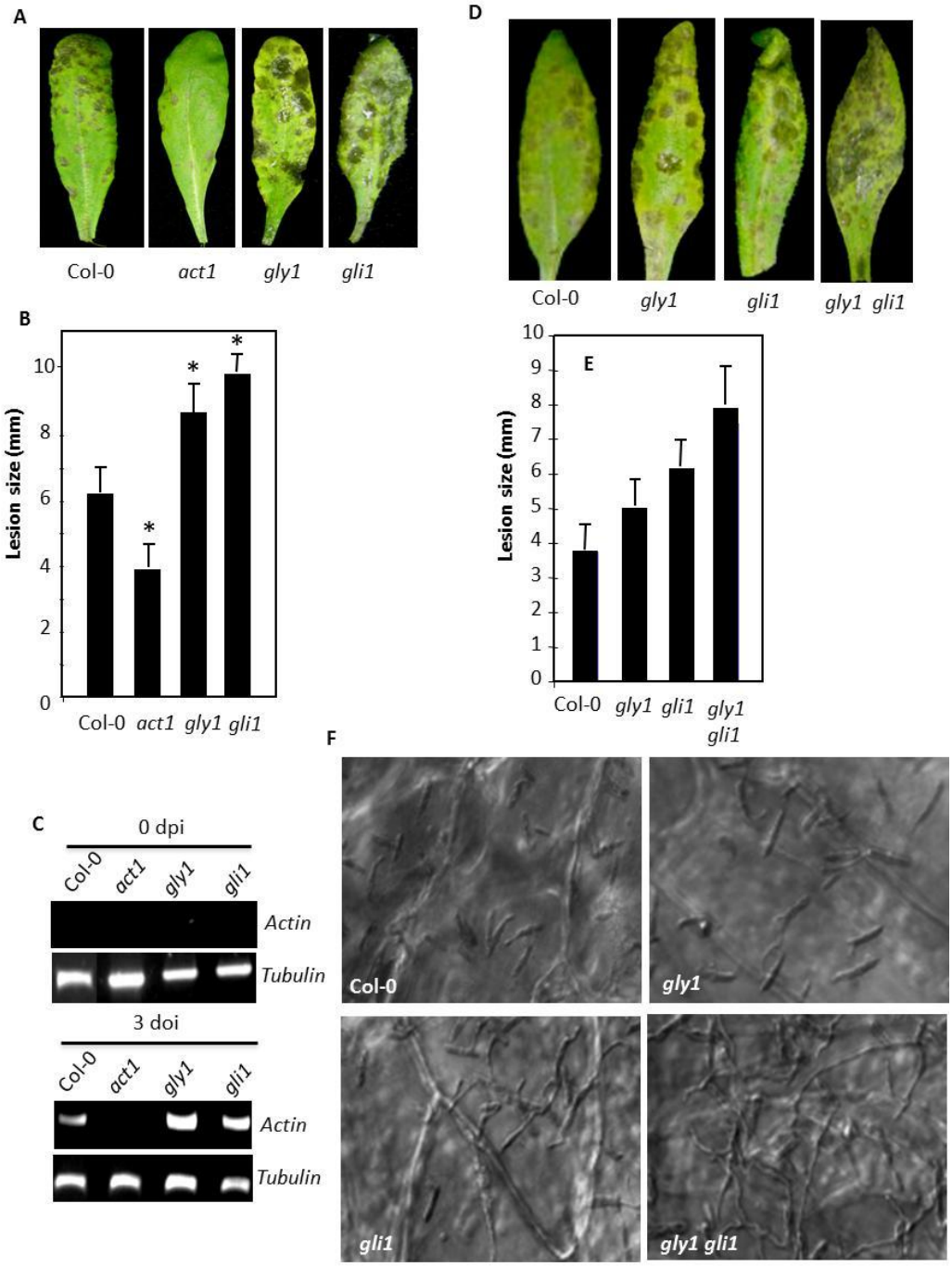

Figure 5.2. Pathogen responses in *Botrytis cinerea*-inoculated plants.

(A) Disease symptoms on Col-0, *act1, gly1* and *gli1* plants spray-inoculated with 2×10^5 spores/mL of *B. cinerea* at 3 dpi. **(B)** Lesion size in spot-inoculated genotypes. The plants were spot inoculated with 10 µL 10^6 spores/mL of *B. cinerea* and the lesion size was measured from 30-50 independent leaves at 7 dpi. Statistical significance was determined using Student's *t* test. Asterisks indicate data statistically significant from that of control (Col-0; $P < 0.05$). Error bars indicate SD. **(C)** RT-PCR analysis showing levels of plant

β-tubulin and fungal actin in *B .cinerea*-inoculated Col-0, *act1, gly1* and *gli1* plants at 0 and 3 dpi. **(D)** Disease symptoms on Col-0, *gly1*, *gli1* and *gly1 gli1* plants spray-inoculated with 2×10^5 spores/mL of *B. cinerea* at 3 dpi. **(E)** Lesion size in spot-inoculated genotypes. The plants were spot inoculated with 10 µL 10^6 spores/mL of *B. cinerea* and the lesion size was measured from 30-50 independent leaves at 7 dpi. **(F)** Microscopy of lactophenol blue-stained leaf petioles from Col-0, *gly1*, *gli1* and *gly1 gli1* plants inoculated with *B. cinerea* after 48 hour.

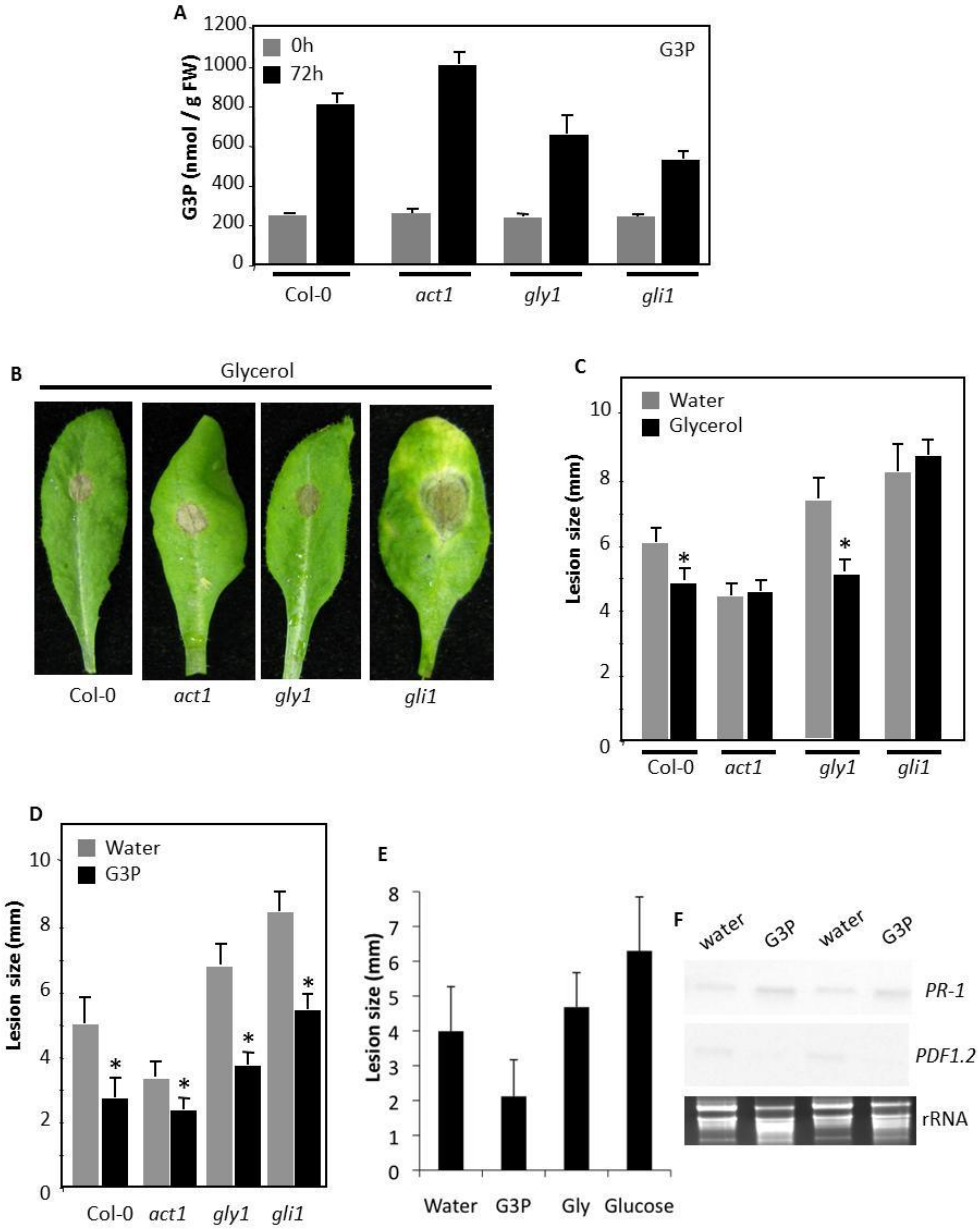

Figure 5.3. Glycerol-3-phosphate (G3P) level in *B. cinerea*-infected plants and pathogen responses in plants pretreated with glycerol or G3P.

(A) G3P level in *B. cinerea*-inoculated Col-0, *act1, gly1* and *gli1* plants at 0 hour and 72 h. **(B)** Disease symptoms on glycerol-pretreated Col-0, *act1, gly1* and *gli1* plants. **(C)** Lesion size in spot-inoculated Col-0, *act1, gly1* and *gli1* plants pretreated with water or glycerol. The plants were spot inoculated with 10 µL 10^6 spores/mL of *B. cinerea* and the lesion size was measured from 30-50 independent leaves at 7 dpi. Statistical significance was determined using Student's *t* test. Asterisks indicate data statistically significant from that of control (Col-0; $P < 0.05$). Error bars indicate SD. **(D)** Lesion size in spot-

inoculated Col-0, *act1, gly1* and *gli1* plants pretreated with water or G3P. The plants were spot inoculated with 10 µL 10^6 spores/mL of *B. cinerea* and the lesion size was measured from 30-50 independent leaves at 7 dpi. **(E)** Lesion size in spot-inoculated Col-0 plants pretreated with water, G3P, glycerol or glucose. The plants were spot inoculated with 10 µL 10^6 spores/mL of *B. cinerea* and the lesion size was measured from 20-30 independent leaves at 7 dpi. **(F)** Northern blot analysis of *PR-1* and *PDF1.2* gene expression in Col-0 plants pretreated with water or glycerol. RNA gel-blot analysis was performed on 7 µg of total RNA. Ethidium bromide staining of rRNA was used as a loading control.

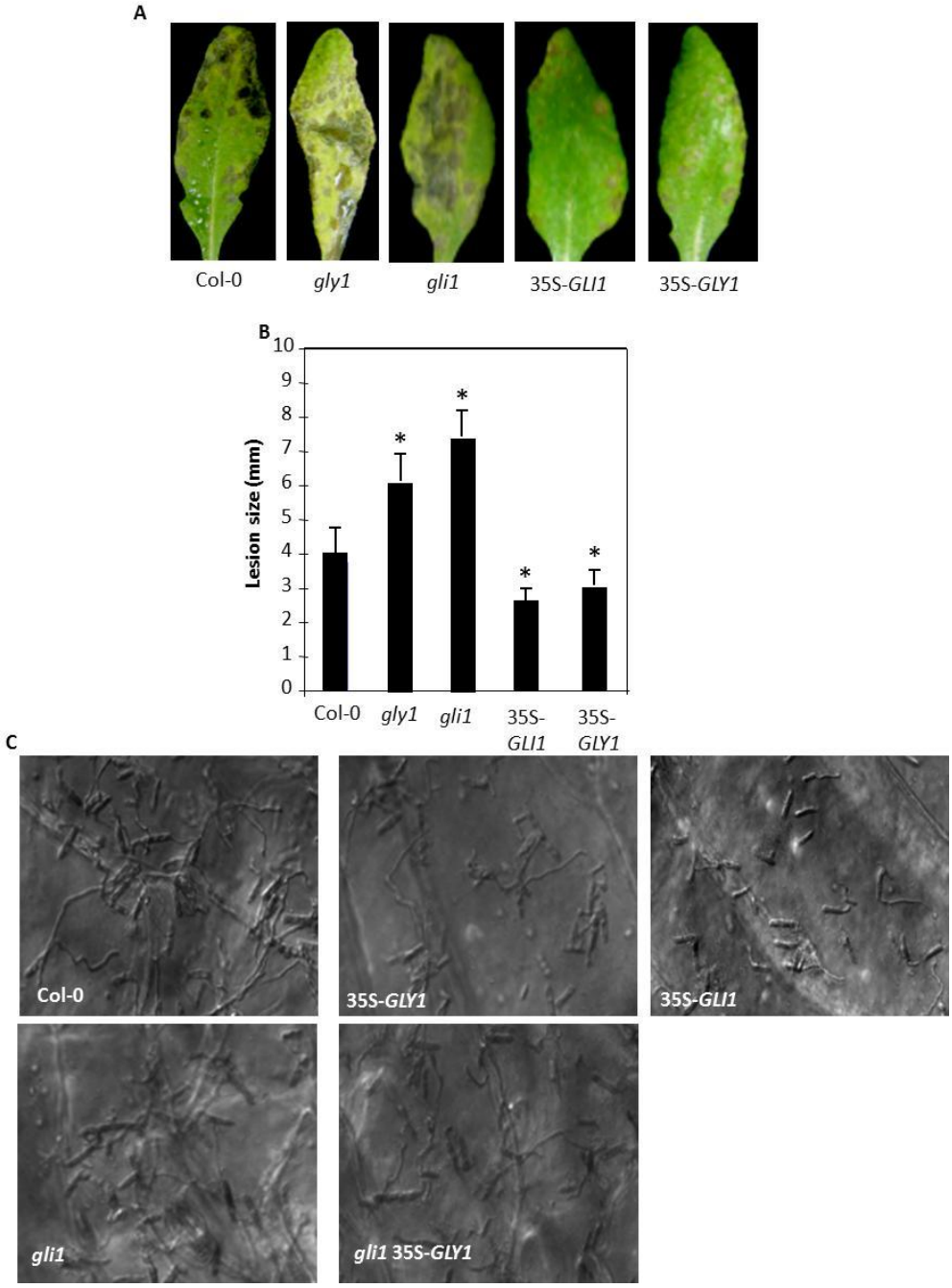

Figure 5.4. Analysis of transgenic lines overexpressing *GLY1* and *GLI1*.

(A) Disease symptoms at 3 dpi on Col-0, *gly1*, *gli1* 35S-*GLY1* and 35S-*GLI1* plants spray-inoculated with 2×10^5 spores/mL of *B. cinerea*. **(B)** Lesion size in spot-inoculated Col-0, *gly1*, *gli1*, 35S-*GLY1* and 35S-*GLI1* plants. The plants were spot inoculated with 10 µL 10^6 spores/mL of *B. cinerea* and the lesion size was measured from 30-50 independent leaves at 7 dpi. **(C)** Microscopy of lactophenol blue-stained leaf petioles

from Col-0, *gli1*, 35S-*GLY1*,35S-*GLI1* and *gli1* 35S-*GLY1* plants inoculated with *B. cinerea* post 48 hour.

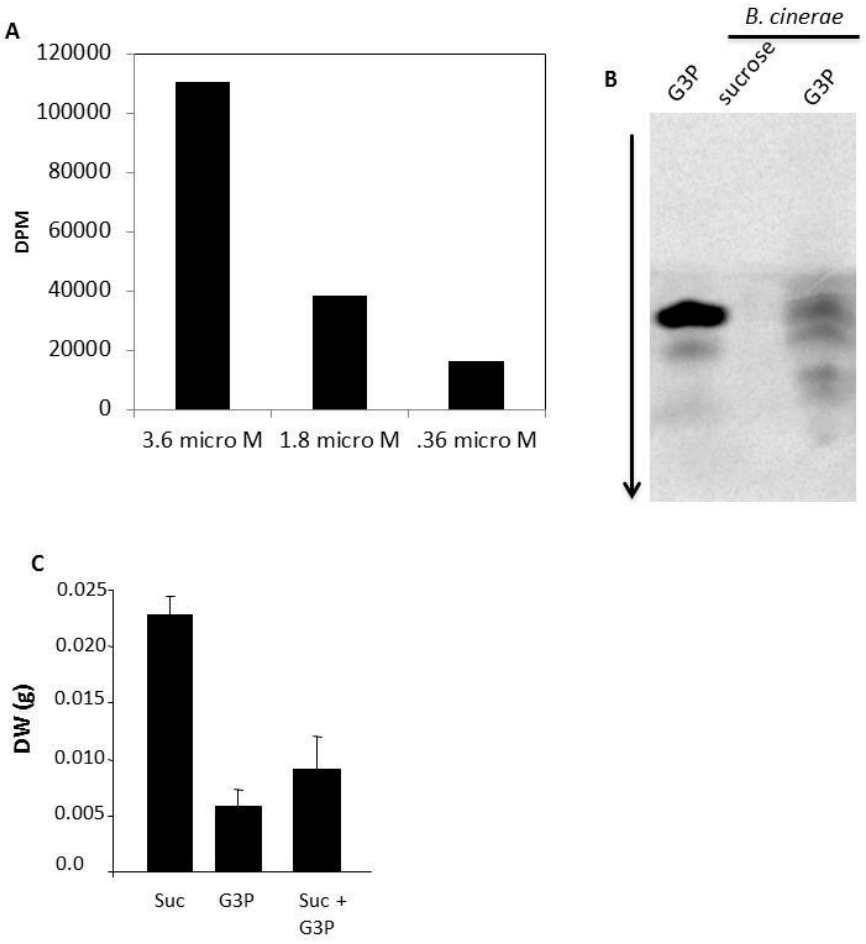

Figure 5.5. Assimilation of [^{14}C]-G3P into *B. cinerea* and the effect of G3P on fungal growth.

(A) DPM (disintegrations per minute) readings from extracted *B. cinerea* mycelium growing in liquid CD (Czapek-Dox) minimal medium for 7 days. Different amounts [^{14}C]-G3P (55 μCi/ umol) were added into the liquid culture as indicated. **(B)** Extraction from [^{14}C]-G3P feeding *B. cinerea* mycelium showing [^{14}C]-G3P and its derivatives on TLC plate. The extraction was obtained from 10 mL 7 day-old culture. **(C)** Dry weight of fungal culture added with 10 mM sucrose (suc), 1mM G3P, and 10 mM sucrose (suc) plus 1mM G3P as carbon sources. In all, 20 mL 7 day old fungal culture was measured and same experiment was repeated twice.

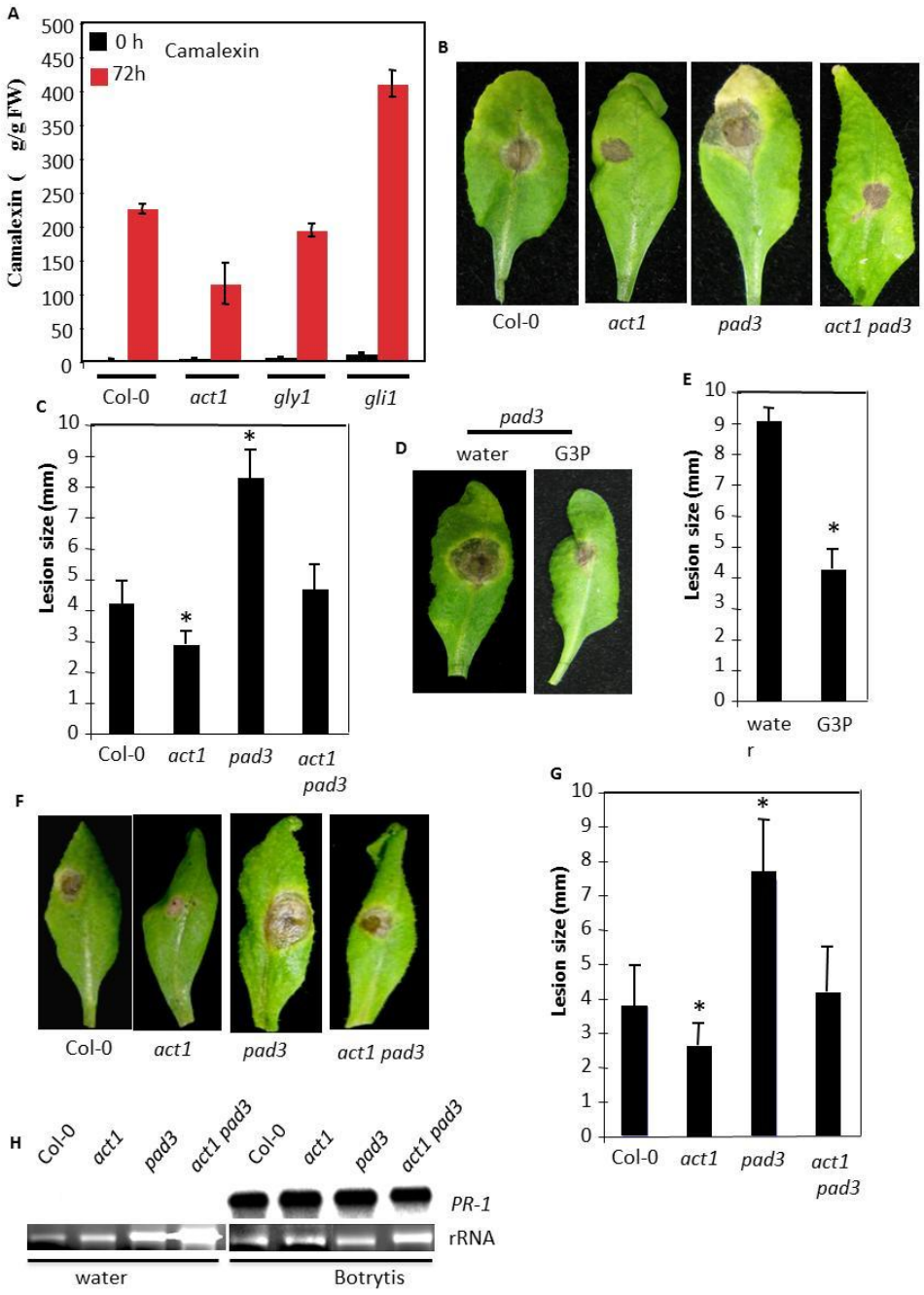

Figure 5.6. Camalexin level in *B. cinerea*-inoculated plants ; G3P confers resistance to necrotrophic pathogens in camalexin-deficient mutant.

(A) Camalexin level in Col-0, *act1, pad3* and *act1 pad3* plants at 0 h and 72 h after *B. cinerea* infection. **(B)** Disease symptoms on Col-0, *act1, gly1* and *gli1* plants spot inoculated with 10 µL 10^6 spores/mL of *B. cinerea*. **(C)** Lesion size in Col-0, *act1, pad3* and *act1 pad3* plants spot inoculated with 10 µL 10^6 spores/mL of *B. cinerea*. The lesion size was measured from 30-50 independent leaves at 7 dpi. Statistical significance was

determined using Student's *t* test. Asterisks indicate data statistically significant from that of control (Col-0; $P < 0.05$). Error bars indicate SD. **(D)** Disease symptoms on *pad3* mutant pretreated with water or G3P. **(E)** Lesion size in *pad3* mutant pretreated with water or G3P. The lesion size was measured from 20-30 independent leaves at 7 dpi**. (F)** Disease symptoms on Col-0, *act1, pad3* and *act1 pad3* spot-inoculated with 10 µL 10^6 spores/mL of *Alternaria brassicae*. **(G)** Lesion size in Col-0, *act1, pad3* and *act1 pad3* plants spot-inoculated with 10 µL 10^6 spores/mL of *Alternaria brassicae*. **(H)** Northern analysis of *PR-1* gene expression in Col-0, *act1, pad3* and *act1 pad3* plants at 0 dpi and 3 dpi post *B. cinerea* infection. RNA gel-blot analysis was performed on 7 µg of total RNA. Ethidium bromide staining of rRNA was used as a loading control.

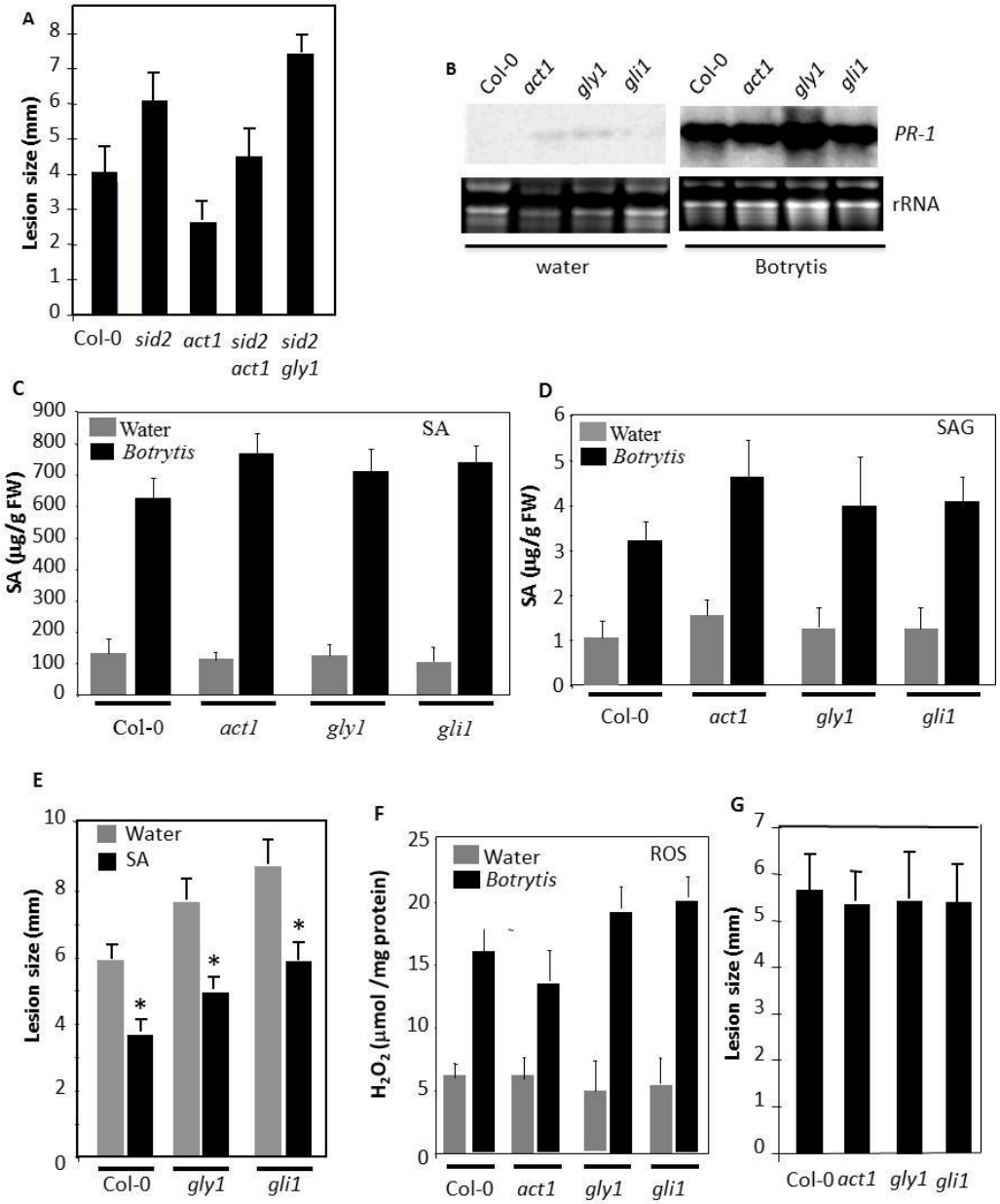

Figure 5.7. SA/SAG and ROS levels in Col-0, *act1*, *gly1* and *gli1* after *B. cinerea* infection and sensitivity to paraquat.

(A) Lesion size in Col-0, *sid2*, *act1*, *sid2 act1* and *sid2 gly1* plants spot-inoculated with 10 µL 10^6 spores/mL of *B. cinerea*. **(B)** Northern analysis of *PR-1* gene expression in Col-0, *act1*, *gly1* and *gli1* plants spray inoculated with water (mock) or *B. cinerea*. RNA gel-blot analysis was performed on 7 µg of total RNA. Ethidium bromide staining of rRNA was used as a loading control. **(C)** SA levels in Col-0, *act1*, *gly1* and *gli1* plants spray inoculated with water (mock) or *B. cinerea*. **(D)** SAG levels in Col-0, *act1*, *gly1* and *gli* plants spray inoculated with water (mock) or *B. cinerea*. **(E)** Lesion size in spot-

inoculated Col-0, *act1*, *gly1* and *gli1* plants pretreated with water and SA. **(F)** ROS levels in Col-0, *act1*, *gly1* and *gli1* plants spray inoculated with water (mock) or *B. cinerea*. **(G)** Lesion size in spot-inoculated Col-0, *act1*, *gly1* and *gli1* plants treated with 10 uM paraquat.

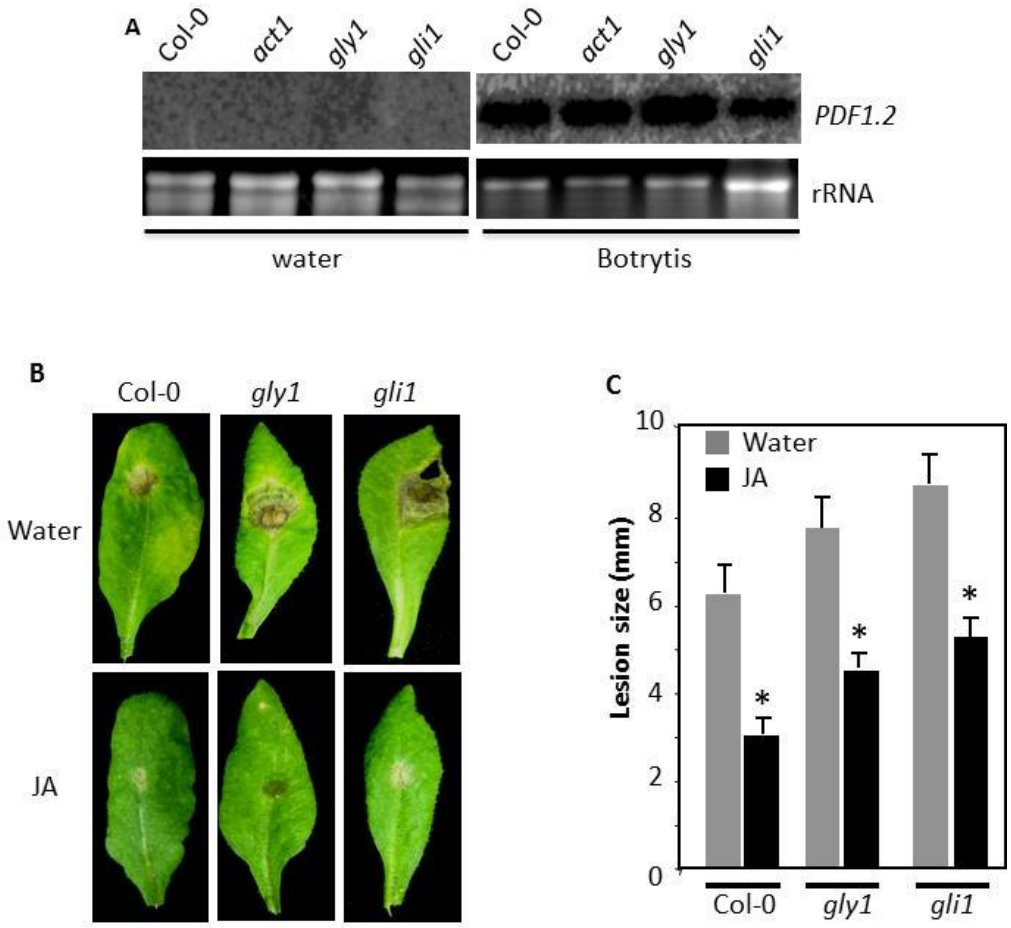

Figure 5.8 Expression of *PDF1.2* gene and pathogen response in plants of indicated genotypes pretreated with JA.

(A) Northern analysis of *PDF 1.2* gene expression in Col-0, *act1*, *gly1* and *gli1* plants spray inoculated with water (mock) or *B. cinerea*. RNA gel-blot analysis was performed on 7 µg of total RNA. Ethidium bromide staining of rRNA was used as a loading control. **(B)** Disease symptoms on spray inoculated Col-0, *gly1* and *gli1* plants pretreated with water or JA. **(C)** Lesion size in spot-inoculated Col-0, *gly1* and *gli1* plants pretreated with water or JA.

.

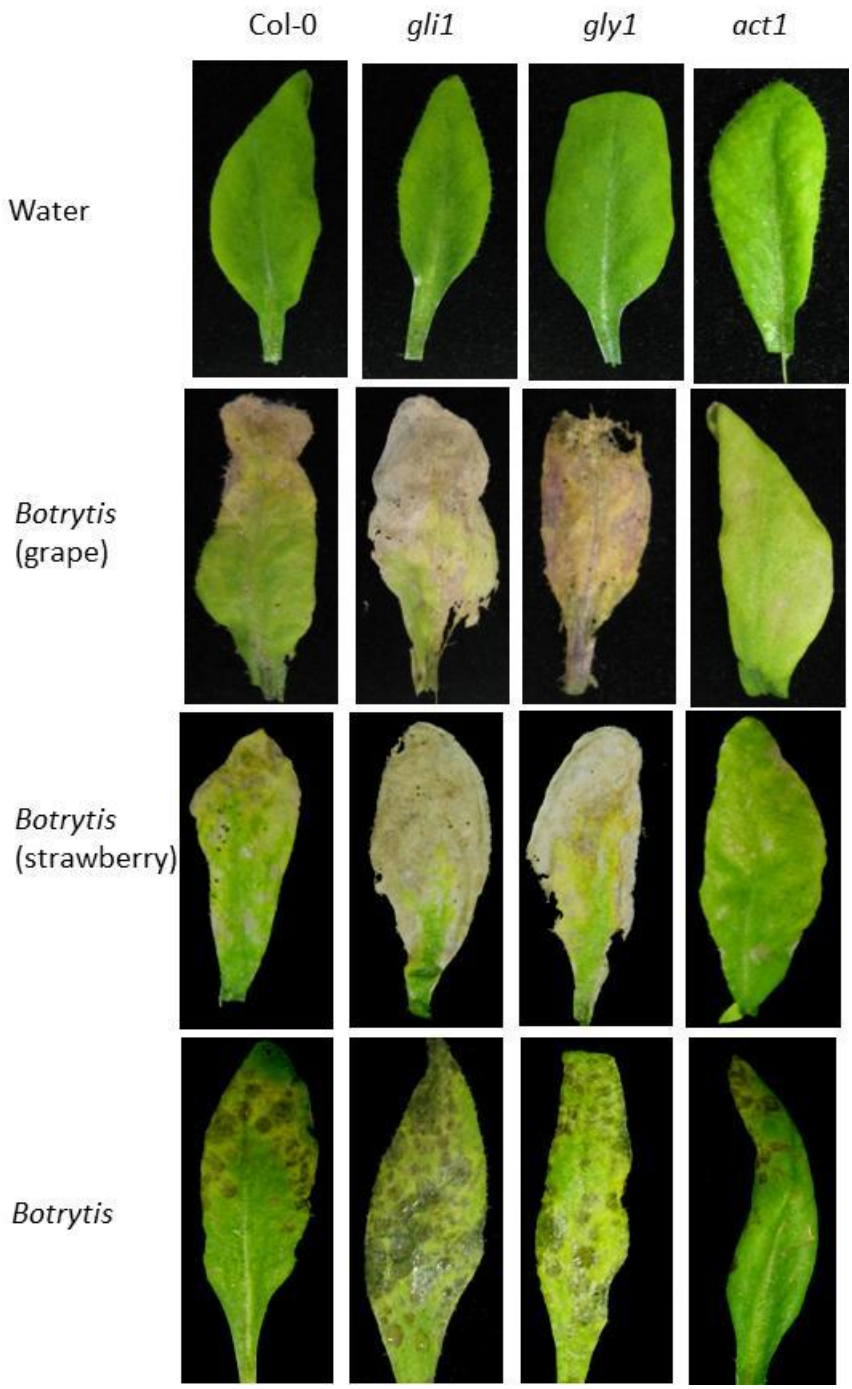

Figure 5.9 Disease symptoms on Col-0, *act1*, *gly1* and *gli1* plants inoculated with different *Botrytis* isolates. The plants were spray inoculated with with 2×10^5 spores/mL of two *Botrytis* spp. isolated from grape and strawberry, and *Botrytis cinerea*. The pictures were taken 9 dpi and 3 dpi, respectively.

APPENDIX

LIST OF ABBREVIATIONS

Acronym/ abbreviation	Expansion
L/mL/μL	Liter/ milliliter/ microliter
M/mM/μM	Molar/millimolar/ micromolar
g/mg/μg/ng	Gram/ milligram/ microgram/ nanogram
h/min/sec	Hours/minutes/seconds
Rh	Relative humidity
^{o}C	Degrees centigrade
BiFC	Bi-molecular fluorescence complementation
BSA	Bovine serum albumin
BTH	Benzo[1,2,3]thiadiazole-7-carbothioic acid *S*-methyl ester
$CaCl_2$	Calcium chroride
CAPS	Cleaved Amplified Polymorphic Sequences
Co-IP	Co-immunoprecipitation
dATP	Deoxyribo adenosine triphosphate
dCAPS	Derived Cleaved Amplified Polymorphic Sequences
dCTP	Deoxyribo cytosine triphosphate
DEPC	Diethyl pyrocarbonate
DNA	Deoxyribonucleic acid
dNTP	Deoxyribo nucleic triphosphate
DMSO	Dimethyl sulfoxide
DPI	Days post inoculation
DPT	Days post treatment
DTT	Dithiothreitol
EDTA	Ethylene diamine tetraacetic acid
EGTA	Ethylene glycol tetraacetic acid
EtBr	Ethidium bromide
K_2HPO_4	Potassium phosphate, dibasic
KH_2PO_4	Potassium phosphate, monobasic
KCl	Potassium chloride
KOH	Potassium hydroxide
LB	Luria-Bertani
$MgCl_2$	Magnesium chloride
MOPS	3-(N-morpholino)propanesulfonic acid
MS	Murashige and Skoog
NaCl	Sodium chloride
NaOAc	Sodium acetate
NaOH	Sodium hydroxide
Na_2HPO_4	Sodium hydrogen phosphate

List of abbreviations (continued)

NaN_3	Sodium azide
PCR	Polymerase chain reaction
PFD	Photon flux density
PBS	Phosphate buffered saline
R	Resistant or resistance
RNA	Ribonucleic acid
SA	Salicylic acid
SAG	Salicylic acid glucoside
SDS	Sodium dodecyl sulfate
SSC	Sodium chloride, sodium citrate
TBE	Tris-borate/ EDTA electrophoresis buffer
TE	TRIS-EDTA
Tfb	Transformation buffer
TRIS	Hydroxymethyl Aminomethane
WT	Wild-type

REFERENCES

Balbi, V. and A. Devoto (2008). Jasmonate signalling network in Arabidopsis thaliana: crucial regulatory nodes and new physiological scenarios. New Phytologist 177(2): 301-318.

Beckers, G. J. M. and S. H. Spoel (2006). Fine-tuning plant defence signalling: Salicylate versus jasmonate." Plant Biology 8(1): 1-10.

Bessire MCC, Jacquat A-C, Humphry M, Borel S, Petétot JMC, Métraux J-P, Nawrath C (2007) A permeable cuticle in *Arabidopsis* leads to a strong resistance to *Botrytis cinerea*. EMBO J 26: 2158-2168.

Brooks DM, Bender CL, Kunkel BN. (2005) The *Pseudomonas syringae* phytotoxin coronatine promotes virulence by overcoming salicylic acid-dependent defences in *Arabidopsis thaliana*. Mol. Plant Pathol. 6: 629-639

Cao, H., S. A. Bowling, et al. (1994). Characterization of an Arabidopsis Mutant That Is Nonresponsive to Inducers of Systemic Acquired-Resistance. Cell 6(11).

Chandra-Shekara AC, Navarre D, Kachroo A, Kang H-G, Klessig DF, Kachroo P. (2004) Signaling requirements and role of salicylic acid in HRT- and rrt- mediated resistance to turnip crinkle virus in Arabidopsis. Plant J. 40: 647-659

Chandra-Shekara AC, Venugopal SC, Barman SR, Kachroo A, Kachroo P. (2007) Plastidial fatty acid levels regulate resistance gene-dependent defense signaling in Arabidopsis. Proc. Natl. Acad. Sci. USA 104: 7277-7282

Chaturvedi R, Krothapalli K, Makandar R, Nandi A, Sparks AA, Roth M, Welti R, Shah J (2008) Plastid ω-3 desaturase-dependent accumulation of a systemic acquired

resistance inducing activity in petiole exudates of *Arabidopsis thaliana* is independent of jasmonic acid. Plant J 54: 106-117.

Chen L-J, Li H-M (1998) A mutant deficient in the plastid lipid DGD is defective in protein import into chloroplasts. Plant J 16: 33-39.

Cui J, Bahrami AK, Pringle EG, Hernandez-Guzman G, Bender CL, Pierce NE, Ausubel FM. (2005) *Pseudomonas syringae* manipulates systemic plant defenses against pathogens and herbivores. Proc. Natl. Acad. Sci. USA 102: 1791-1796

Dahmer ML, Fleming PD, Collins GB, Hildebrand DF. (1989) A rapid screening for determining the lipid composition of soybean seeds. J. Am. Oil Chem. 66: 534-538

Dangl JL, Dietrich RA, Richberg MH. (1996) Death don't have no mercy: Cell death programs in plant-microbe interactions. Plant Cell 8: 1793-1807

Delaney, T. P., L. Friedrich, et al. (1995). Arabidopsis Signal-Transduction Mutant Defective in Chemically and Biologically Induced Disease Resistance. 92(14).

Dickman MB, Park YK, Oltersdorf T, Li W, Clemente T, French R. (2001) Abrogation of disease development in plants expressing animal antiapoptotic genes. Proc. Natl. Acad. Sci. USA. 98: 6957-6962

Doherty HM, Selvendran RR, Bowles DJ. (1988) The wound response of tomato plants can be inhibited by aspirin and related hydroxy-benzoic acids. Physiol. Mol. Plant Pathol. 33: 377-384

Dong J, Chen C, Chen Z. (2003) Expression profiles of the *Arabidopsis WRKY* gene superfamily during plant defense response. Plant Mol. Biol. 51: 21-37

Durrant, W. E. and X. Dong (2004). Systemic acquired resistance. 42.

Eulgem T, Rushton PJ, Robatzek S, Somssich IE. (2000) The WRKY superfamily of plant transcription factors. Trends Plant Sci. 5: 199-206

Eulgem, T. (2005). Regulation of the Arabidopsis defense transcriptome. Trends in Plant Science 10(2): 71-78.

Eulgem T. (2006) Dissecting the WRKY web of plant defense regulators. PLoS Pathog. 2: e126

Eulgem T, Somssich IE. (2007) Networks of WRKY transcription factors in defense signaling. Curr. Opin. Plant Biol. 10: 366-371

Farrington JA, Ebert M, Land EJ, Fletcher K. (1973) Bipyridylium quaternary salts and related compounds. V. Pulse radiolysis studies of the reaction of paraquat radical with oxygen. Implications for the mode of action of bipyridyl herbicides. Biochim. Biophys. Acta 314: 372-381

Friedrich, L., K. Lawton, et al. (1996). A benzothiadiazole derivative induces systemic acquired resistance in tobacco. 10(1).

Gaffney, T., L. Friedrich, et al. (1993). Requirement of Salicylic-Acid for the Induction of Systemic Acquired-Resistance. 261(5122).

Glazebrook J. (2005) Contrasting mechanisms of defense against biotrophic and necrotrophic pathogens. Annu. Rev. Phytopathol. 43: 205-227

Govrin E, Levine A. (2000) The hypersensitive response facilitates plant infection by the necrotrophic pathogen *Botrytis cinerea*. Curr. Biol. 10: 751-757

Govrin EM, Rachmilevitch S, Tiwari BS, Solomon M, Levine A. (2006) An elicitor from *Botrytis cinerea* induces the hypersensitive response in *Arabidopsis thaliana* and other plants and promotes the gray mold disease. Phytopathol. 96: 299-307

Gupta V, Willits MG, Glazebrook J. (2000) *Arabidopsis thaliana* EDS4 contributes to salicylic acid (SA)-dependent expression of defense responses: evidence for inhibition of jasmonic acid signaling by SA. Mol. Plant Microbe Interact. 13: 503-511

Halim, V. A., A. Vess, et al. (2006). The role of salicylic acid and jasmonic acid in pathogen defence. 8(3).

Higashi K, Ishiga Y, Inagaki Y, Toyoda K, Shiraishi T, Ichinose Y. (2008) Modulation of defense signal transduction by flagellin-induced WRKY41 transcription factor in Arabidopsis thaliana. Mol. Genet. Genomics. 279: 303-312

Hiyama T, Ohinata A, Kobayashi S. (1993) Paraquat (methylviologen): Its interference with primary photochemical reactions. Z. Naturforsch 48c: 374-378

Jiang CJ, Shimono M, Maeda S, Inoue H, Mori M, Hasegawa M, Sugano S, Takatsuji H. (2009) Suppression of the rice fatty-acid desaturase gene OsSSI2 enhances resistance to blast and leaf blight diseases in rice. Mol. Plant Microbe Interact. 22: 820-829

Jones, J. D. G. and J. L. Dangl (2006). The plant immune system. Nature 444(7117): 323-329.

Kachroo A, Kachroo P (2009) Fatty acid derived signals in plant defense. Ann Rev Phytopath 47: 153-176.

Kachroo A, Kachroo P (2006) Salicylic Acid-, Jasmonic Acid- and Ethylene-Mediated Regulation of Plant Defense Signaling In Genetic Regulation of Plant Defense Mechanisms, Ed Jane Setlow, Springer pubs, 28: 55-83.

Kachroo A, Venugopal SC, Lapchyk L, Falcone D, Hildebrand D, Kachroo P (2004) Oleic acid levels regulated by glycerolipid metabolism modulate defense gene expression in Arabidopsis. Proc Natl Acad Sci USA 101: 5152-5257.

Kachroo P, Venugopal SC, Navarre DA, Lapchyk L, Kachroo A (2005) Role of salicylic acid and fatty acid desaturation pathways in *ssi2*-mediated signaling. Plant Physiol 139: 1717-1735.

Kachroo P, Shanklin J, Shah J, Whittle E, Klessig D (2001) A fatty acid desaturase modulates the activation of defense signaling pathways in plants. Proc Natl Acad Sci USA 98: 9448-9453.

Kachroo A, Lapchyk L, Fukushigae H, Hildebrand D, Klessig D, Kachroo P. (2003) Plastidial fatty acid signaling modulates salicylic acid- and jasmonic acid-mediated defense pathways in the Arabidopsis *ssi2* mutant. Plant Cell 12: 2952-2965.

Kachroo A, Daqi F, Havens W, Navarre D, Kachroo P, Ghabrial S (2008) An oleic acid–mdiated pathway induces constitutive defense signaling and enhanced resistance to multiple pathogens in soybean. Mol. Plant-Microbe Interact 21: 564-575.

Kachroo A, Shanklin J, Lapchyk L, Whittle E, Hildebrand D, Kachroo P (2007) The Arabidopsis stearoyl-acyl carrier protein-desaturase family and the contribution of leaf isoforms to oleic acid synthesis. Plant Mol Biol 63: 257-271.

Kachroo A, Fu DQ, Havens W, Navarre D, Kachroo P, Ghabrial SA. (2008) An oleic Acid-mediated pathway induces constitutive defense signaling and enhanced resistance to multiple pathogens in soybean. Mol. Plant Microbe Interact. 21: 564-575

Kachroo A, Kachroo P. (2007a) Regulation of plant defense pathways. In "Genetic Engineering, Principles and Methods". Eds Jane K. Setlow. 28: 55-83

Kachroo P, Shanklin J, Shah J, Whittle EJ, Klessig DF. (2001) A fatty acid desaturase modulates the activation of defense signaling pathways in plants. Proc. Natl. Acad. Sci. USA 98: 9448-9453

Koornneef A, Pieterse CMJ. (2008) Cross-talk in defense signaling. Plant Physiol. 146: 839-844

Kunkel BN, Brooks DM. (2002) Cross talk between signaling pathways in pathogen defense. Curr. Opin. Plant Biol. 5: 325-331

Li Y, Beisson F, Koo AJK, Molina I, Pollard M, Ohlrogge J (2007) Identification of acyltransferases required for cutin biosynthesis and production of cutin with suberin-like monomers. Proc Natl Acad Sci USA 104: 18339-18344.

Li J, Brader G, Palva ET. (2004) The WRKY70 transcription factor: a node of convergence for jasmonate-mediated and salicylate-mediated signals in plant defense. Plant Cell. 16: 319-331

Li, C. Y., G. H. Liu, et al. (2003). The tomato Suppressor of prosystemin-mediated responses2 gene encodes a fatty acid desaturase required for the biosynthesis of jasmonic acid and the production of a systemic wound signal for defense gene expression. Plant Cell 15(7): 1646-1661.

Lorenzo, O. and R. Solano (2005). Molecular players regulating the jasmonate signalling network. Current Opinion in Plant Biology 8(5): 532-540.

Lü S, Song T, Kosma DK, Parsons EP, Rowland O, Jenks MA (2009) *Arabidopsis CER8* encodes LONG-CHAIN ACYL-COA SYN-THETASE 1 (LACS1) that has overlapping functions with LACS2 in plant wax and cutin synthesis. Plant J 59: 553-564.

Malamy, J., J. P. Carr, et al. (1990). Salicylic-Acid - a Likely Endogenous Signal in the Resistance Response of Tobacco to Viral-Infection. 250(4983).

Maleck K, Levine A, Eulgem T, Morgan A, Schmid J, Lawton K, Dangl JL, Dietrich RA. (2000) The transcriptome of *Arabidopsis thaliana* during systemic acquired resistance. Nat. Genet. 26: 403-410

Mao P, Duan M, Wei C, Li Y. (2007) WRKY62 transcription factor acts downstream of cytosolic NPR1 and negatively regulates jasmonate-responsive gene expression. Plant Cell Physiol. 48: 833-842

Mauch-Mani, B. and F. Mauch (2005). The role of abscisic acid in plant-pathogen interactions." Current Opinion in Plant Biology 8(4): 409-414.

Mengiste T, Chen X, Salmeron JM, Dietrich RA. (2003) The BOS1 gene encodes an R2R3MYB transcription factor protein that is required for biotic and abiotic stress responses in Arabidopsis. Plant Cell 15: 2551-2565

Miao Y, Laun T, Zimmermann P, Zentgraf U. (2004) Targets of the WRKY53 transcription factor and its role during leaf senescence in Arabidopsis. Plant Mol. Biol. 55: 853-867

Pandey SP, Somssich IE. (2009) The role of WRKY transcription factors in plant immunity. Plant Physiol. 150: 1648-1655

Park S-W, Kaimoyo E, Kumar D, Mosher S, Klessig, DF (2007) Methyl salicylate is a critical mobile signal for plant systemic acquired resistance. Science 318: 113-116. Rasmussen, JB, Hammerschmidt, R and Zook, MN (1991) Systemic induction of salicylic acid accumulation in cucumber after inoculation with *Pseudomonas syringae* pv *syringae*. Plant Physiol 97: 1342-1347.

Peña-Cortés H, Albrecht T, Prat S, Weiler EW, Willmitzer L. (1993) Aspirin prevents wound-induced gene expression in tomato leaves by blocking jasmonic acid biosynthesis. Planta 191: 123-128

Petersen M, Brodersen P, Naested H, Andreasson E, Lindhart U, Johansen B, Nielsen HB, Lacy M, Austin MJ, Parker JE, Sharma SB, Klessig DF, Martienssen R, Mattsson O, Jensen AB. Mundy J. (2000) Arabidopsis map kinase 4 negatively regulates systemic acquired resistance. Cell 103: 1111-1120

Pieterse, C. M. J., J. A. Van Pelt, et al. (2000). Rhizobacteria-mediated induced systemic resistance (ISR) in Arabidopsis requires sensitivity to jasmonate and ethylene but is not accompanied by an increase in their production. 57(3).

Rowe HC, Walley JW Corwin J, Chan EK-F, Dehesh K, Kliebenstein DJ (2010) Deficiencies in jasmonate-mediated plant defense reveal quantitative variation in *Botrytis cinerea* pathogenesis. PLOS Pathogen 6: e1000861.

Rushton PJ, Somssich IE, Ringler P, Shen QJ. (2010) WRKY transcription factors. Trends Plant Sci. 15: 247-258

Rushton PJ, Torres JT, Parniske M, Wernert P, Hahlbrock K, Somssich IE. (1996) Interaction of elicitor-induced DNA-binding proteins with elicitor response elements in the promoters of parsley PR1 genes. EMBO J. 15: 5690-5700

Ryals, J. A., U. H. Neuenschwander, et al. (1996). Systemic acquired resistance. 8(10).

Schellmann S, Hülskamp M (2005) Epidermal differntiation: trichomes in *Arabidopsis* as a model system. Int J Dev Bio 49: 579-584.

Schnurr J, Shockey J, Browse J (2004) The acyl-CoA synthetase encoded by *LACS2* is essential for normal cuticle development in *Arabidopsis*. Plant Cell 16: 629–642.

Shah, J. (2003). The salicylic acid loop in plant defense. Current Opinion in Plant Biology 6(4): 365-371.

Shah, J., P. Kachroo, et al. (2001). A recessive mutation in the Arabidopsis SSI2 gene confers SA- and NPR1-independent expression of PR genes and resistance against bacterial and oomycete pathogens. Plant Journal 25(5): 563-574.

Shah, J., F. Tsui, et al. (1997). Characterization of a salicylic acid-insensitive mutant (sai1) of Arabidopsis thaliana, identified in a selective screen utilizing the SA-inducible expression of the tms2 gene. 10(1).

Shirasu K, Nakajima H, Rajasekhar VK, Dixon RA, Lamb, C (1997) Salicylic acid potentiates an agonist-dependent gain control that amplifies pathogen signals in the activation of defense mechanisms. Plant Cell **9**: 261-270.

Smith-Becker J, Marois E, Huguet EJ, Midland SL, Sims JJ, Keen NT (1998) Accumulation of salicylic acid and 4-hydroxybenzoic acid in phloem fluids of cucumber during systemic acquired resistance is preceded by a transient increase in phenylalanine ammonia-lyase activity in petioles and stems. Plant Physiol 116: 231-238.

Spoel SH, Dong X. (2008) Making sense of hormone crosstalk during plant immune responses. Cell Host Microbe 3: 348-351

Spoel SH, Koornneef A, Claessens SMC, Korzelius JP, Van Pelt JA, Mueller MJ, Buchala AJ, Métraux JP, Brown R, Kazan K, Van Loon LC, Dong X, Pieterse CM. (2003) NPR1 modulates cross talk between salicylate- and jasmonate-dependent defense pathways through a novel function in the cytosol. Plant Cell 15: 760-770

Spoel, S. H., J. S. Johnson, et al. (2007). Regulation of tradeoffs between plant defenses against pathogens with different lifestyles. 104(47).

Tanaka T, Tanaka H, Machida C, Watanabe M, Machida Y (2004) A new method for rapid visualization of defects in leaf cuticle reveals five intrinsic patterns of surface defects in Arabidopsis. Plant J 37: 139-146.

Thomma, B., K. Eggermont, et al. (1998). Separate jasmonate-dependent and salicylate-dependent defense-response pathways in Arabidopsis are essential for resistance to distinct microbial pathogens. 95(25).

Thordal-Christensen, H. (2003). "Fresh insights into processes of nonhost resistance." Current Opinion in Plant Biology 6(4): 351-357.

Tierens KF, Thomma BP, Bari RP, Garmier M, Eggermont K, Brouwer M, Penninckx IA, Broekaert WF, Cammue BP. (2002) Esa1, an Arabidopsis mutant with enhanced

susceptibility to a range of necrotrophic fungal pathogens, shows a distorted induction of defense responses by reactive oxygen generating compounds. Plant J. 29: 131-140.

Truman W, Bennett MH, Kubigsteltig I, Turnbull C, Grant M (2007) Arabidopsis systemic immunity uses conserved defense signaling pathways and is mediated by jasmonates. Proc Natl Acad Sci USA 104: 1075-10780.

Truman W, Bennett MH, Turnbull CGN, Grant MR (2010) Arabidopsis auxin mutants are compromised in systemic acquired resistance and exhibit aberrant accumulation of various indolic compounds. Plant Physiol 152: 1562-1573.

Venugopal SC, Jeong RD, Mandal MK, Zhu S, Chandra-Shekara AC, Xia Y, Hersh M, Stromberg AJ, Navarre D, Kachroo A, Kachroo P. (2009) Enhanced disease susceptibility 1 and salicylic acid act redundantly to regulate resistance gene-mediated signaling. PLoS Genet. 5: e1000545

Veronese P, Chen X, Bluhm B, Salmeron J, Dietrich RA. Mengiste T. (2004) The BOS loci of Arabidopsis are required for resistance to *Botrytis cinerea* infection. Plant J. 40: 558-574

Vijayan, P., J. Shockey, et al. (1998) A role for jasmonate in pathogen defense of Arabidopsis." Proc Natl Acad Sci USA 95(12): 7209-7214.

Vlot AC, Dempsey DA, Klessig DF (2009) Salicylic acid, a multifaceted horomone to combat disease. Ann Rev Phytopath 47: 177-206.

Ward, E. R., S. J. Uknes, et al. (1991) Coordinate Gene Activity in Response to Agents That Induce Systemic Acquired-Resistance. 3(10).

Walker AR, Davison PA, Bolognesi-Winfield AC, James CM, Srinivasan N, Blundell TL, Esch JJ, Marks MD, Gray JC (1999) The *TRANSPARENT TESTA GLABRA1* locus, which regulates trichome differentiation and anthocyanin biosynthesis in *Arabidopsis*, encodes a WD40 repeat protein. Plant Cell 11: 1337-1350

Wasternack, C. (2007) Jasmonates: An update on biosynthesis, signal transduction and action in plant stress response, growth and development. Annals of Botany 100(4): 681-697.

Weng H, Molina I, Shockey J, Browse J (2010) Organ fusion and defective cuticle function in *lacs1 lacs2* double mutant of *Arabidopsis*. Planta 231: 1089-1100.

Wildermuth MC, Dewdney J, Wu G, Ausubel FM. (2001) Isochorismate synthase is required to synthesize salicylic acid for plant defence. Nature. 414: 562-565

von Tiedemann AV. (1997) Evidence for a primary role of active oxygen species in induction of host cell death during infection of bean leaves with *Botrytis cinerea*. Physiol. Mol. Plant Pathol. 50: 151–166

Xia Y, Gao Q-M, Navarre D, Hildebrand D, Kachroo A, Kachroo P. (2009) Acyl carrier protein regulates oleate levels and systemic acquired resistance in Arabidopsis. Cell H & M. 5: 151-165

Yu D, Chen C, Chen Z. (2001) Evidence for an important role of WRKY DNA binding proteins in the regulation of *NPR1* gene expression. Plant Cell 13: 1527-1539

Zhao Y, Thilmony R, Bender CL, Schaller A, He SY, Howe GA. (2003) Virulence systems of *Pseudomonas syringae* pv. *tomato* promote bacterial speck disease in tomato by targeting the jasmonate signaling pathway. Plant J. 36: 485-499

Zheng Z, Mosher SL, Fan B, Klessig DF, Chen Z. (2007) Functional analysis of Arabidopsis WRKY25 transcription factor in plant defense against Pseudomonas syringae. BMC Plant Biol. 7: 2

Zheng Z, Qamar SA, Chen Z, Mengiste T. (2006) Arabidopsis WRKY33 transcription factor is required for resistance to necrotrophic fungal pathogens. Plant J. 48: 592-605

Vita

Birth place- Chifeng, China

Birth date- Apr. 7th 1981

Education

1. Master of Science (Biology) Microbiology
   Institute of Microbiology, Chinese Academy of Sciences (Beijing), China
   July 2006

2. Bachelor of Science (Biology)
   Inner Mongolia University (Hohhot), China
   July 2003

Professional positions held

1. Graduate Research Assistant (August 2006-April 2012), University of Kentucky, USA

Scholastic and professional honors

1. Honored with the Myrle E. and Verle D. Nietzel Visiting Distinguished Faculty Award in conjunction with Ph.D. defense, University of Kentucky (2012)
2. Recipient of Kentucky Opportunity Fellowship (2010, 2011)
3. Recipient of Travel Award (The Kyung Soo Kim Award and the Malcolm C. Shurtleff Award) from the American Phytopathological Society (2009)
4. Recipient of Graduate School Fellowship from University of Kentucky (2007, 2008)
5. Recipient of Di-Ao Scholarships for excellent graduates of Graduate University of Chinese Academy of Sciences (GUCAS) (2006)
6. Recipient of George Gao Scholarships for graduate students having good performance in study and research (2004, 2005)
7. Recipient of University Scholarships for top undergraduate students (1999-2003)

Professional publications

In preparation

1. **Gao Q.M.**, Kachroo P., Kachroo A. (2012). Long-chain acyl-CoA synthetases (LACS) are required for basal defense and systemic immunity in Arabidopsis.
2. Xia Y., **Gao Q.M.**, Yu K., Navarre D., Kachroo A., Kachroo P. (2012). Digalatosyl-diacylglycol synthase is required for normal cuticle formation and plant response to microbes.
3. **Gao Q.M.**, Sekine K.T., Venugopal S, Kachroo P., Kachroo A. (2012). Glycerol-3-phosphate mediates basal defense against necrotrophic pathogens.

Published

4. Mandal M.K., Chanda B., Xia Y., Yu K., **Gao Q.M.**, Selote D., Kachroo A., Kachroo P. (2011). Glycerol-3-phosphate and systemic immunity. **Plant Signaling & Behavior** 6:1-4.
5. Chanda B., Xia Y., Mandal M.K., Yu K., Sekine K.T., **Gao Q.M.**, Selote D., Hu Y., Stromberg A., Navarre D., Kachroo A., Kachroo P. (2011). Glycerol-3-phosphate is a critical mobile inducer of systemic immunity in plants. **Nature Genetics** 43:421-427.
6. **Gao Q.M.**, Venugopal S., Navarre D., Kachroo A. (2011). Low 18:1-derived repression of jasmonic acid-inducible defense responses requires the WRKY50 and WRKY51 proteins. **Plant Physiology** 155:464-476.
7. **Gao Q.M.**, Guo L.D. (2010). A comparative study of arbuscular mycorrhizal fungi in forest, grassland and cropland in the Tibetan Plateau, China. **Mycology** 3:163-170.
8. Xia Y., **Gao Q.M.**, Yu K., Navarre D., Hildebrand D., Kachroo A., Kachroo P. (2009). An intact cuticle in distal tissues is essential for the induction of systemic acquired resistance in plants. **Cell Host & Microbe** 5:151-165.
9. Zhang Y., **Gao Q.M.**, Guo L.D. (2007). Seven new records of arbuscular mycorrhizal fungi in China. **Mycosystema** 26:174-178.
10. **Gao Q.M.**, Zhang Y., Guo L.D. (2006). Arbuscular mycorrhiza fungi in the Southeast region of Tibet. **Mycosystema** 25:234-243.

Qing-Ming GAO
April 14th 2012